App Met Sat Summary

AOS 745
Lectures in Benevento
Jun 2007

Paul Menzel
UW/CIMSS/AOS

Satellite remote sensing of the Earth-atmosphere

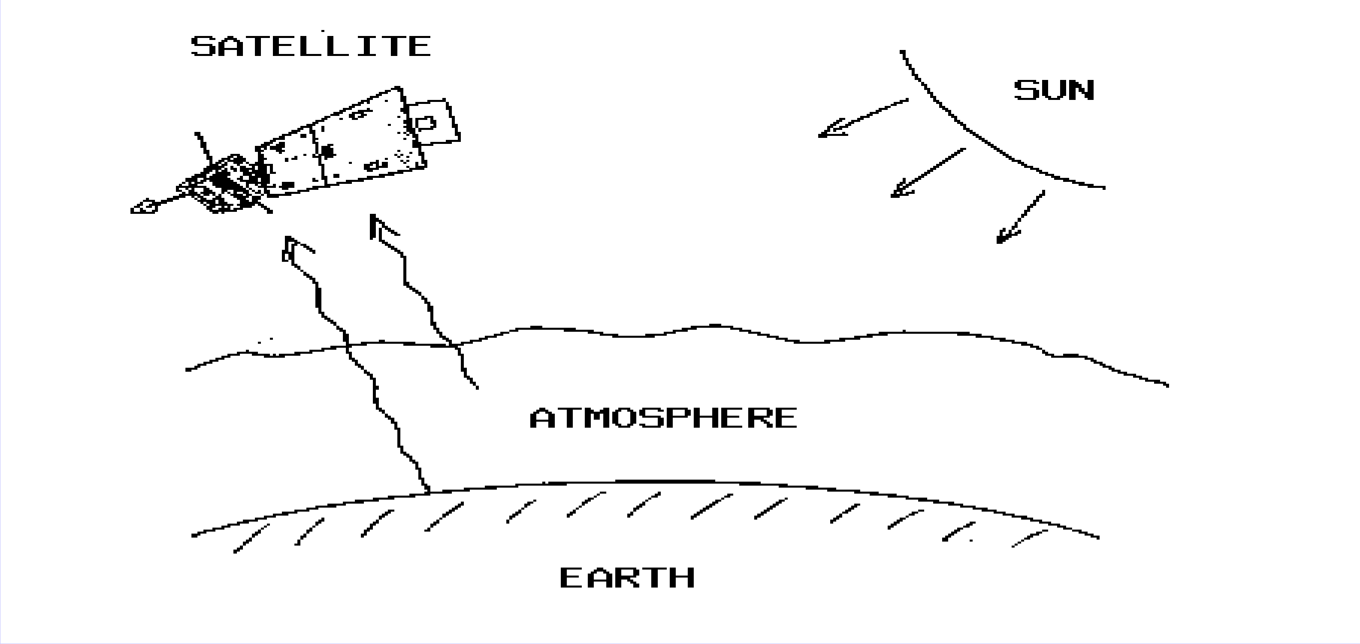

Observations depend on

- telescope characteristics (resolving power, diffraction)
- detector characteristics (signal to noise)
- communications bandwidth (bit depth)
- spectral intervals (window, absorption band)
- time of day (daylight visible)
- atmospheric state (T, Q, clouds)
- earth surface (Ts, vegetation cover)

Spectral Characteristics of Energy Sources and Sensing Systems

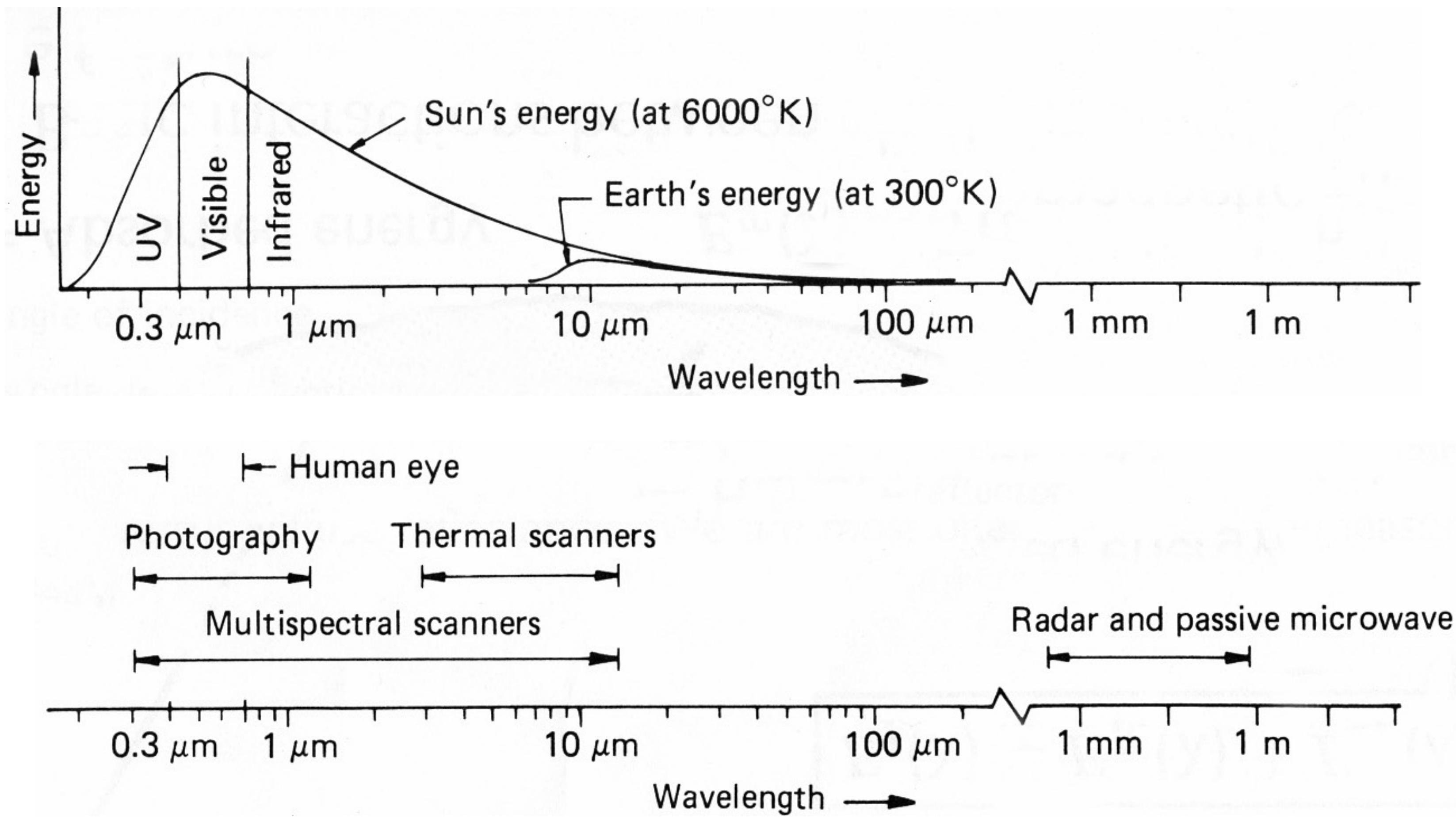

Terminology of radiant energy

Energy from the Earth Atmosphere

over time is

Flux

which strikes the detector area

Irradiance

at a given wavelength interval

Monochromatic Irradiance

over a solid angle on the Earth

Radiance observed by satellite radiometer

is described by

The Planck function

can be inverted to

Brightness temperature

Definitions of Radiation

QUANTITY	SYMBOL	UNITS
Energy	dQ	Joules
Flux	dQ/dt	Joules/sec = Watts
Irradiance	dQ/dt/dA	Watts/meter^2
Monochromatic Irradiance	dQ/dt/dA/dλ	W/m^2/micron
	or	
	dQ/dt/dA/dν	W/m^2/cm^{-1}
Radiance	dQ/dt/dA/dλ/dΩ	W/m^2/micron/ster
	or	
	dQ/dt/dA/dν/dΩ	W/m^2/cm^{-1}/ster

Using wavenumbers

Planck's Law $$B(\nu,T) = c_1\nu^3 / [e^{c_2\nu/T} - 1] \quad (mW/m^2/ster/cm^{-1})$$

where ν = # wavelengths in one centimeter (cm-1)

T = temperature of emitting surface (deg K)

c_1 = 1.191044 x 10-5 ($mW/m^2/ster/cm^{-4}$)

c_2 = 1.438769 (cm deg K)

Wien's Law $dB(\nu_{max},T) / d\nu = 0$ where $\nu max) = 1.95T$

indicates peak of Planck function curve shifts to shorter wavelengths (greater wavenumbers) with temperature increase.

Stefan-Boltzmann Law $$E = \pi \int_o^{\infty} B(\nu,T)\, d\nu = \sigma T^4$$, where σ = 5.67 x 10-8 W/m2/deg4.

states that irradiance of a black body (area under Planck curve) is proportional to T^4 .

Brightness Temperature

$$T = c_2\nu/[\ln(\frac{c_1\nu^3}{B_\nu} + 1)]$$ is determined by inverting Planck function

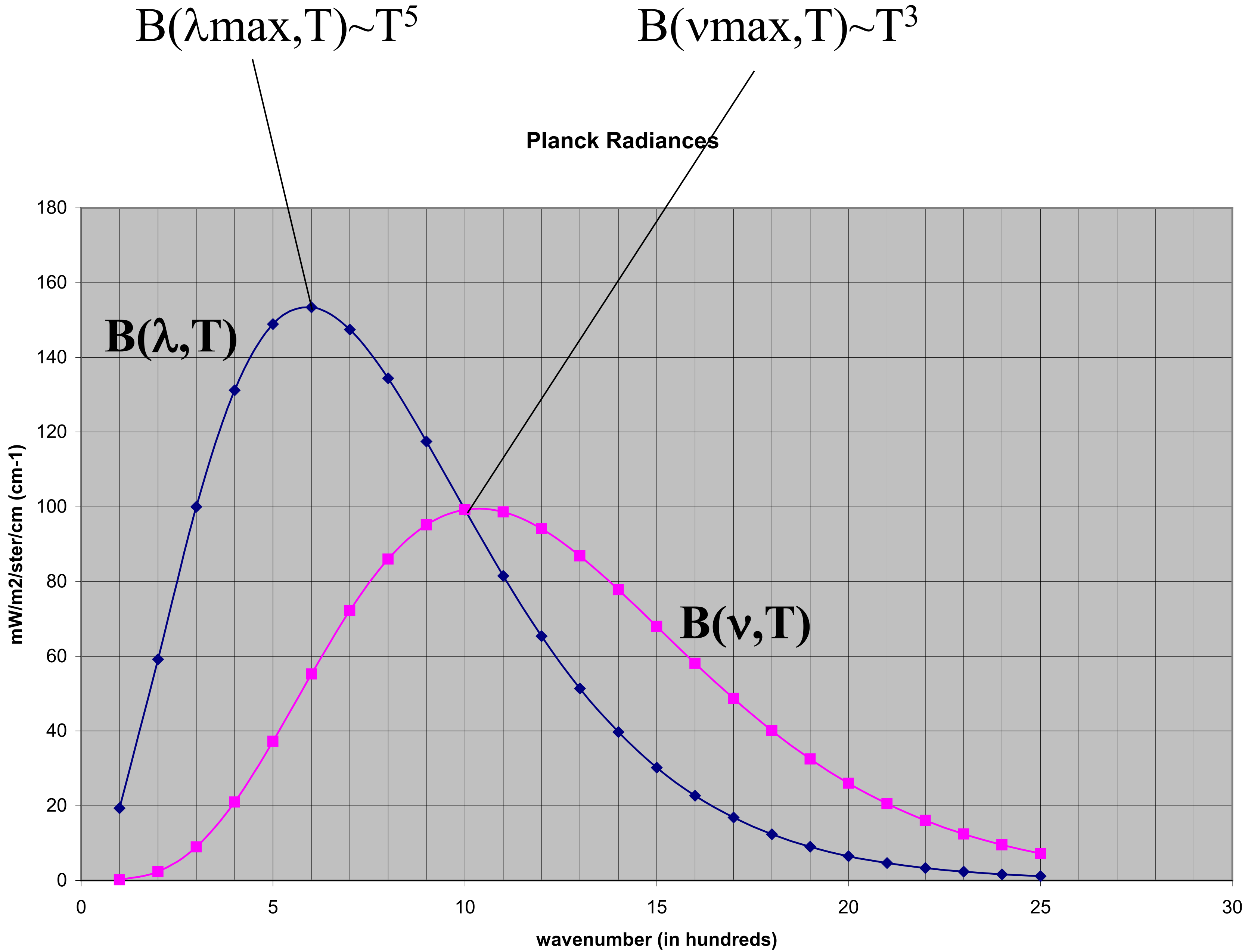

B(λ,T) versus B(ν,T)

Using wavenumbers

$$B(\nu,T) = c_1\nu^3 / [e^{c_2\nu/T} - 1]$$

(mW/m²/ster/cm⁻¹)

ν(max in cm-1) = 1.95T

$B(\nu_{max},T) \sim T^{**}3.$

$$E = \pi \int_o^\infty B(\nu,T)\, d\nu = \sigma T^4,$$

$$T = c_2\nu / [\ln(\frac{c_1\nu^3}{B_\nu} + 1)]$$

Using wavelengths

$$B(\lambda,T) = c_1 / \{ \lambda^5 [e^{c_2/\lambda T} - 1] \}$$

(mW/m²/ster/μm)

λ(max in cm)T = 0.2897

$B(\lambda_{max},T) \sim T^{**}5.$

$$E = \pi \int_o^\infty B(\lambda,T)\, d\lambda = \sigma T^4,$$

$$T = c_2 / [\lambda \ln(\frac{c_1}{\lambda^5 B_\lambda} + 1)]$$

Spectral Distribution of Energy Radiated from Blackbodies at Various Temperatures

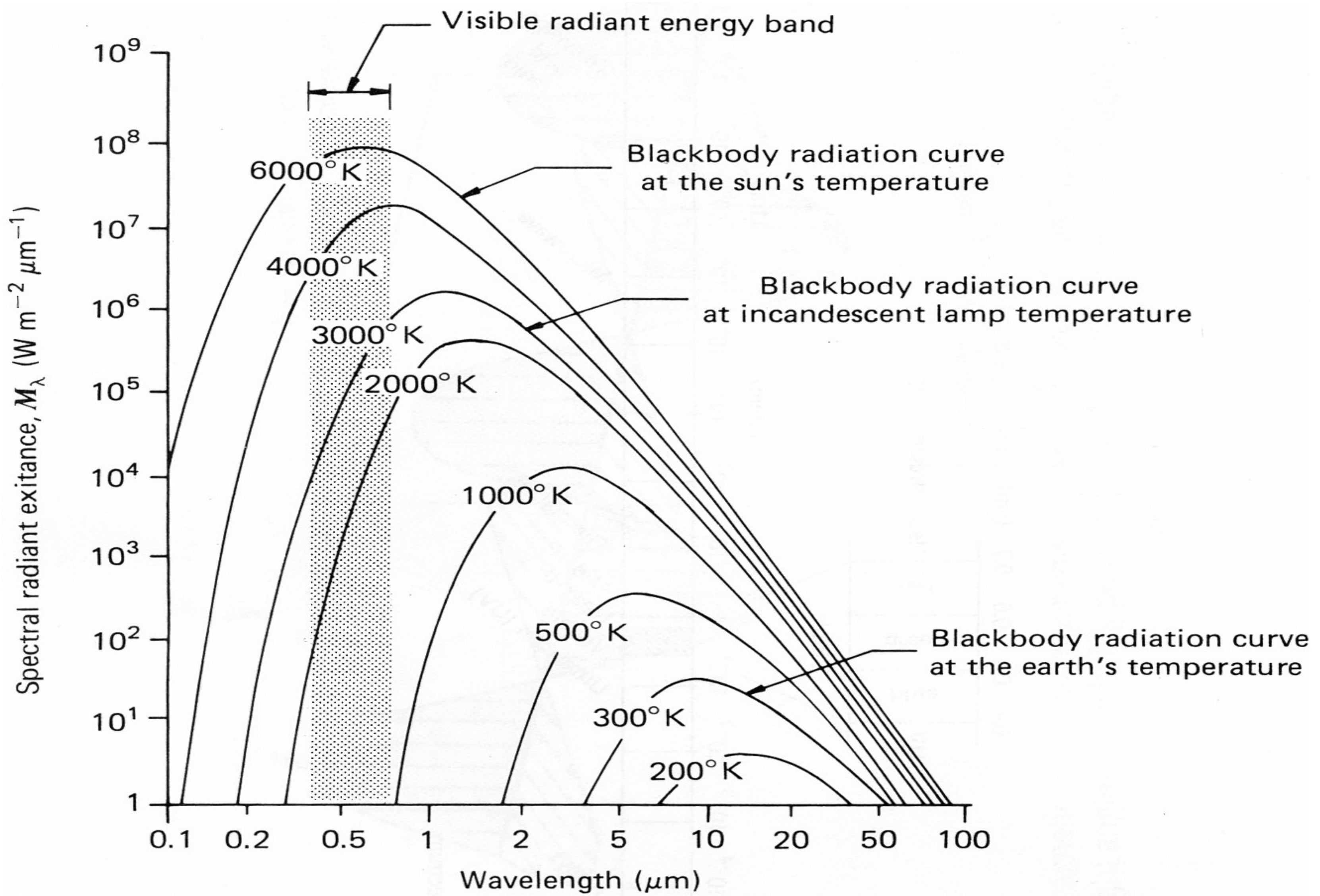

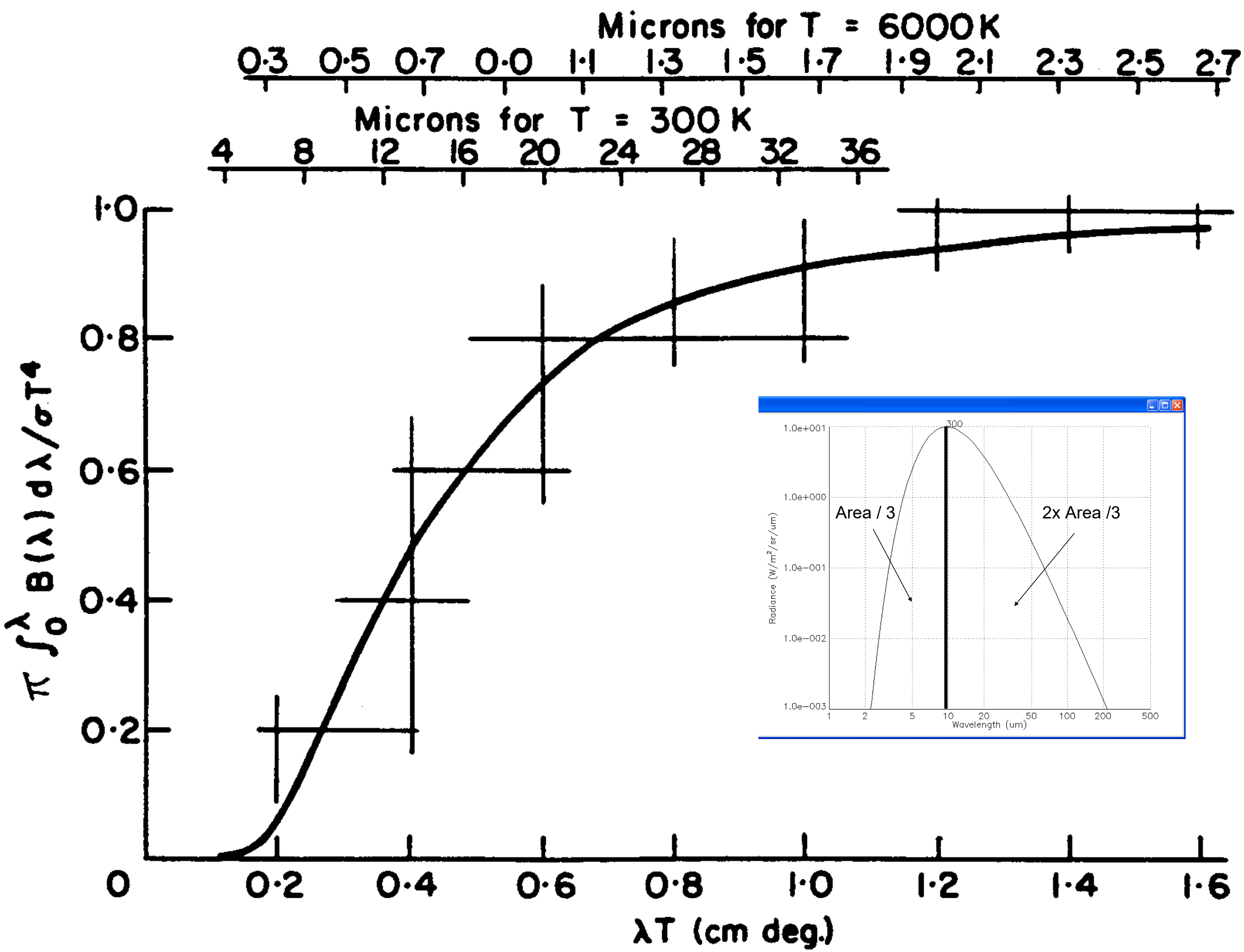
Microns for T = 6000K
0·3 0·5 0·7 0·0 1·1 1·3 1·5 1·7 1·9 2·1 2·3 2·5 2·7
Microns for T = 300 K
4 8 12 16 20 24 28 32 36
1·0 0·8 0·6 0·4 0·2
$\pi \int_0^\lambda B(\lambda)\, d\lambda / \sigma T^4$
0 0·2 0·4 0·6 0·8 1·0 1·2 1·4 1·6
λT (cm deg.)
Area / 3
2x Area /3
300
1.0e+001
1.0e+000
1.0e−001
1.0e−002
1.0e−003
Radiance (W/m²/sr/um)
1 2 5 10 20 50 100 200 500
Wavelength (um)

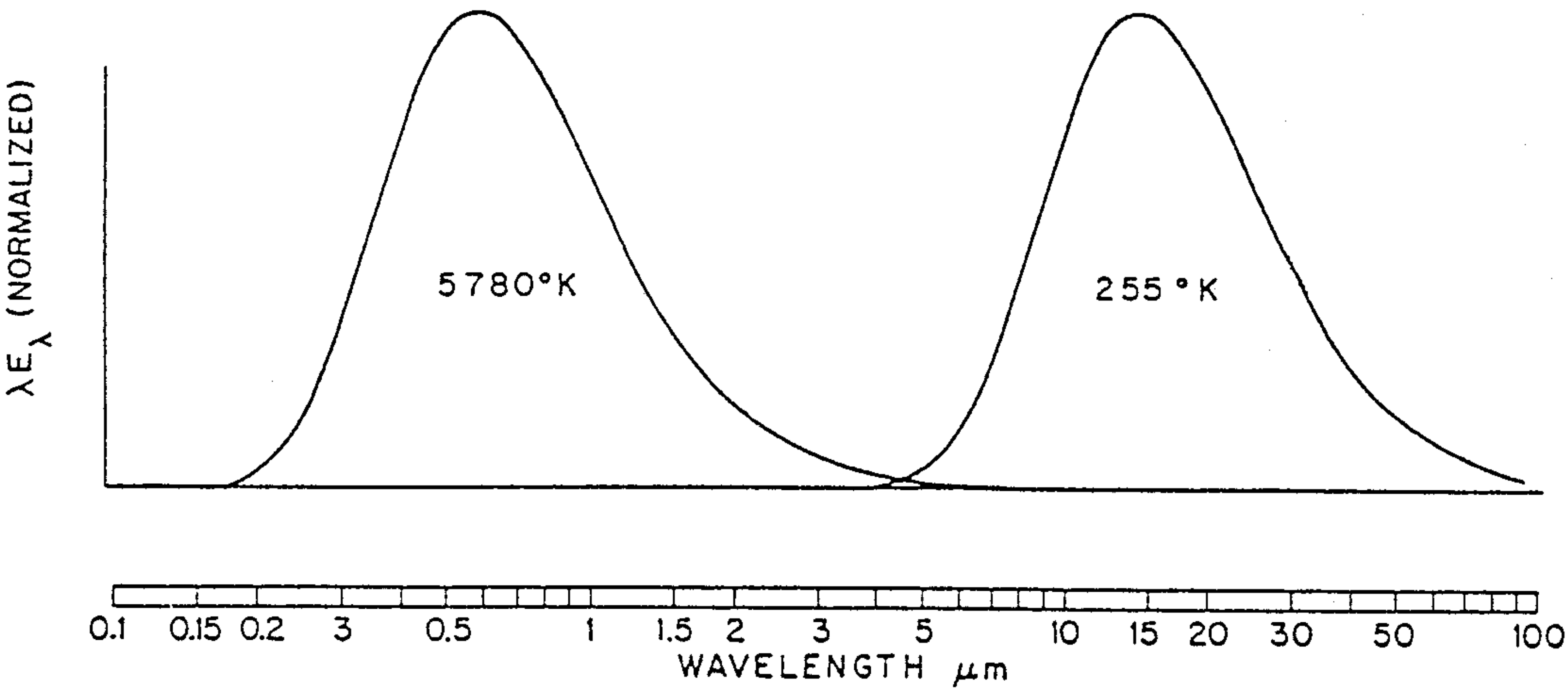

Normalized black body spectra representative of the sun (left) and earth (right), plotted on a logarithmic wavelength scale. The ordinate is multiplied by wavelength so that the area under the curves is proportional to irradiance.

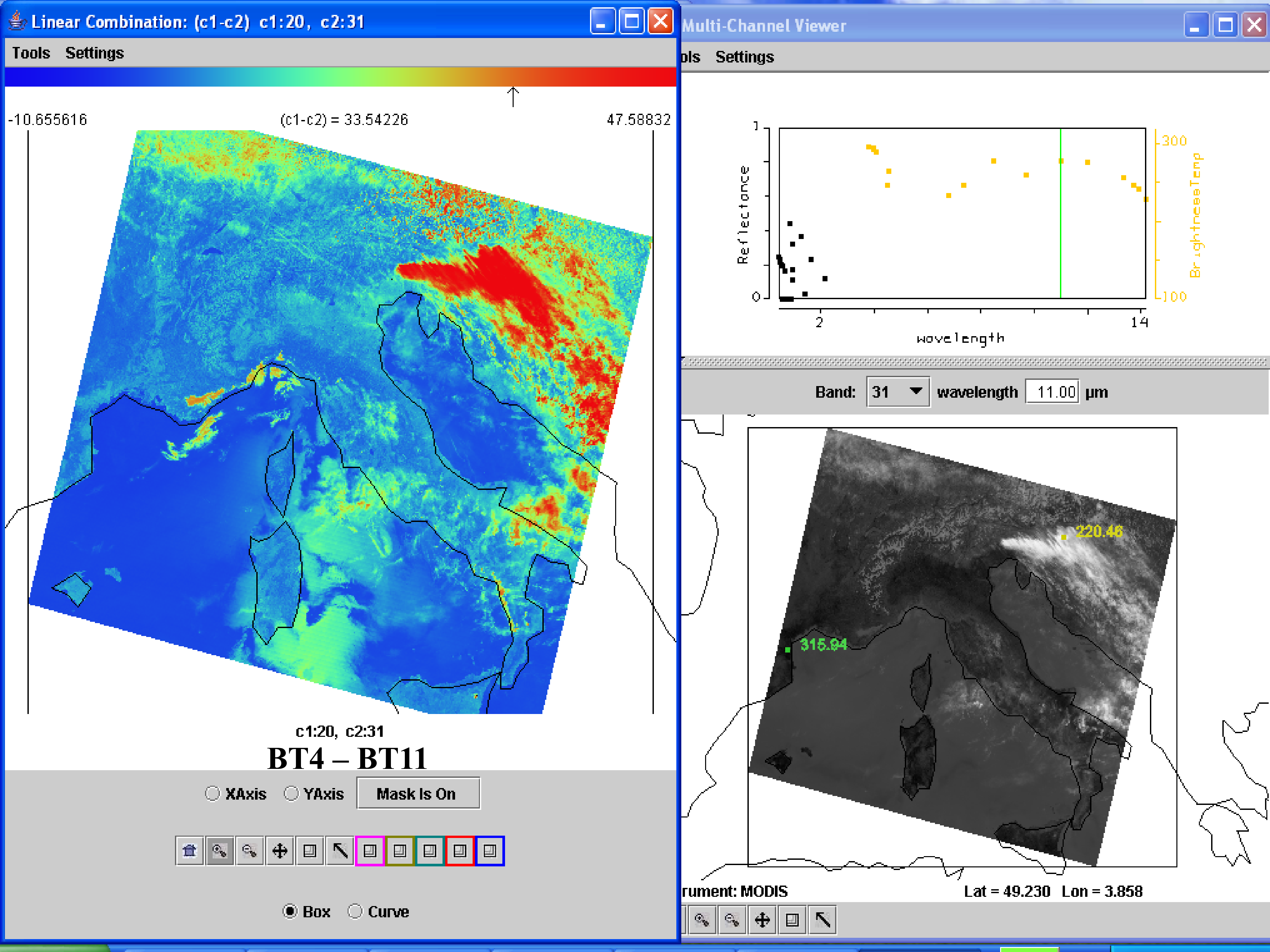
Linear Combination: (c1-c2) c1:20, c2:31
Tools Settings
-10.655616
(c1-c2) = 33.54226
47.58832
c1:20, c2:31
BT4 – BT11
XAxis
YAxis
Mask Is On
Box
Curve
Multi-Channel Viewer
ols Settings
Reflectance
BrightnessTemp
300
100
0
1
2
14
wavelength
Band: 31
wavelength 11.00 μm
220.46
315.04
rument: MODIS
Lat = 49.230 Lon = 3.858

Temperature Sensitivity of B(λ,T) for typical earth temperatures

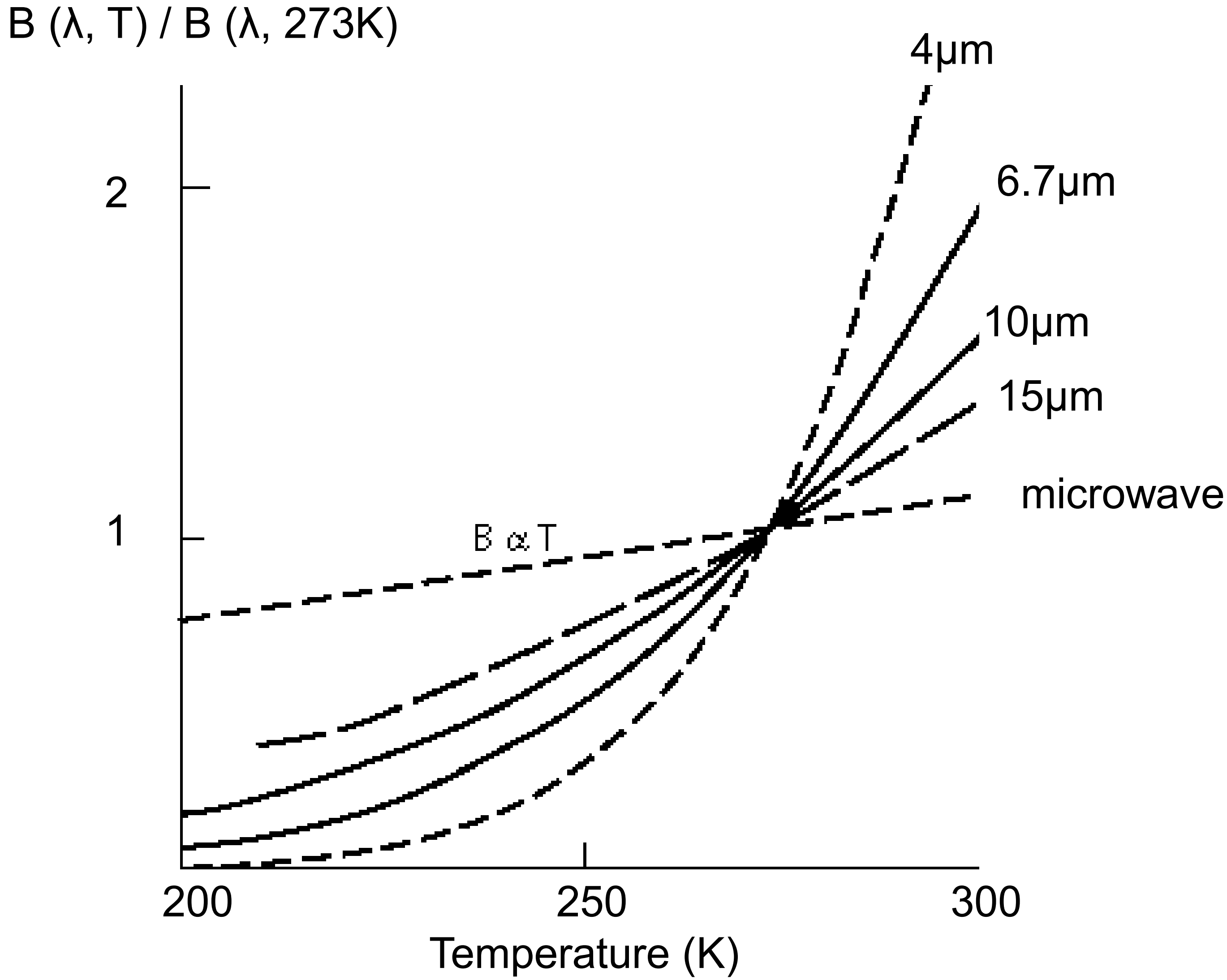

Observed BT at 4 micron

Window Channel:
•little atmospheric absorption
•surface features clearly visible

Range [250 335]

Clouds are cold

Values over land
Larger than over water

Reflected Solar everywhere
Stronger over Sunglint

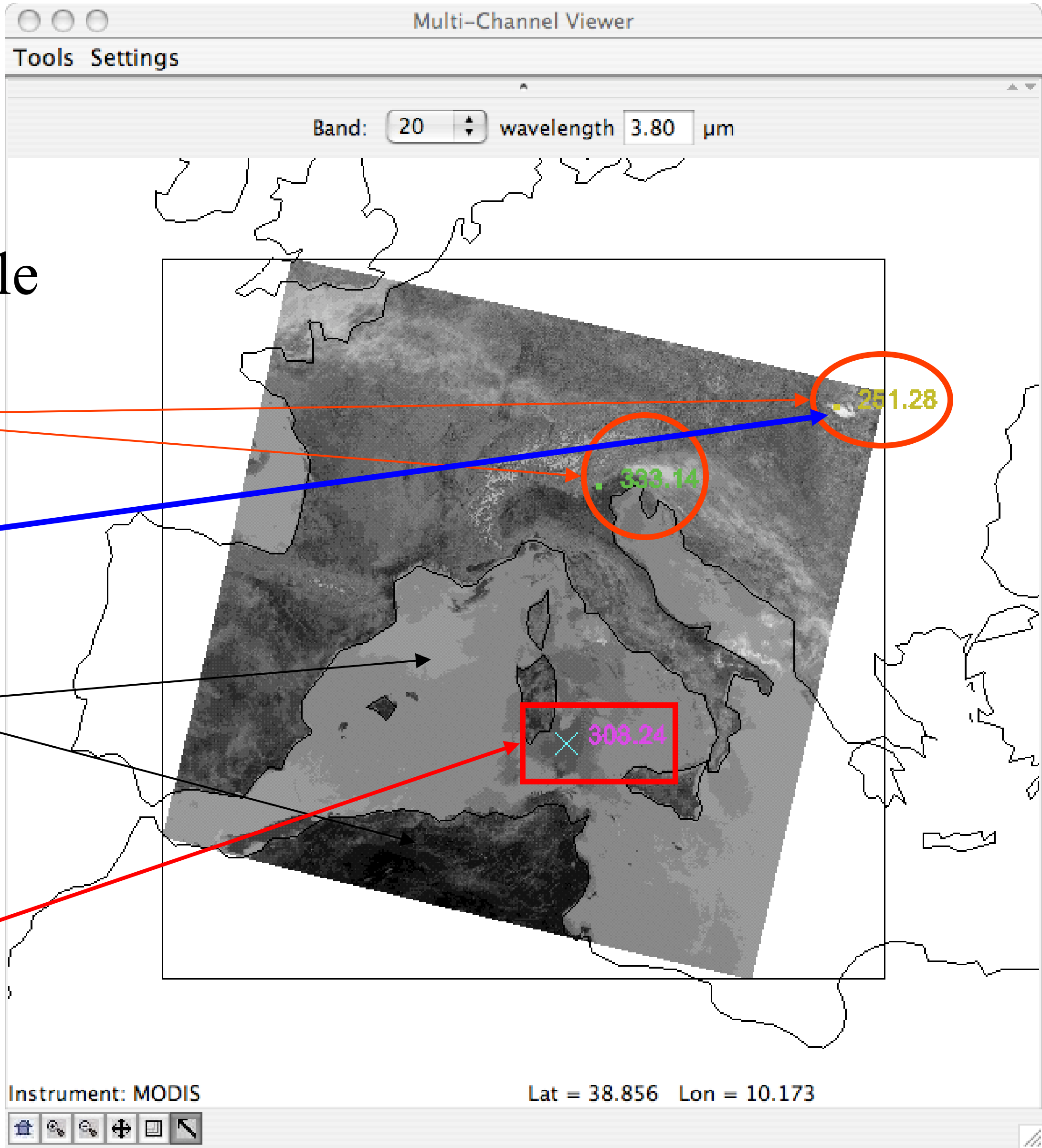

Observed BT at 11 micron

Window Channel:
- little atmospheric absorption
- surface features clearly visible

Range [220 320]

Clouds are cold

Values over land
Larger than over water

Undetectable Reflected Solar
Even over Sunglint

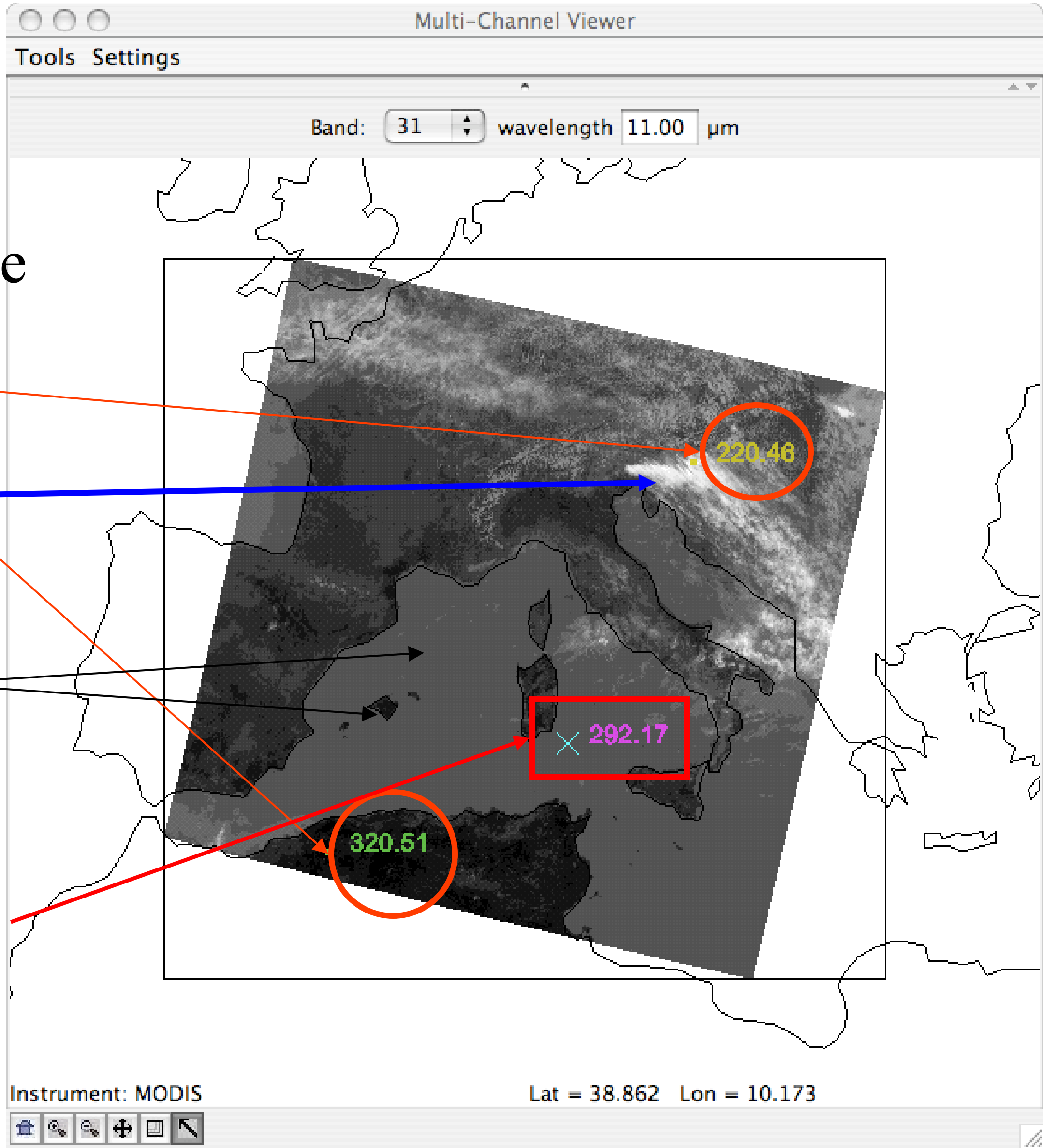

Solar (visible) and Earth emitted (infrared) energy

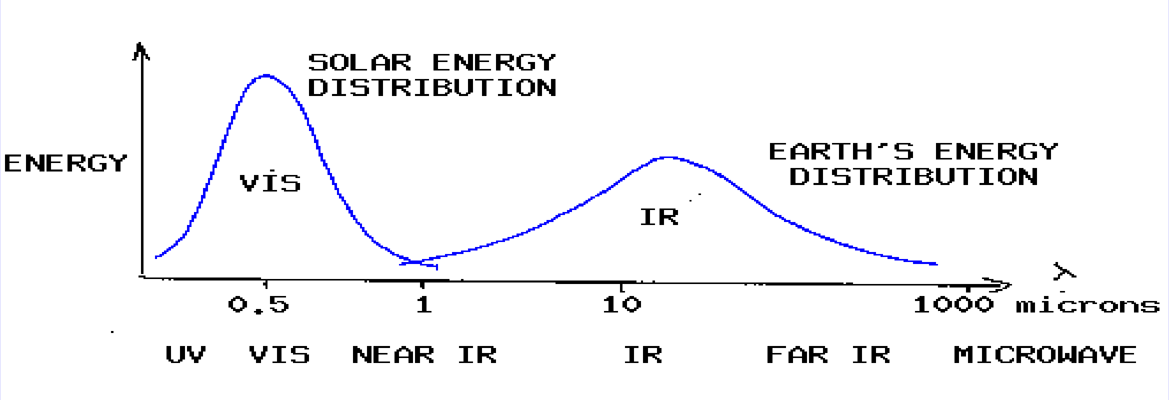

Incoming solar radiation (mostly visible) drives the earth-atmosphere (which emits infrared).

Over the annual cycle, the incoming solar energy that makes it to the earth surface (about 50 %) is balanced by the outgoing thermal infrared energy emitted through the atmosphere.

The atmosphere transmits, absorbs (by H2O, O2, O3, dust) reflects (by clouds), and scatters (by aerosols) incoming visible; the earth surface absorbs and reflects the transmitted visible. Atmospheric H2O, CO2, and O3 selectively transmit or absorb the outgoing infrared radiation. The outgoing microwave is primarily affected by H2O and O2.

Selective Absorption
Atmosphere transmits visible and traps infrared

Incoming solar   Outgoing IR

$\downarrow E$ $\uparrow (1-a_l)\, Y_{sfc}$ $\uparrow Y_a$

top of the atmosphere

$\downarrow (1-a_s)\, E$ $\uparrow Y_{sfc}$ $\downarrow Y_a$

earth surface.

$$Y_{sfc} = \frac{(2-a_S)}{(2-a_L)} E = \sigma T_{sfc}^4$$

thus if $a_s < a_L$ then $Y_{sfc} > E$

Solar Spectrum

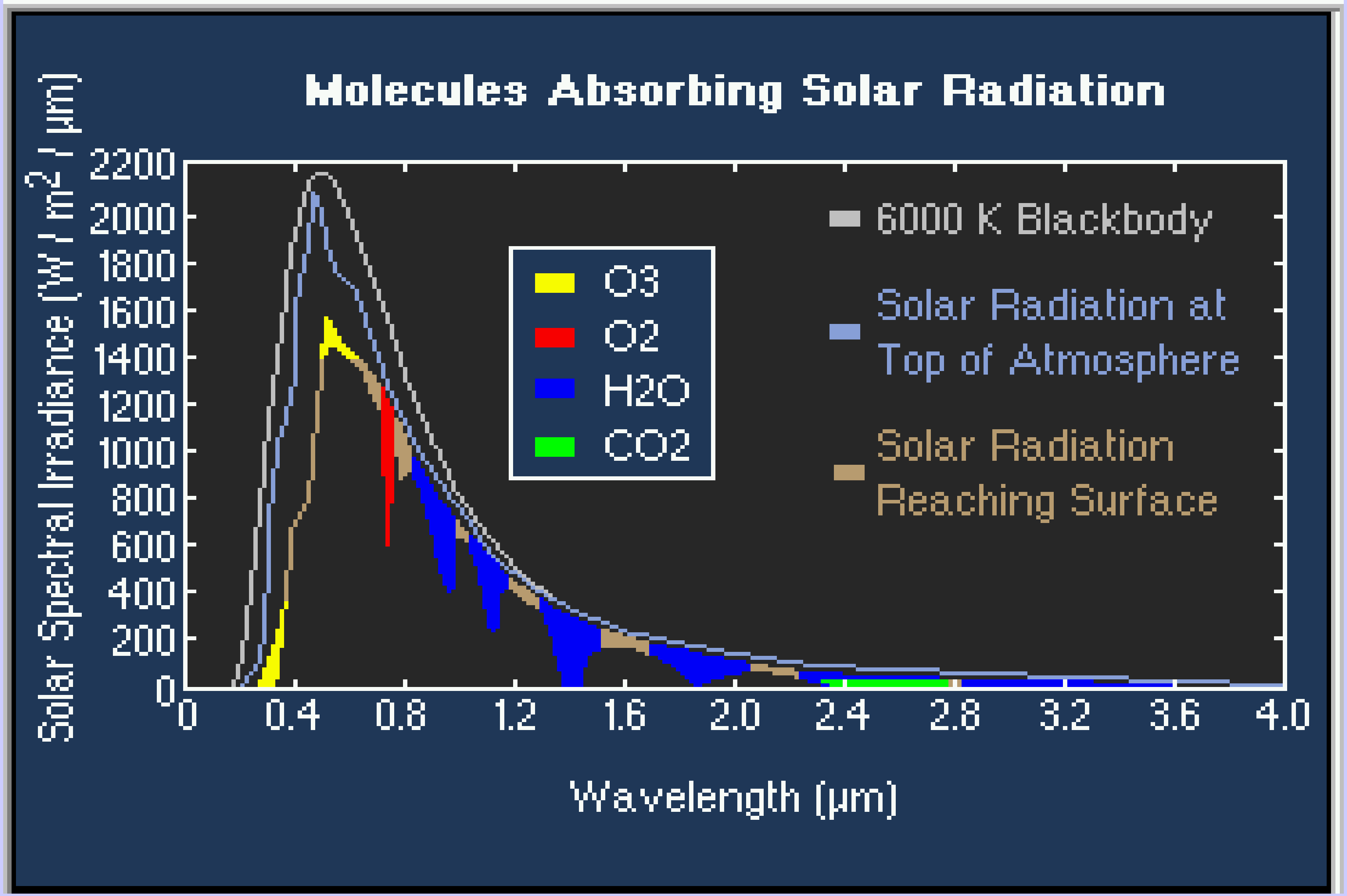

VIIRS, MODIS, FY-1C, AVHRR

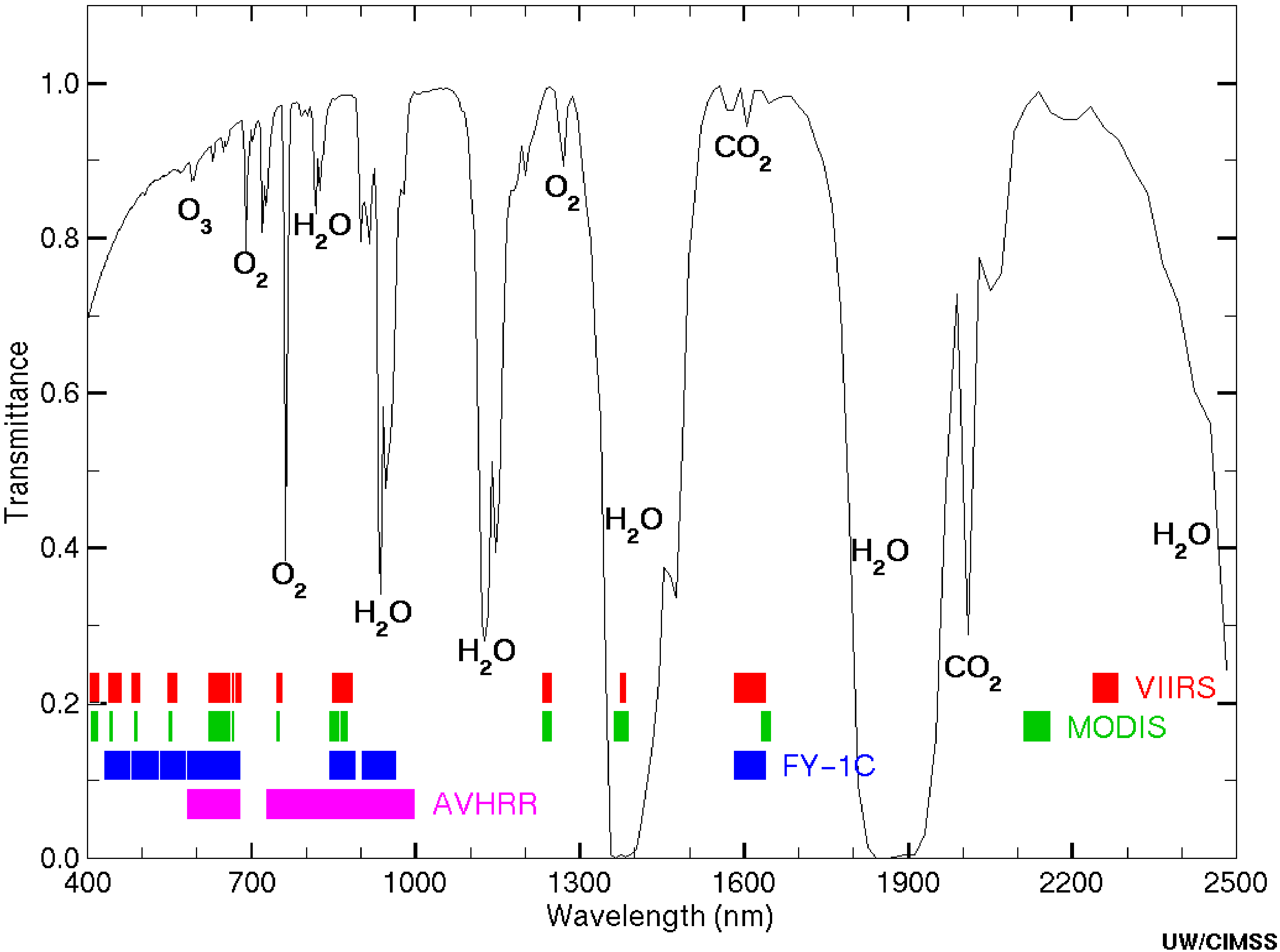

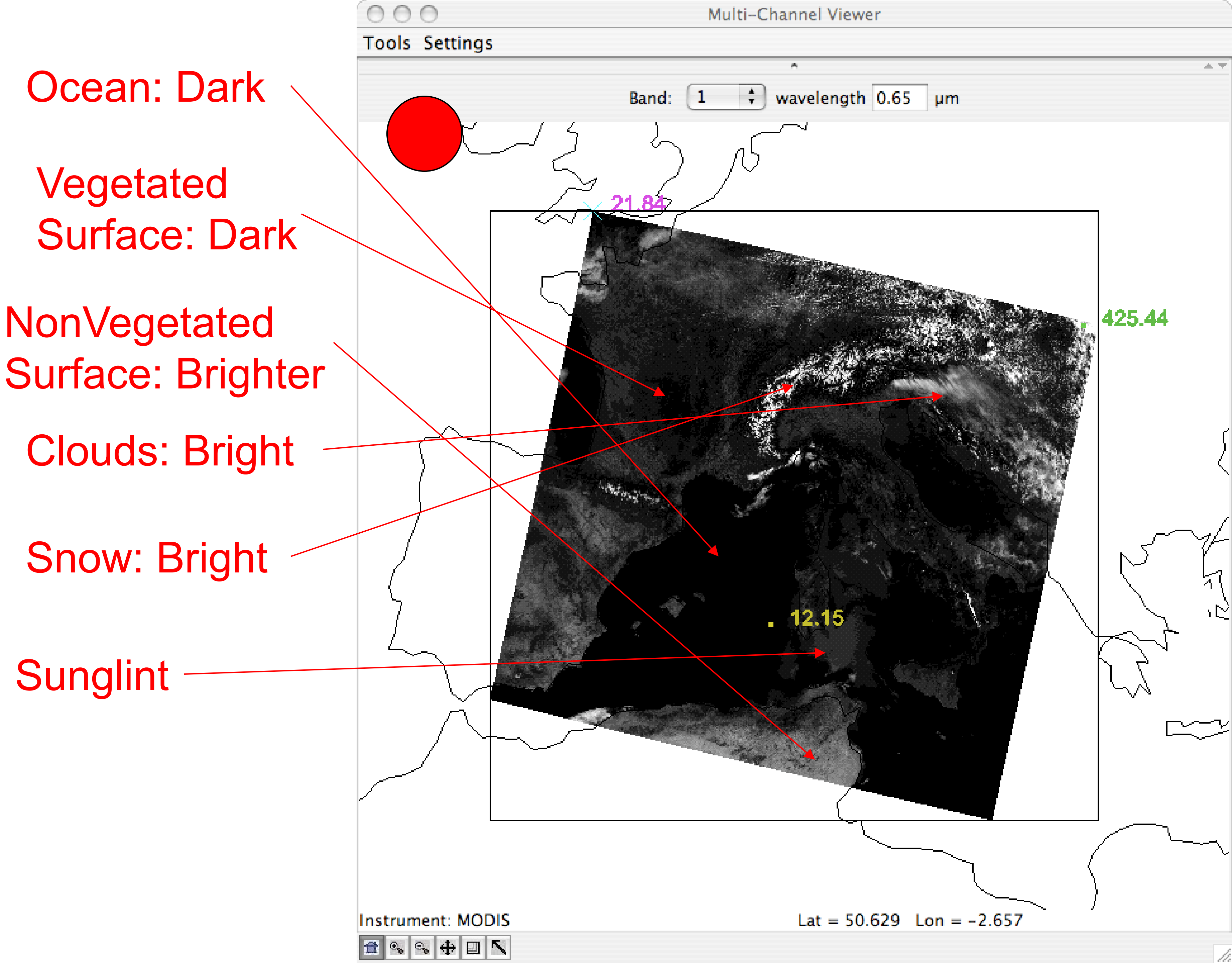
Ocean: Dark
Vegetated Surface: Dark
NonVegetated Surface: Brighter
Clouds: Bright
Snow: Bright
Sunglint
Multi-Channel Viewer
Tools Settings
Band: 1 wavelength 0.65 μm
21.84
425.44
12.15
Instrument: MODIS
Lat = 50.629 Lon = -2.657

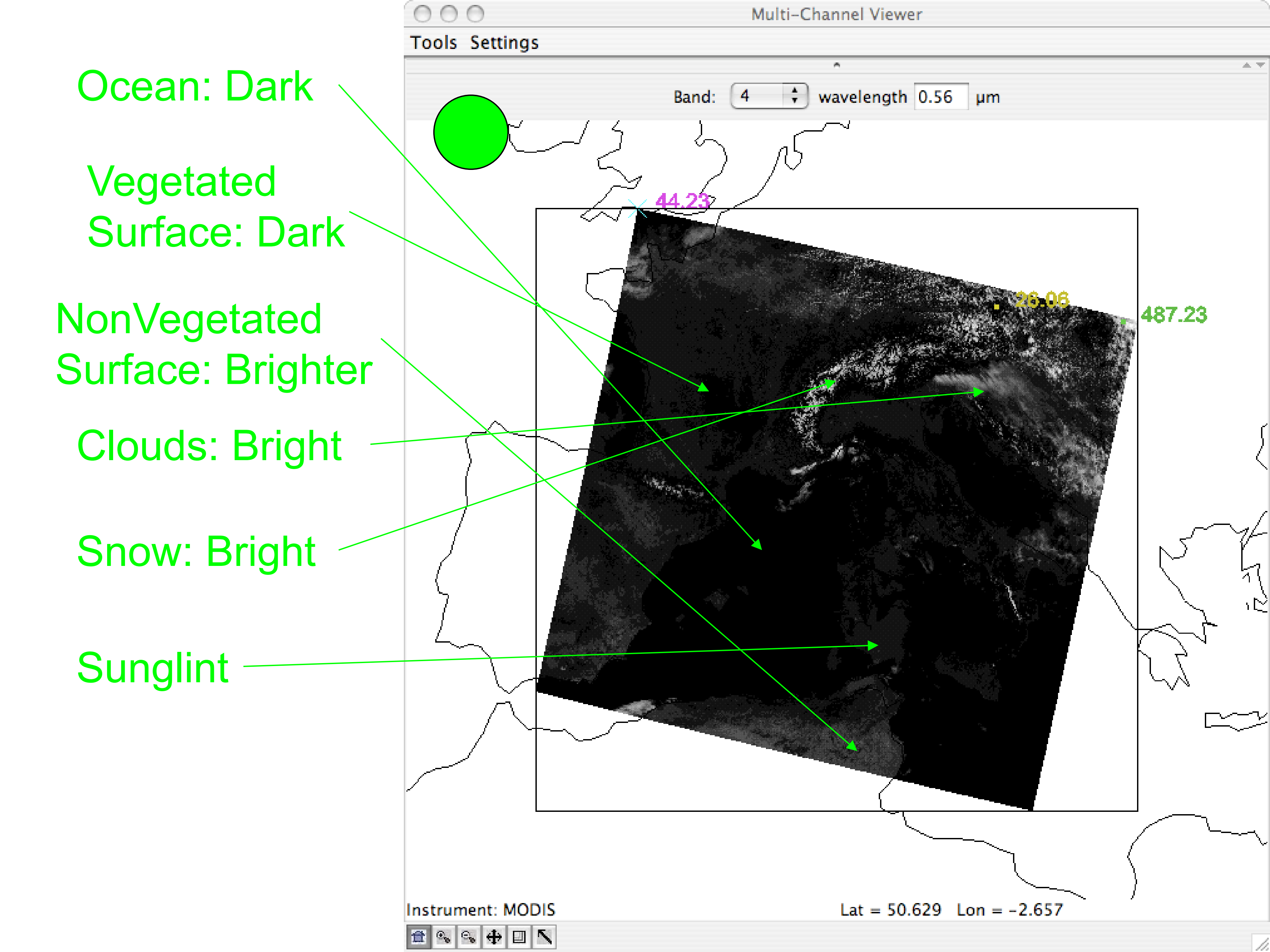

Ocean: Dark
Vegetated Surface: Dark
NonVegetated Surface: Brighter
Clouds: Bright
Snow: Bright
Sunglint
Multi-Channel Viewer
Tools Settings
Band: 4 wavelength 0.56 µm
44.23
26.06
487.23
Instrument: MODIS
Lat = 50.629 Lon = -2.657

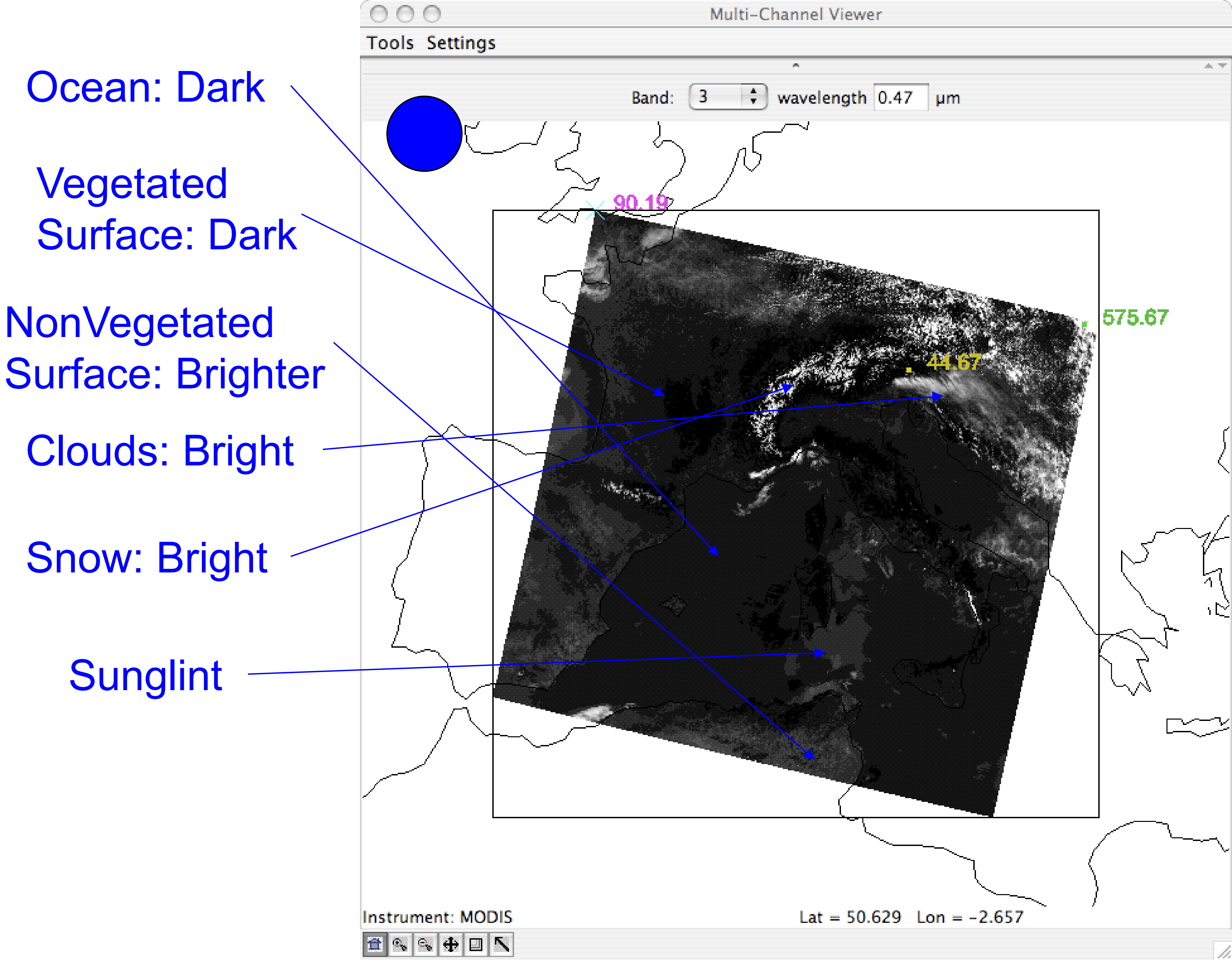

Ocean: Dark
Vegetated Surface: Dark
NonVegetated Surface: Brighter
Clouds: Bright
Snow: Bright
Sunglint
Multi-Channel Viewer
Tools Settings
Band: 3 wavelength 0.47 µm
90.19
575.67
44.67
Instrument: MODIS
Lat = 50.629 Lon = -2.657

AVIRIS Movie #2

AVIRIS Image - Porto Nacional, Brazil
20-Aug-1995
224 Spectral Bands: 0.4 - 2.5 μm
Pixel: 20m x 20m   Scene: 10km x 10km

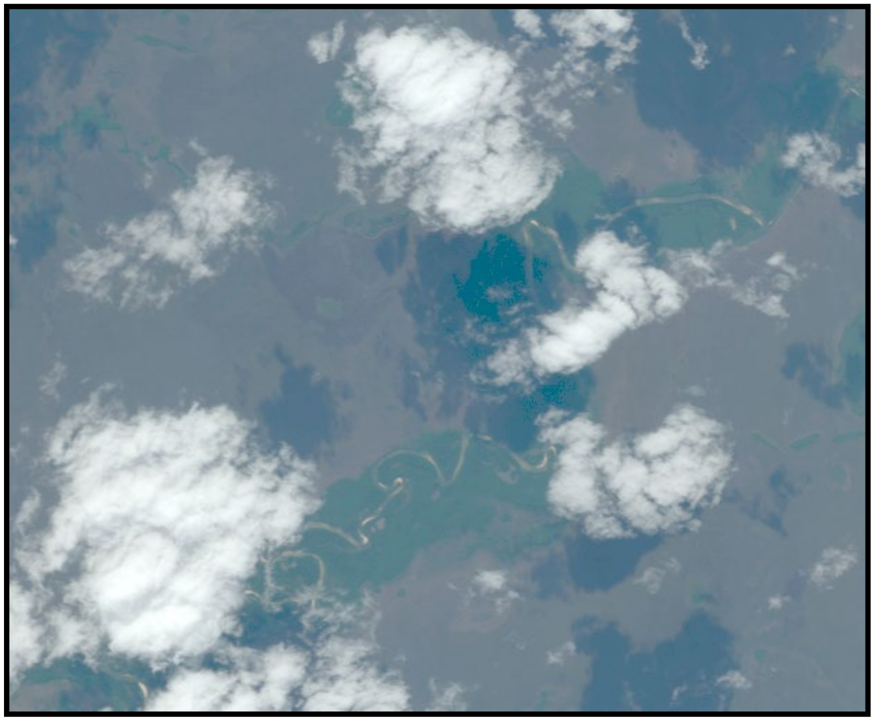

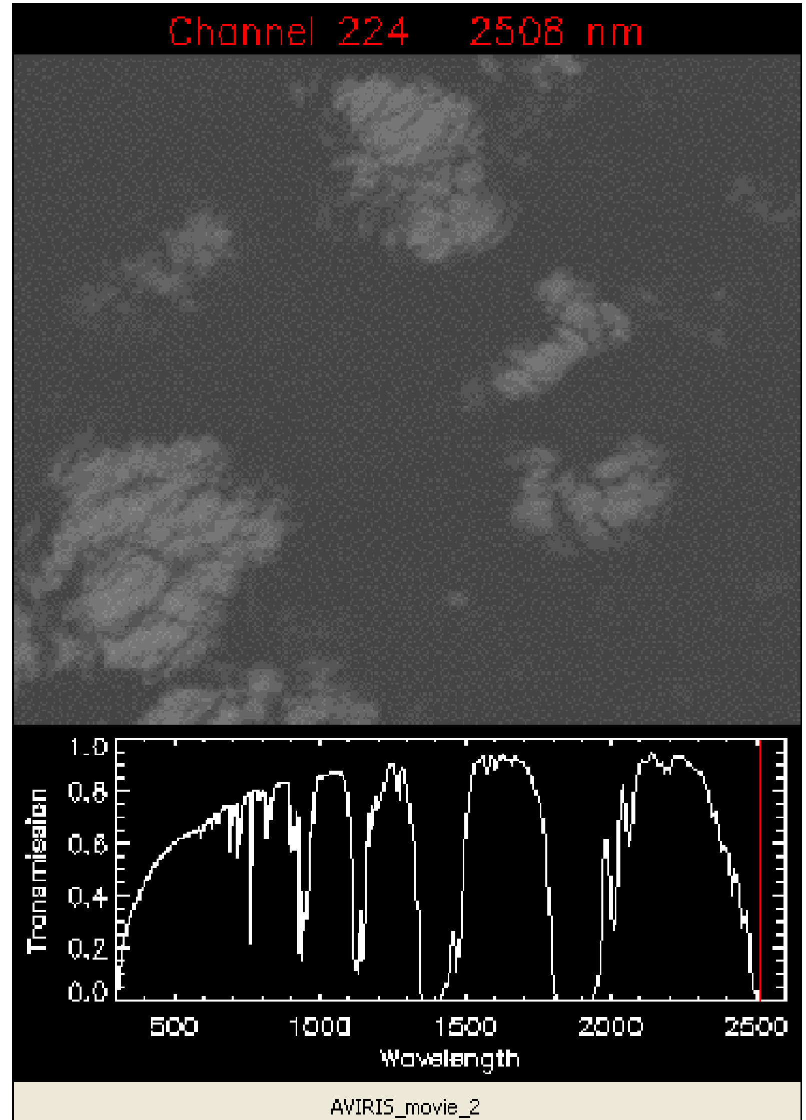

AVIRIS Movie #1

AVIRIS Image - Linden CA 20-Aug-1992
224 Spectral Bands: 0.4 - 2.5 μm
Pixel: 20m x 20m   Scene: 10km x 10km

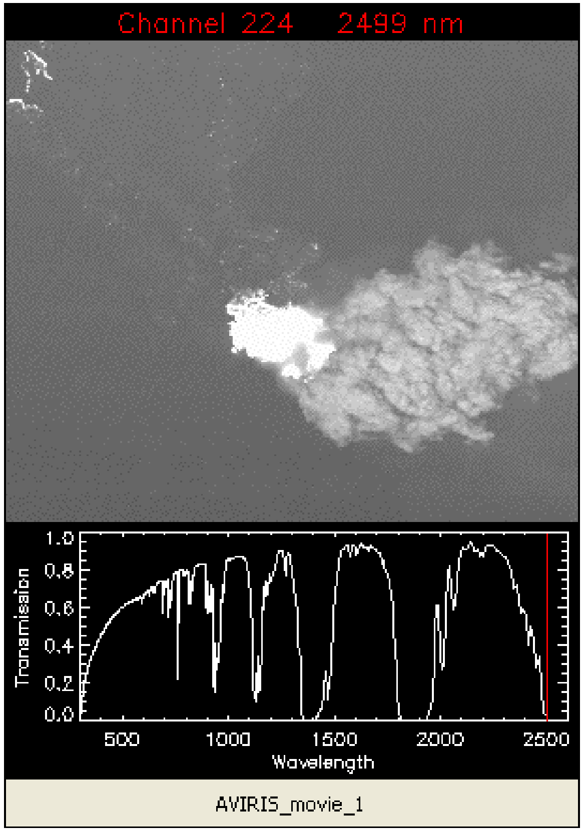

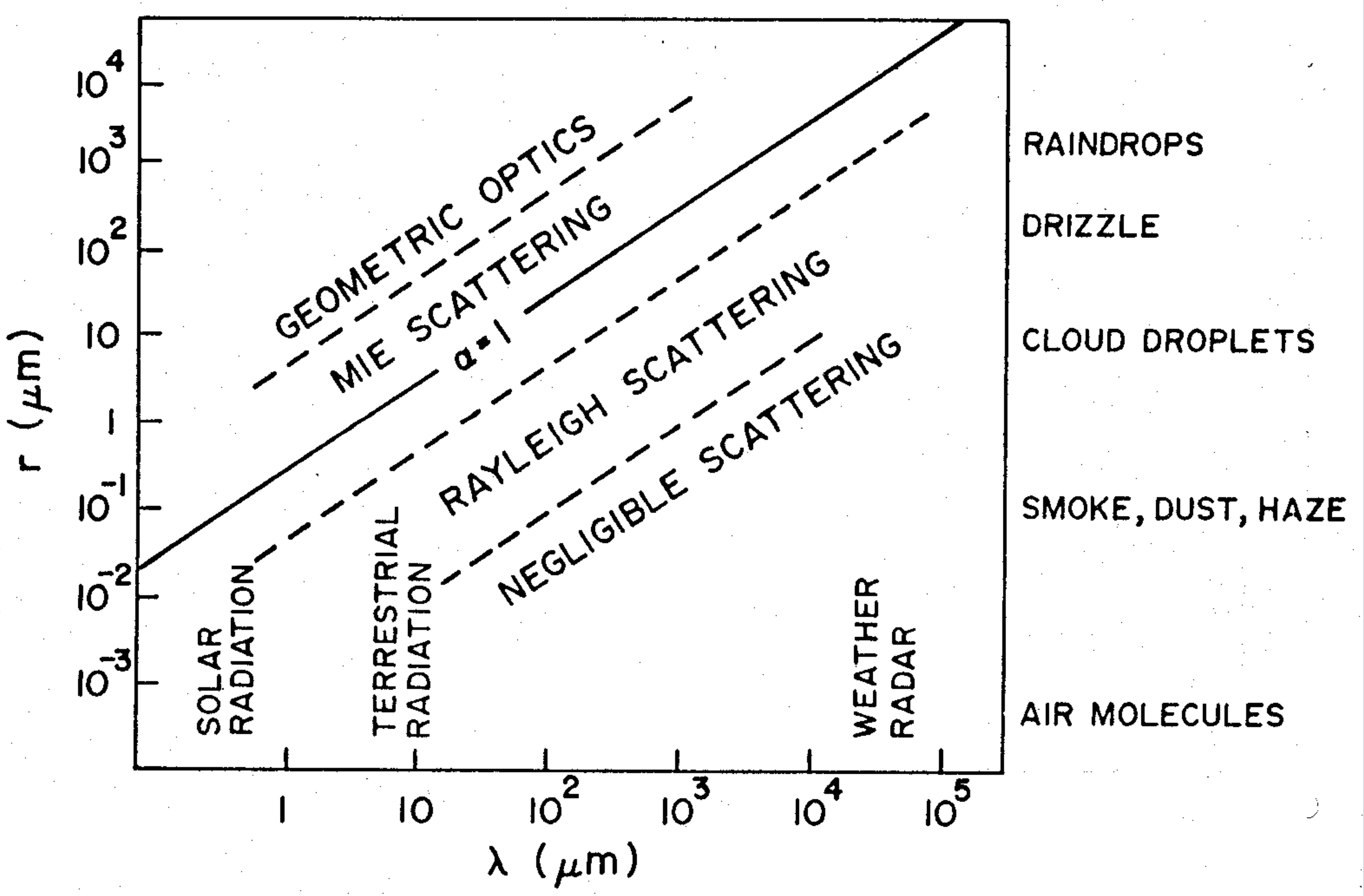

GEOMETRIC OPTICS
MIE SCATTERING
α = 1
RAYLEIGH SCATTERING
NEGLIGIBLE SCATTERING
SOLAR RADIATION
TERRESTRIAL RADIATION
WEATHER RADAR
RAINDROPS
DRIZZLE
CLOUD DROPLETS
SMOKE, DUST, HAZE
AIR MOLECULES
r (μm)
λ (μm)
10⁴
10³
10²
10
1
10⁻¹
10⁻²
10⁻³
1
10
10²
10³
10⁴
10⁵

Aerosol Size Distribution

There are 3 modes :

- « **nucleation** »: radius is between 0.002 and 0.05 µm. They result from combustion processes, photo-chemical reactions, etc.

- « **accumulation »:** radius is between 0.05 µm and 0.5 µm**.** Coagulation processes.

- « **coarse** »: larger than 1 µm**.** From mechanical processes like aeolian erosion.

« fine » particles (nucleation and accumulation) result from anthropogenic activities, coarse particles come from natural processes.

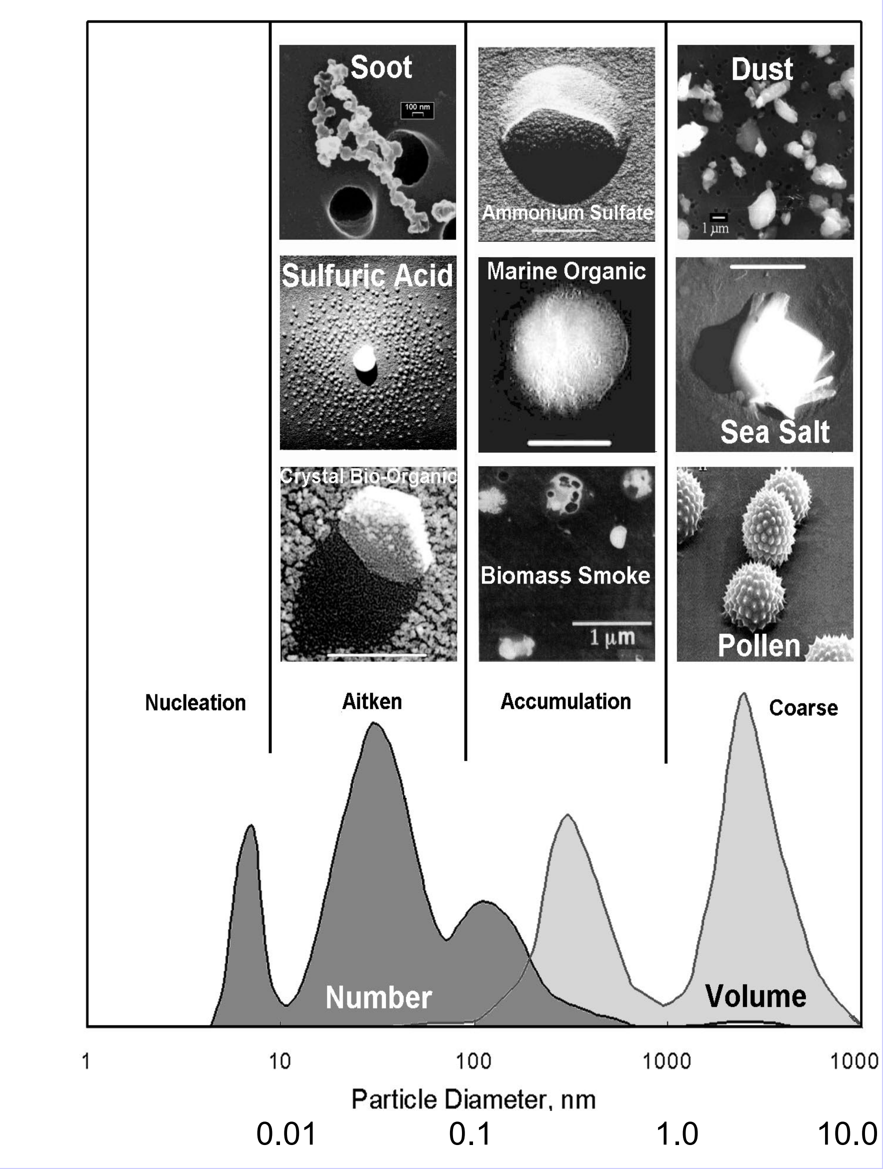

Aerosols over Ocean

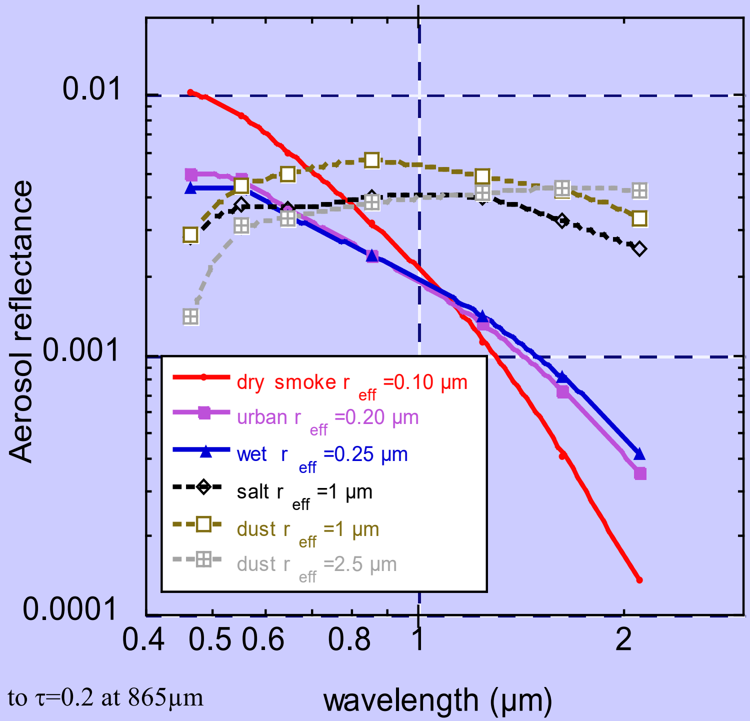

Normalized to τ=0.2 at 865µm

- Radiance data in 6 bands (550-2130nm).
- Spectral radiances (LUT) to derive the aerosol size distribution
- Two modes (accumulation 0.10-0.25µm; coarse1.0-2.5µm); ratio is a free parameter
- Radiance at 865µm to derive τ

Ocean products :

- The total Spectral Optical thickness
- The effective radius
- The optical thickness of small & large modes/ratio between the 2 modes

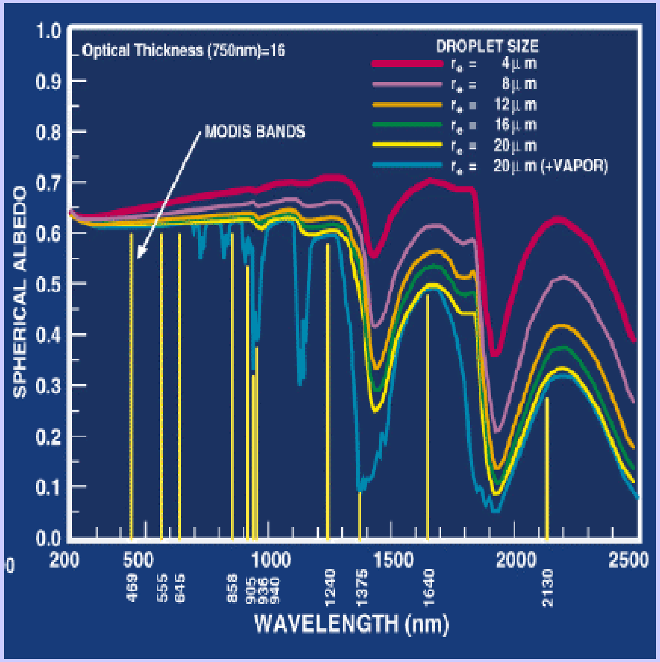
Optical Thickness (750nm)=16
DROPLET SIZE
r_e = 4µm
r_e = 8µm
r_e = 12µm
r_e = 16µm
r_e = 20µm
r_e = 20µm (+VAPOR)
MODIS BANDS
SPHERICAL ALBEDO
WAVELENGTH (nm)
469 555 645 858 905 936 940 1240 1375 1640 2130

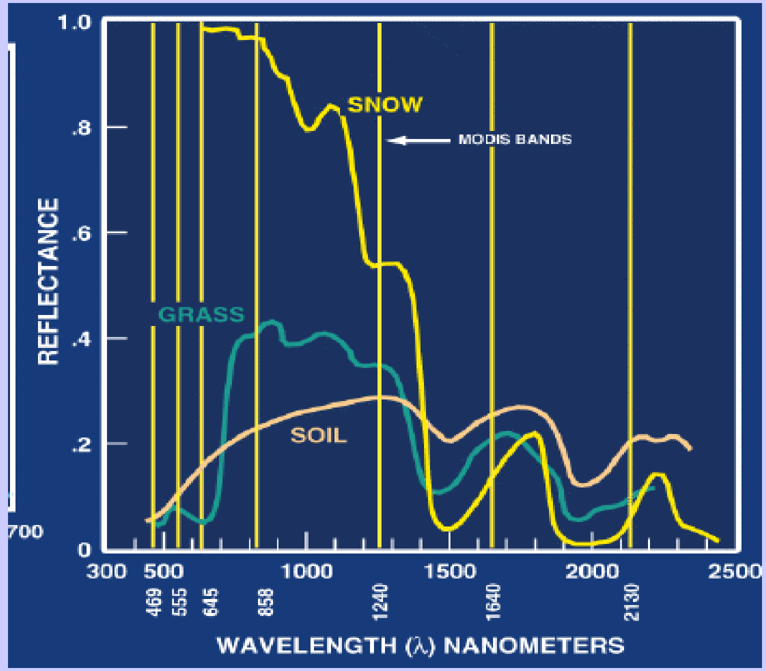
SNOW
MODIS BANDS
GRASS
SOIL
REFLECTANCE
WAVELENGTH (λ) NANOMETERS
469 555 645 858 1240 1640 2130

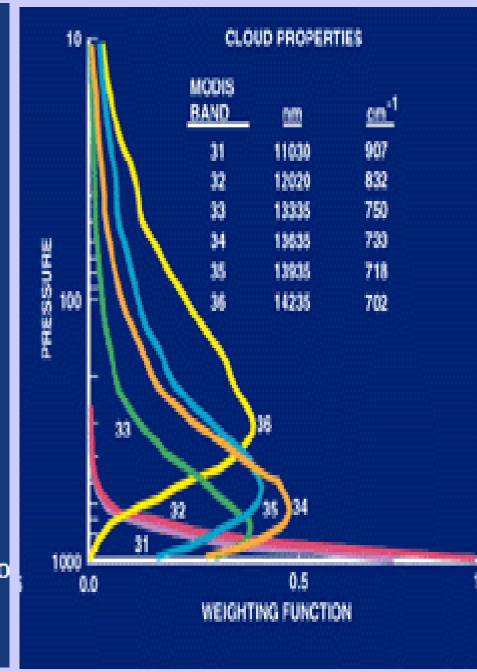
CLOUD PROPERTIES
MODIS BAND nm cm⁻¹
31 11030 907
32 12020 832
33 13335 750
34 13635 733
35 13935 718
36 14235 702
PRESSURE
WEIGHTING FUNCTION

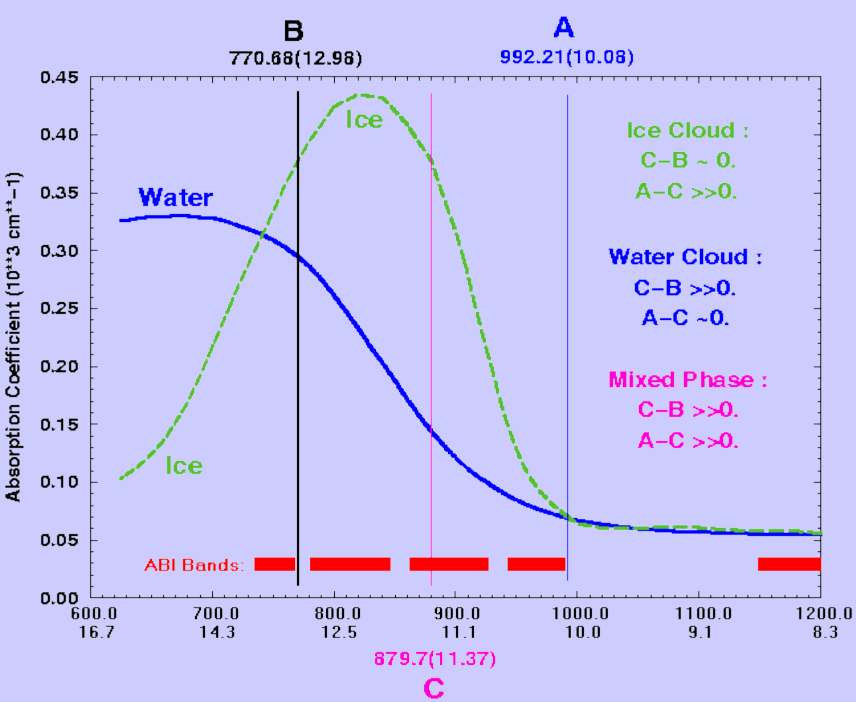
B
770.68(12.98)
A
992.21(10.08)
Water
Ice
Ice Cloud :
C–B ~ 0.
A–C >>0.
Water Cloud :
C–B >>0.
A–C ~0.
Mixed Phase :
C–B >>0.
A–C >>0.
ABI Bands:
Absorption Coefficient (10**3 cm**-1)
879.7(11.37)
C

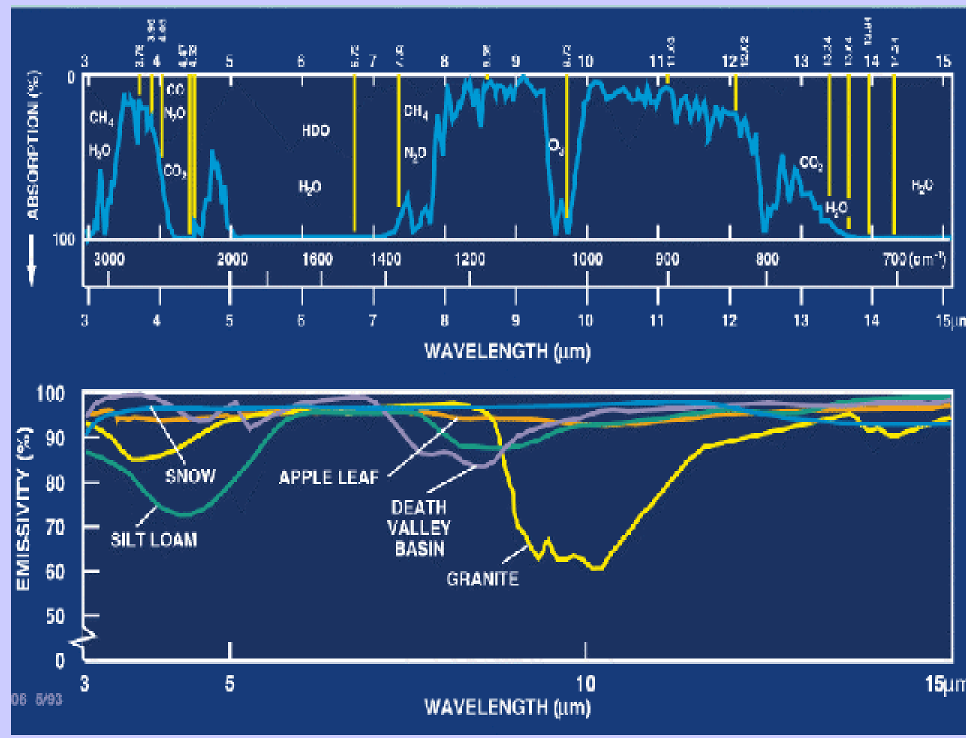
ABSORPTION (%)
CH4
H2O
CO
N2O
CO2
HDO
O3
WAVELENGTH (µm)
EMISSIVITY (%)
SNOW
APPLE LEAF
DEATH VALLEY BASIN
SILT LOAM
GRANITE
WAVELENGTH (µm)

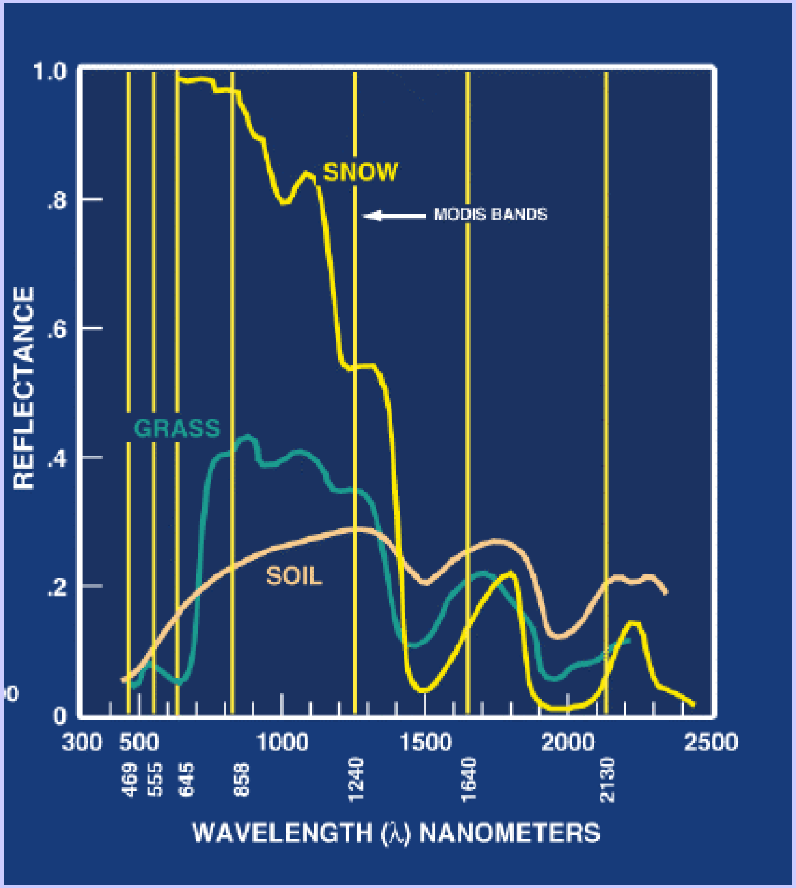

Investigating with Multi-spectral Combinations

Given the spectral response of a surface or atmospheric feature

Select a part of the spectrum where the reflectance or absorption changes with wavelength

e.g. reflection from snow/ice

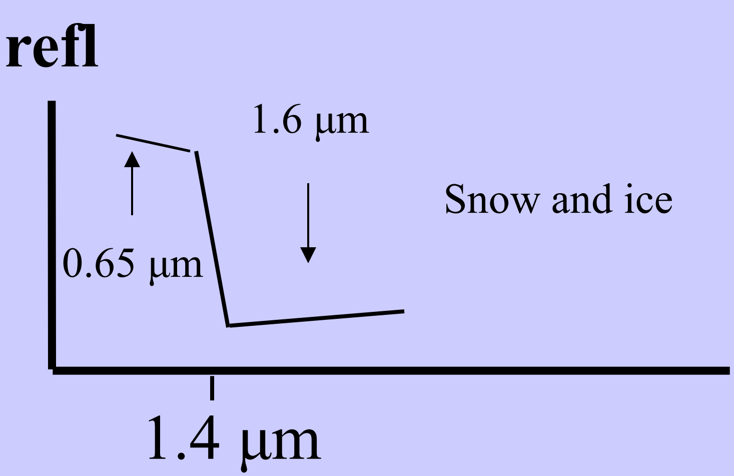

If 0.65 µm and 1.6 µm channels see the same reflectance than surface viewed is not snow;
if 1.6 µm sees considerably lower reflectance than 0.65 µm then surface might be snow

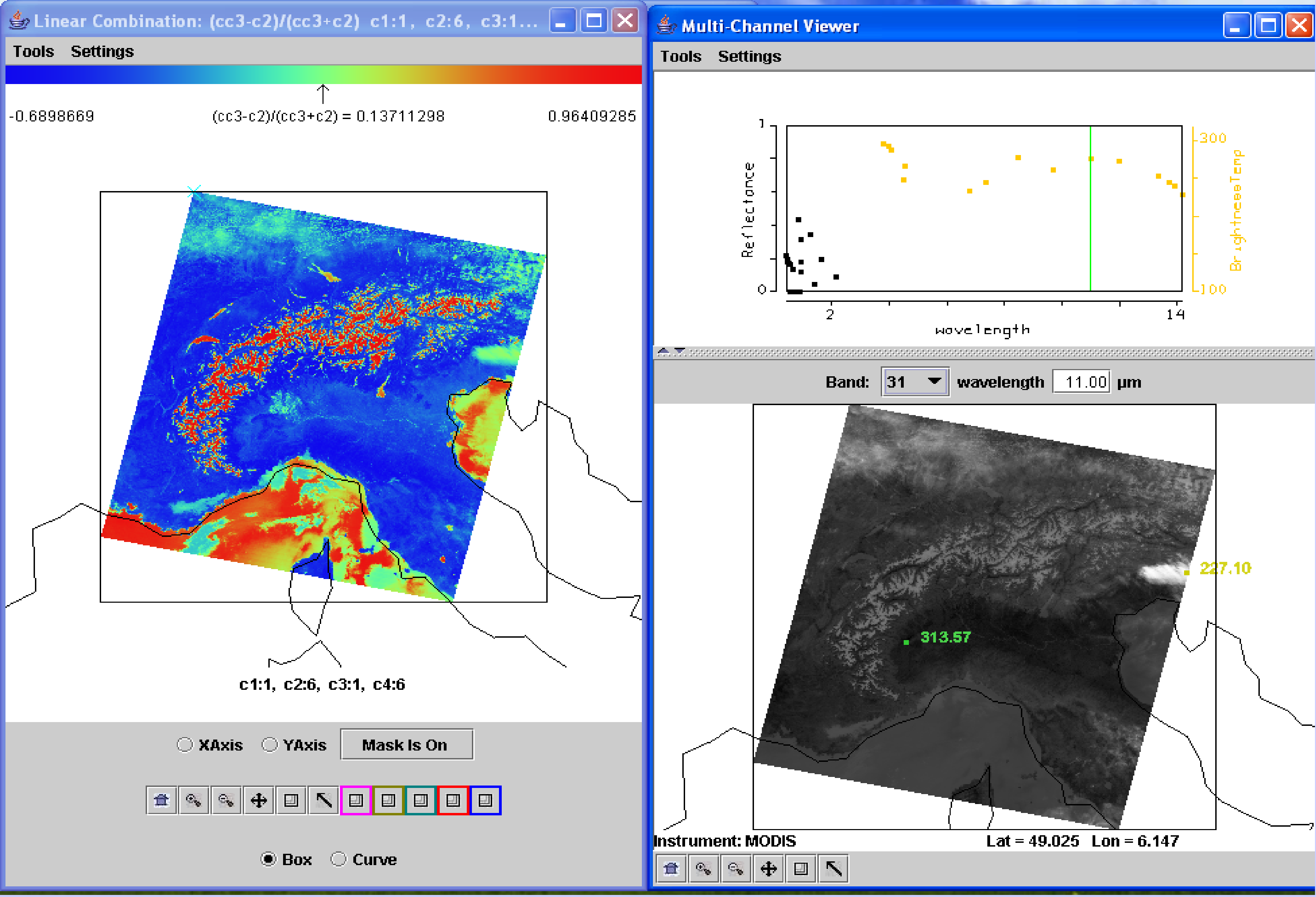

NDSI = [r0.6-r1.6]/[r0.6+r1.6] is near one in snow in Alps

Cloud Mask Tests

• BT11	threshold over ocean
• BT13.9	high clouds
• BT6.7	high clouds
• BT3.9-BT11	broken or scattered clouds
• BT11-BT12	high clouds in tropics
• BT8.6-BT11	ice clouds
• BT6.7-BT11	clouds in polar regions
• BT11+aPW(BT11-BT12)	clouds over ocean
• r0.65	clouds over land
• r0.85	clouds over ocean
• r1.38	thin cirrus
• r1.6	clouds over snow, ice cloud
• r0.85/r0.65	clouds over vegetation
• Sig(BT11)	clouds over ocean

12 channel SEVIRI

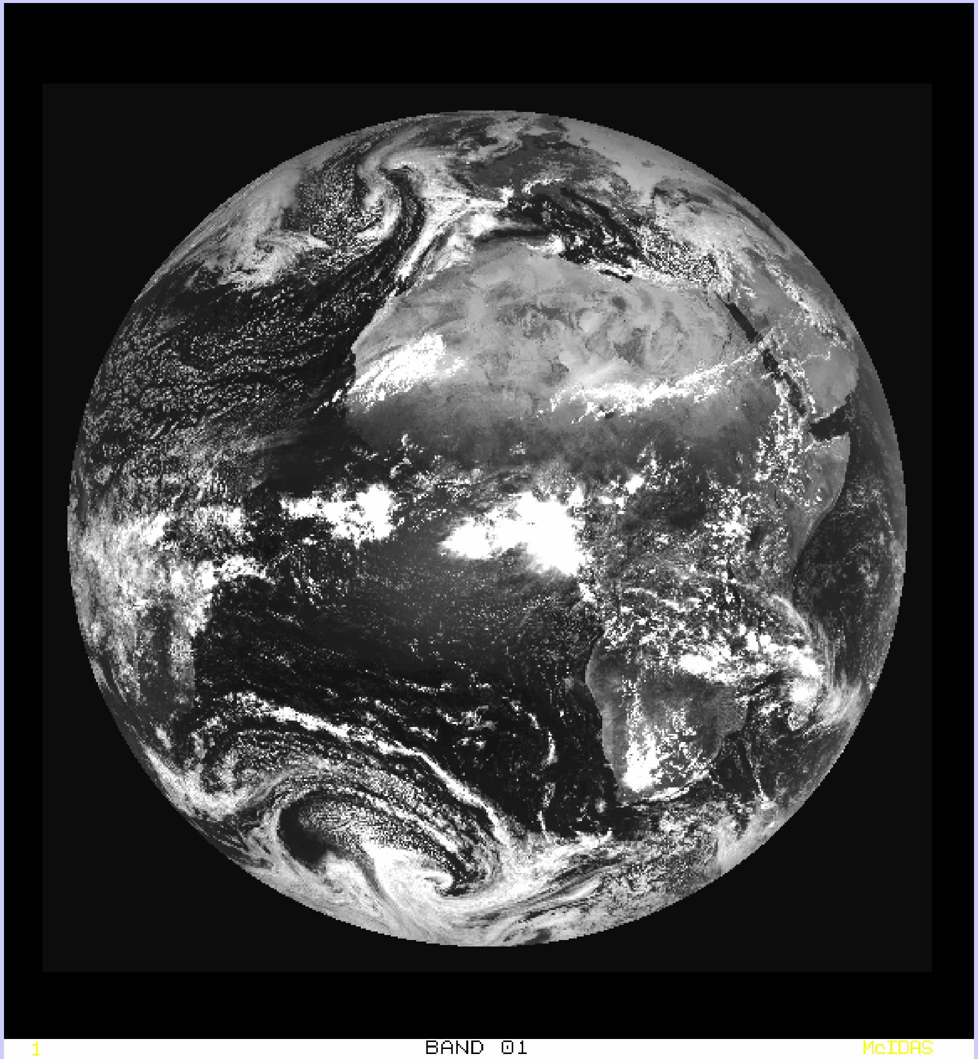

See image gallery at http://www.eumetsat.int/idcplg

Convective Initiation RGB 0.6-1.6-10.8 um

	Red VIS0.6	Green NIR1.6	Blue IR10.8	RGB
I. Very early stage yellow	255	255	200	white-light
II. First convection	255	255	100	yellow
III. First icing	255	200	0	orange
IV. Large icing	255	100	0	red-orange

First Icing

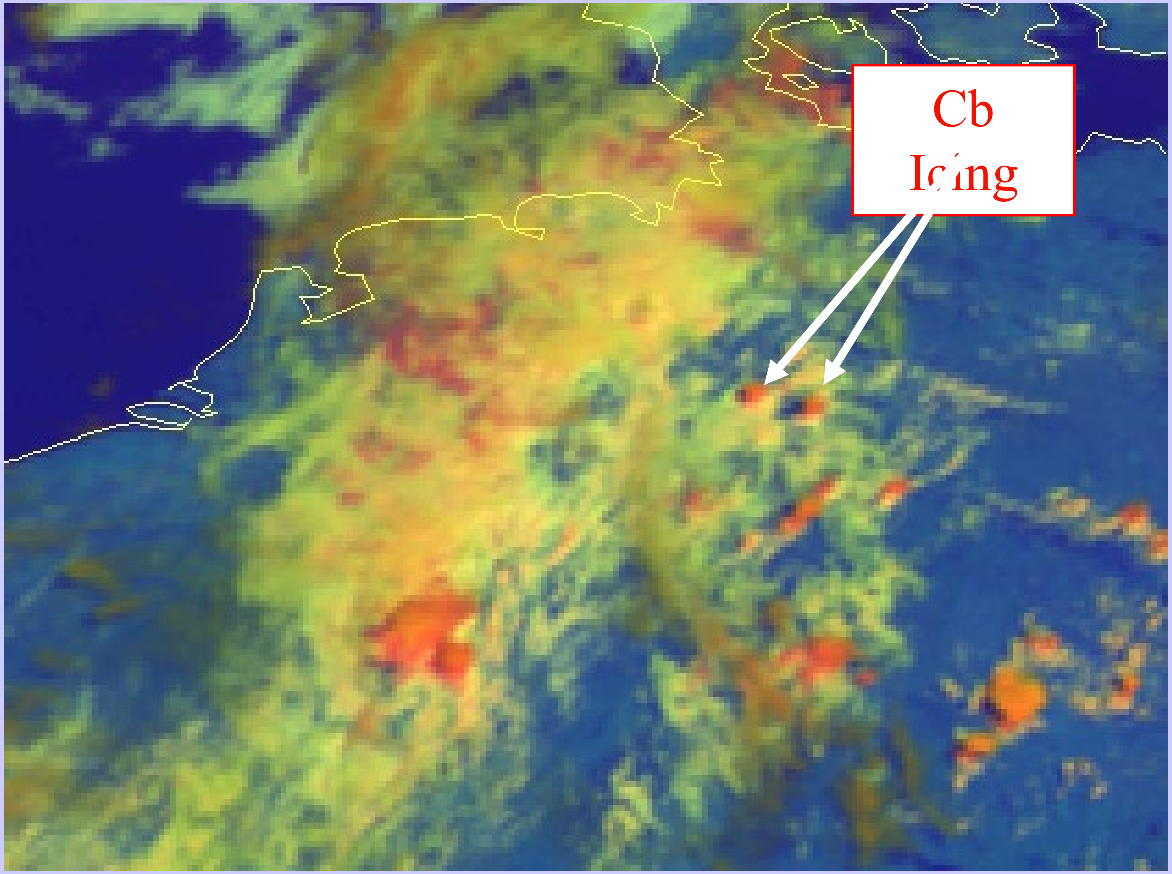

MSG-1, 5 June 2003, 10:30 UTC, RGB 01-03-09

Large Icing

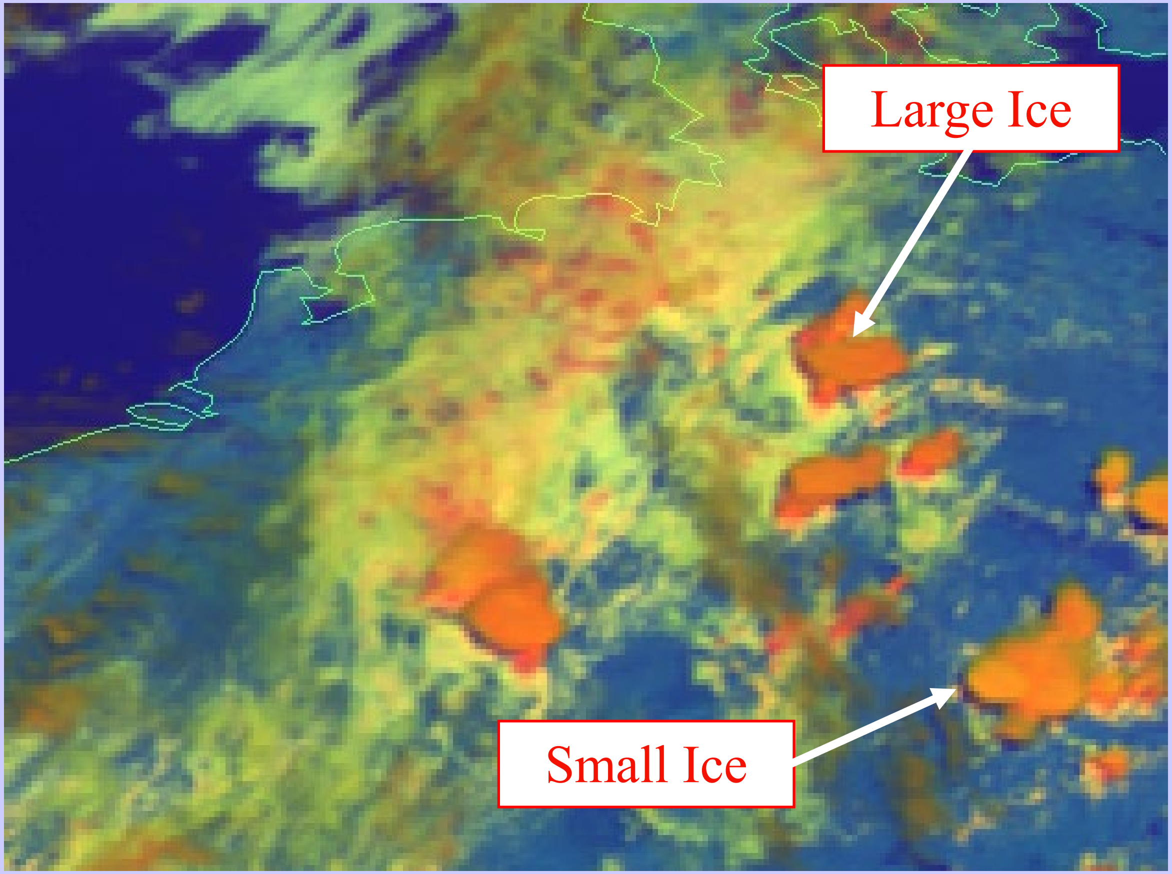

MSG-1, 5 June 2003, 11:30 UTC, RGB 01-03-09

Very Large Icing

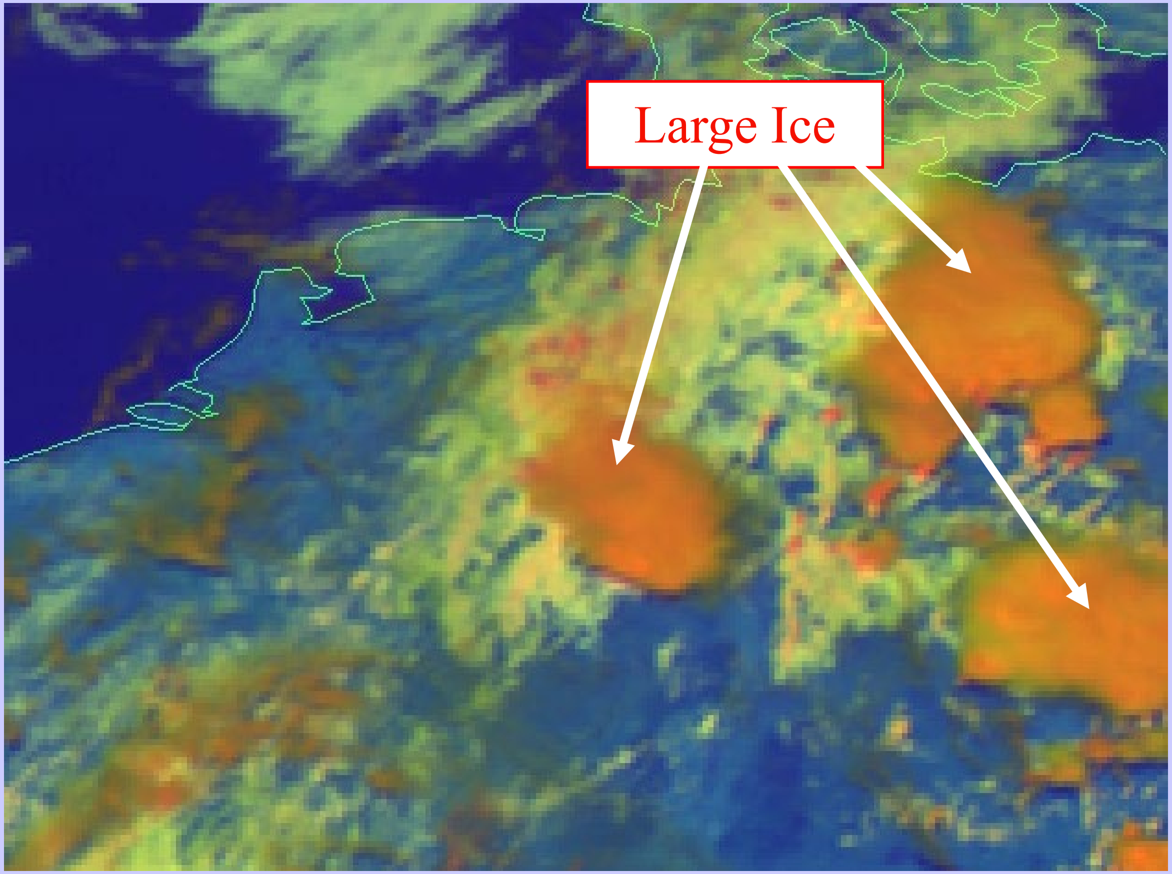

MSG-1, 5 June 2003, 13:30 UTC, RGB 01-03-09

SEVIRI sees dust storm over Africa

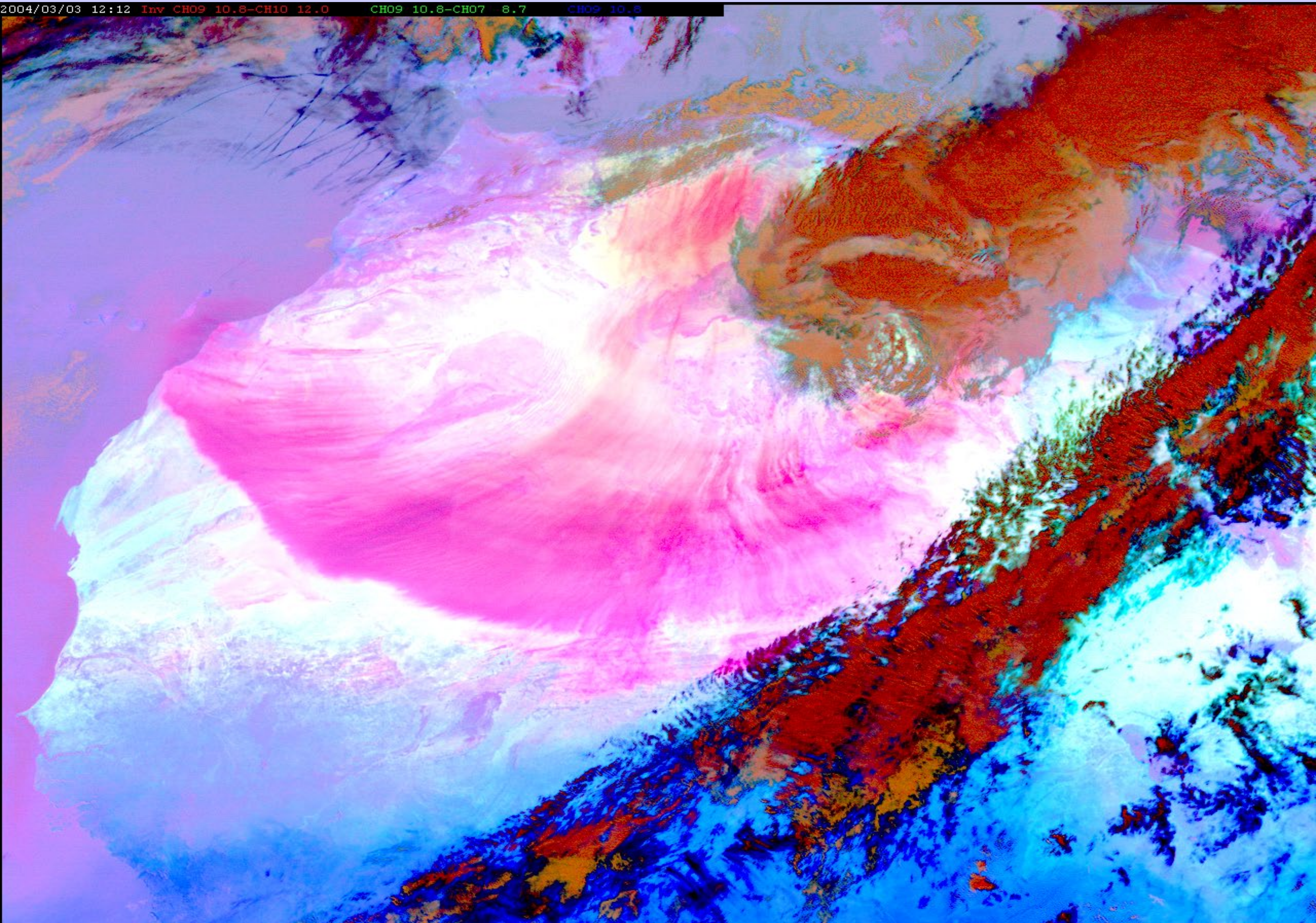

SEVIRI sees volcanic ash & SO2 and downwind inhibition of convection

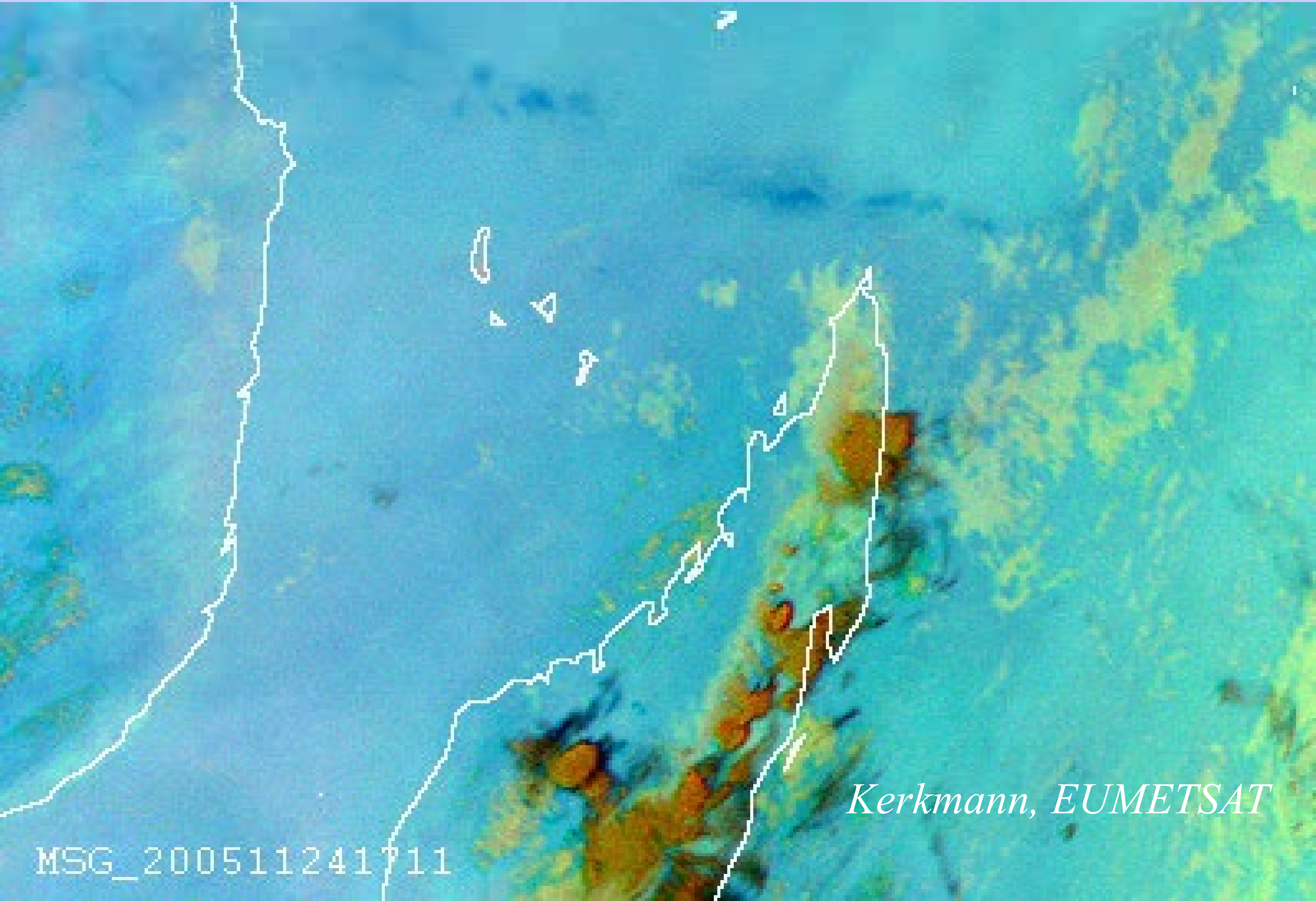

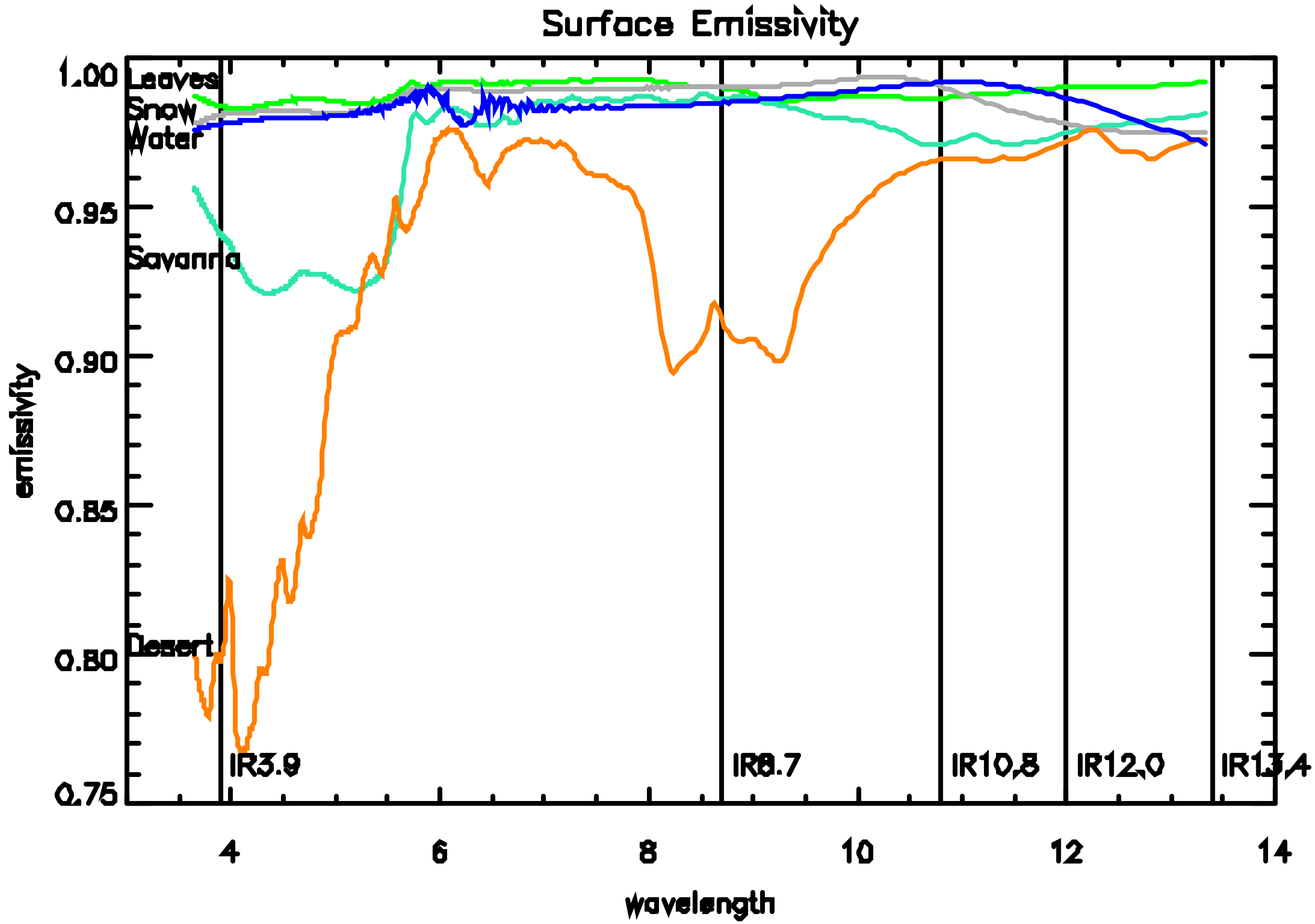

Surface Emissivity
Leaves
Snow
Water
Savanna
Desert
IR3.9
IR8.7
IR10.8
IR12.0
IR13.4
1.00
0.95
0.90
0.85
0.80
0.75
4
6
8
10
12
14
emissivity
wavelength

Dust and Cirrus Signals

Imaginary Index of Refraction of Ice and Dust

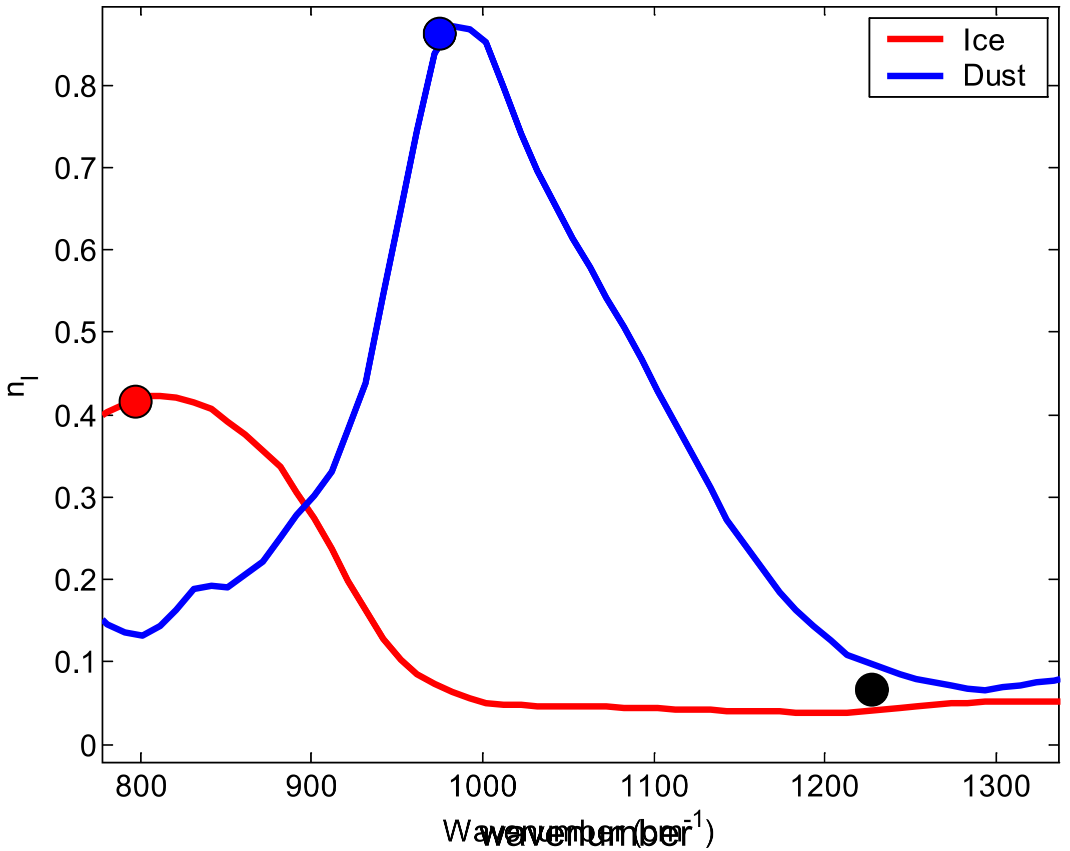

- Both ice and silicate absorption small in 1200 cm^{-1} window
- In the 800-1000 cm^{-1} atmospheric window:

  Silicate index *increases*

  Ice index *decreases*

  with wavenumber

Volz, F.E. : Infrared optical constant of ammonium sulphate, Sahara Dust, volcanic pumice and flash, Appl Opt 12 564-658 (1973)

MODIS IR Spectral Bands

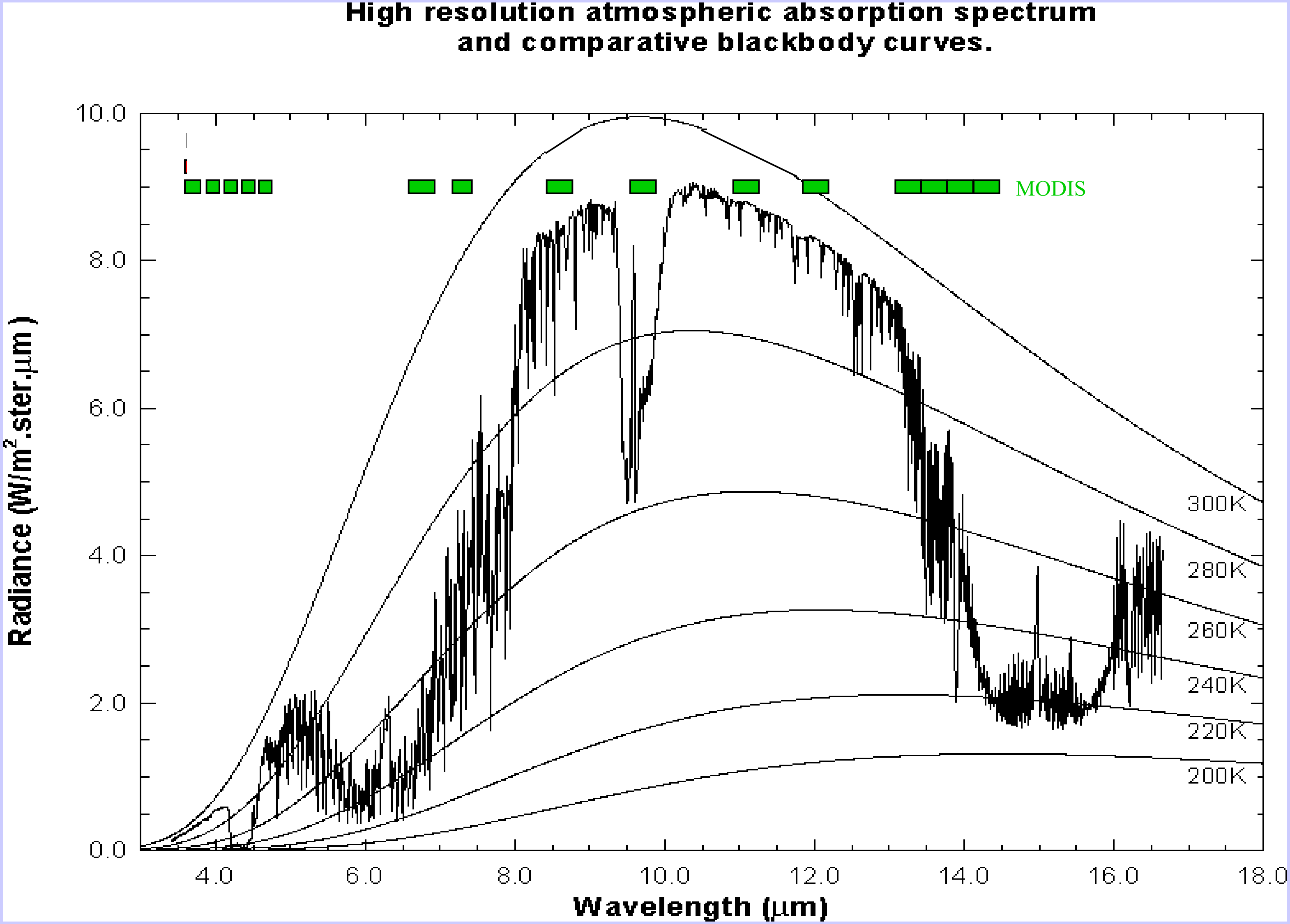

Vibrational Lines

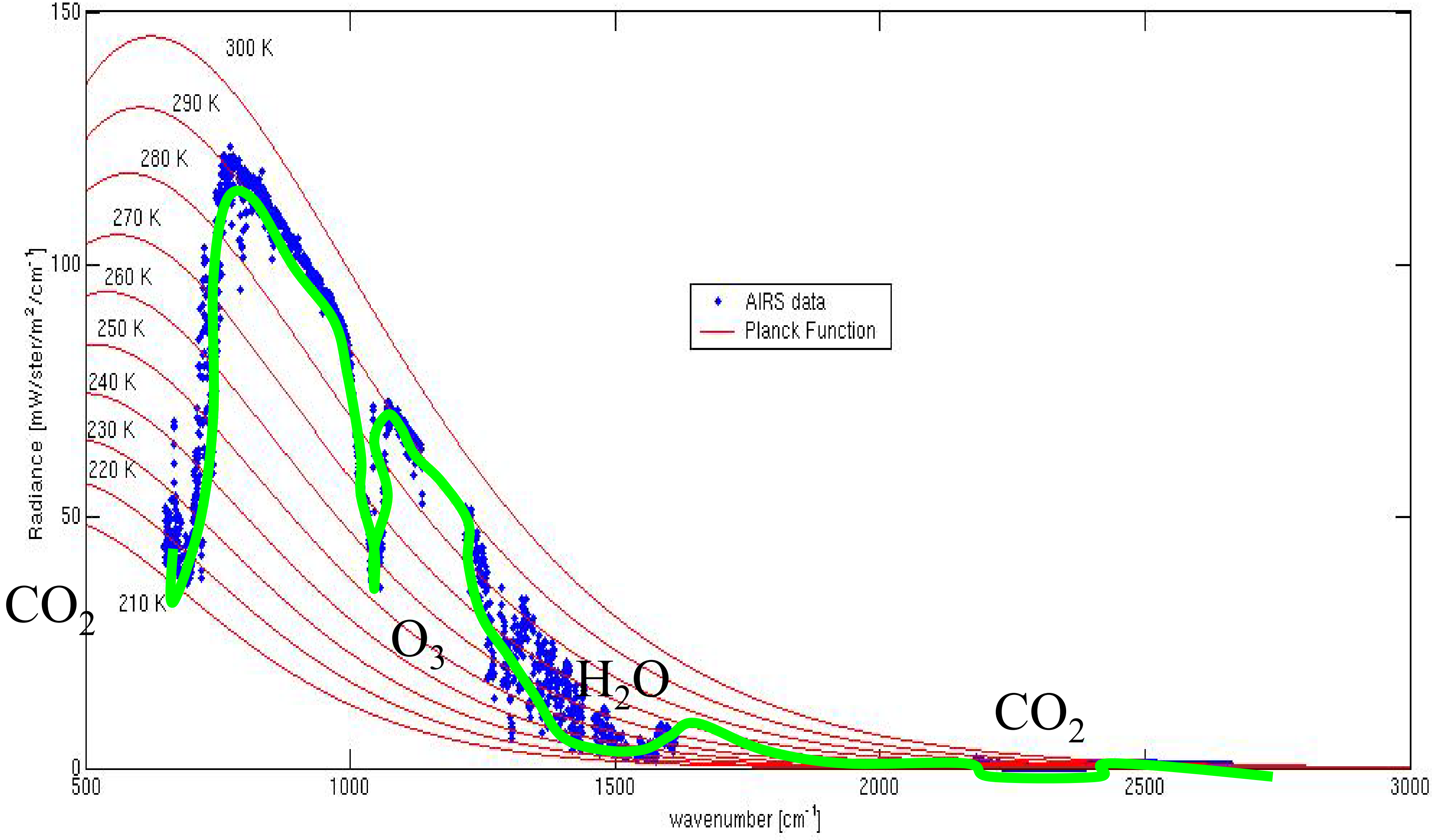

Rotational Lines

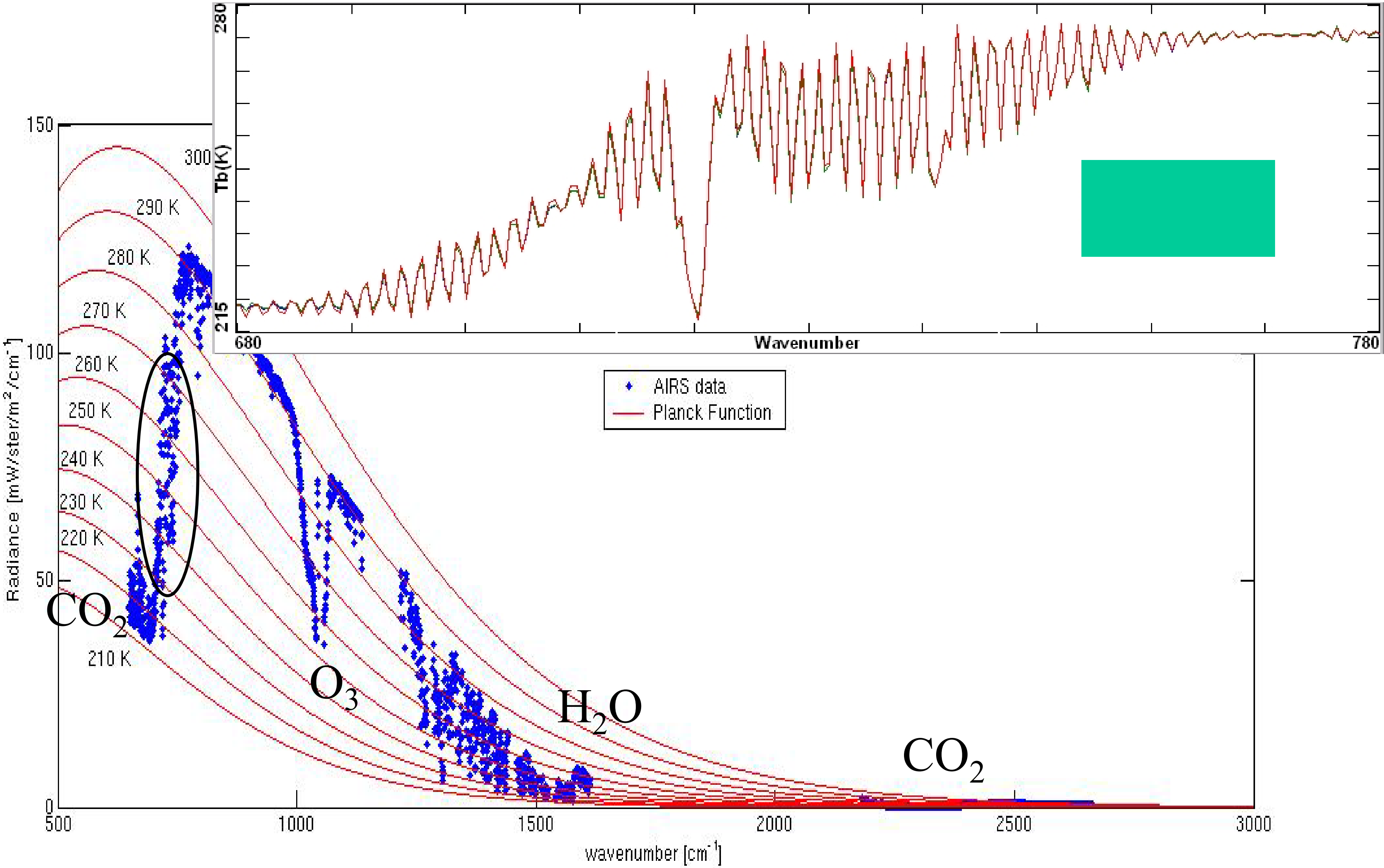

GOES Sounder Spectral Bands: 14.7 to 3.7 um and vis

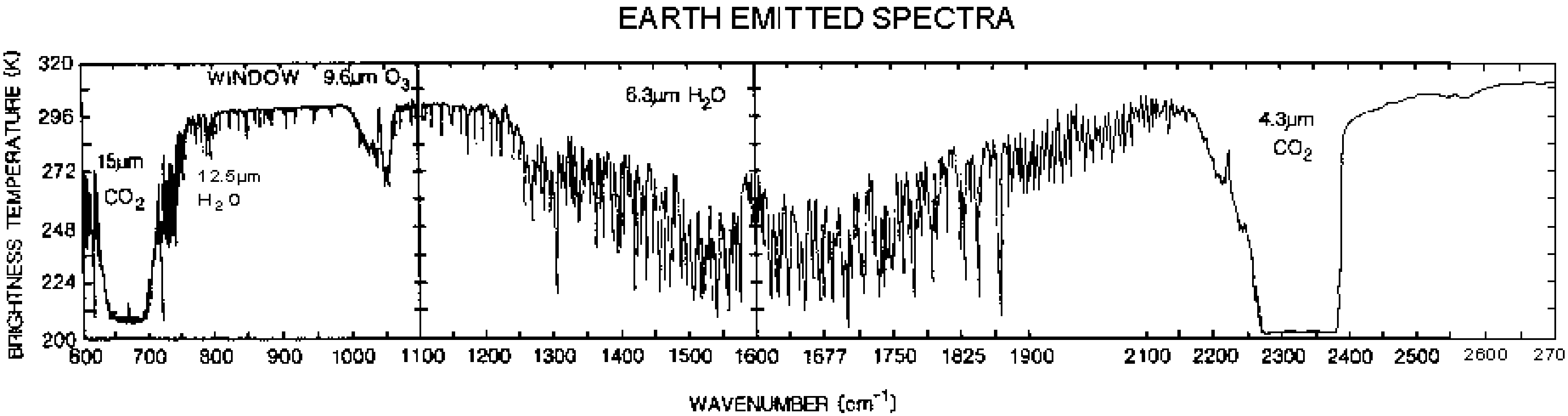

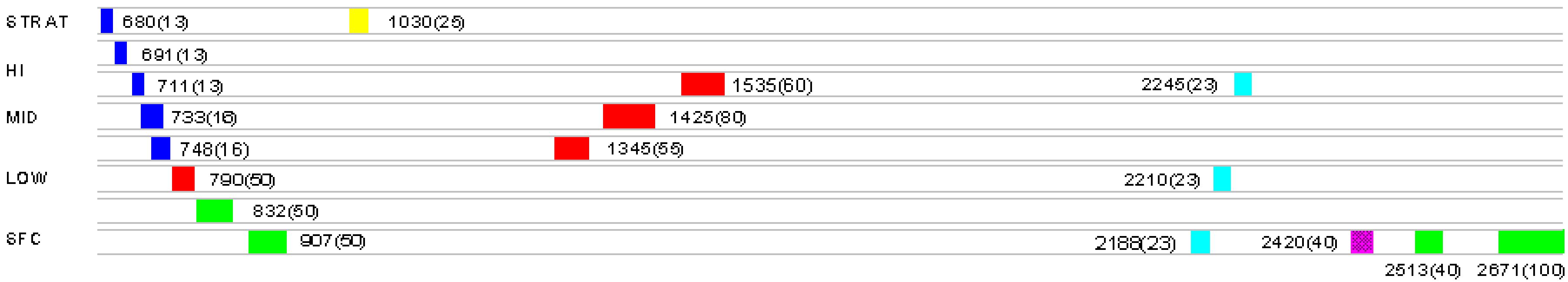

GOES-I SOUNDER SPECTRAL BANDS

COOPERATIVE INSTITUTE FOR METEOROLOGICAL SATELLITE STUDIES

Radiative Transfer through the Atmosphere

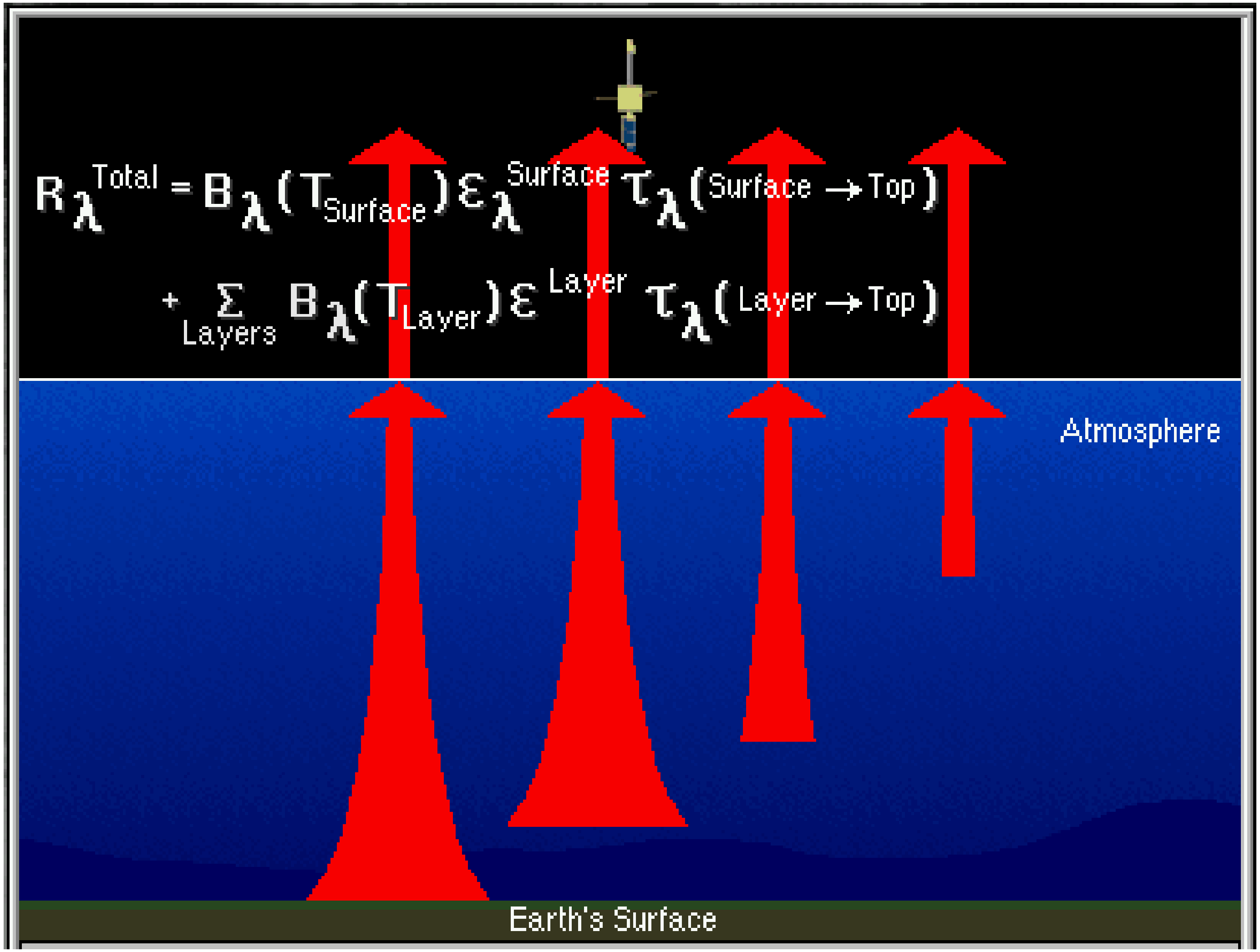

line broadening with pressure helps to explain weighting functions

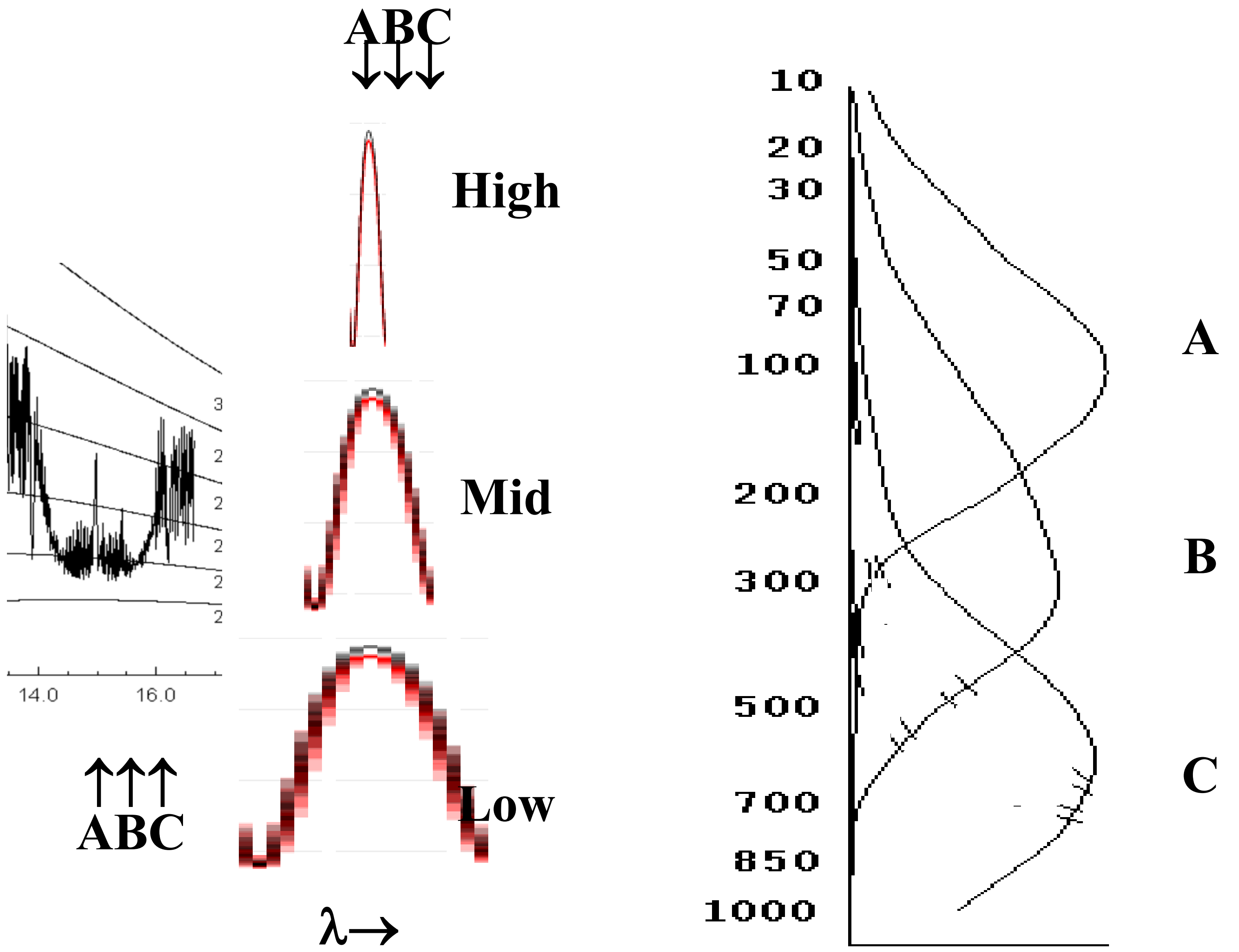

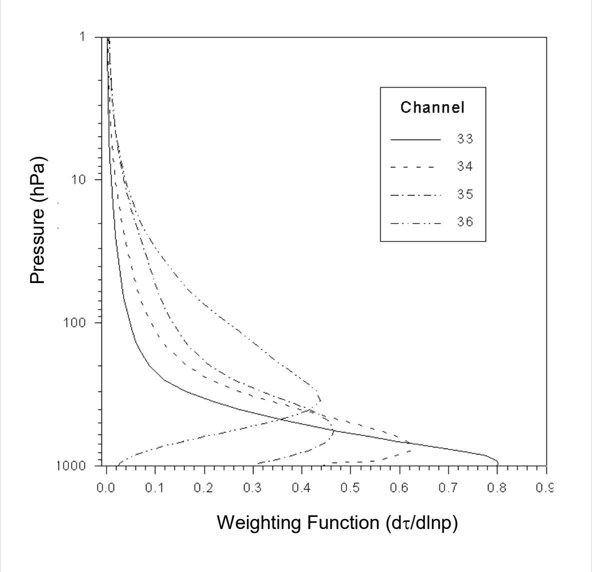

CO_2 channels see different layers in the atmosphere

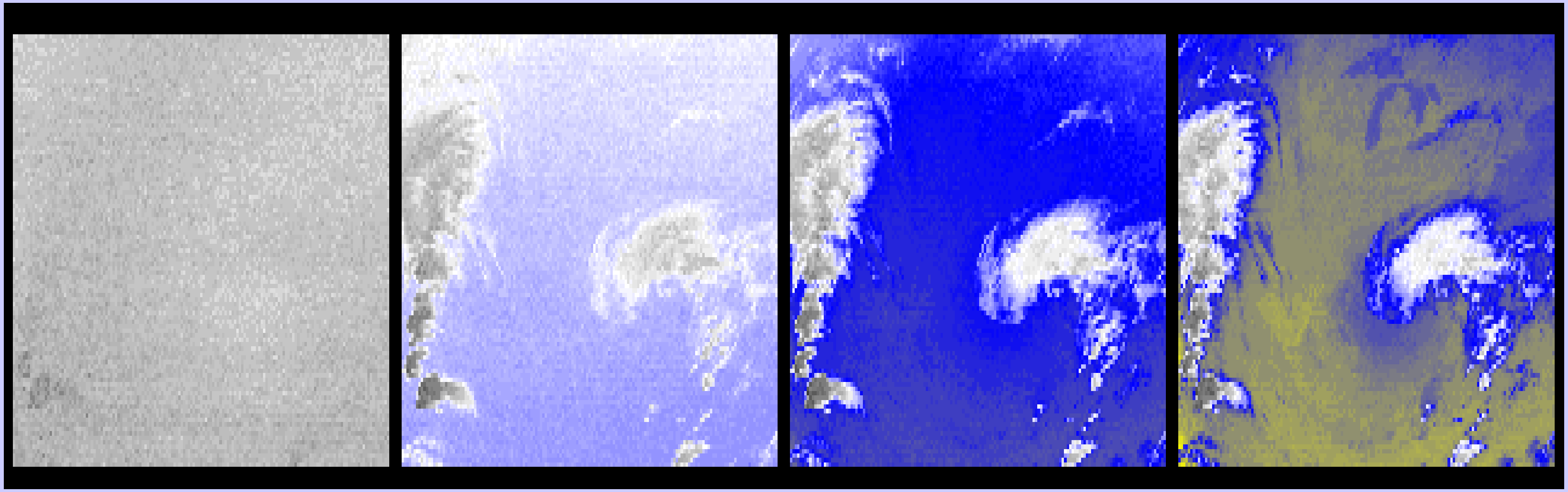

14.2 um | 13.9 um | 13.6 um | 13.3 um

Radiative Transfer Equation

When reflection from the earth surface is also considered, the RTE for infrared radiation can be written

$$I_\lambda = \varepsilon_\lambda^{sfc} B_\lambda(T_s)\, \tau_\lambda(p_s) + \int_{p_s}^{o} B_\lambda(T(p))\, F_\lambda(p)\, [d\tau_\lambda(p)/ dp]\, dp$$

where

$$F_\lambda(p) = \{ 1 + (1 - \varepsilon_\lambda)\, [\tau_\lambda(p_s) / \tau_\lambda(p)]^2 \}$$

The first term is the spectral radiance emitted by the surface and attenuated by the atmosphere, often called the boundary term and the second term is the spectral radiance emitted to space by the atmosphere directly or by reflection from the earth surface.

The atmospheric contribution is the weighted sum of the Planck radiance contribution from each layer, where the weighting function is [$d\tau_\lambda(p) / dp$]. This weighting function is an indication of where in the atmosphere the majority of the radiation for a given spectral band comes from.

MODIS TPW

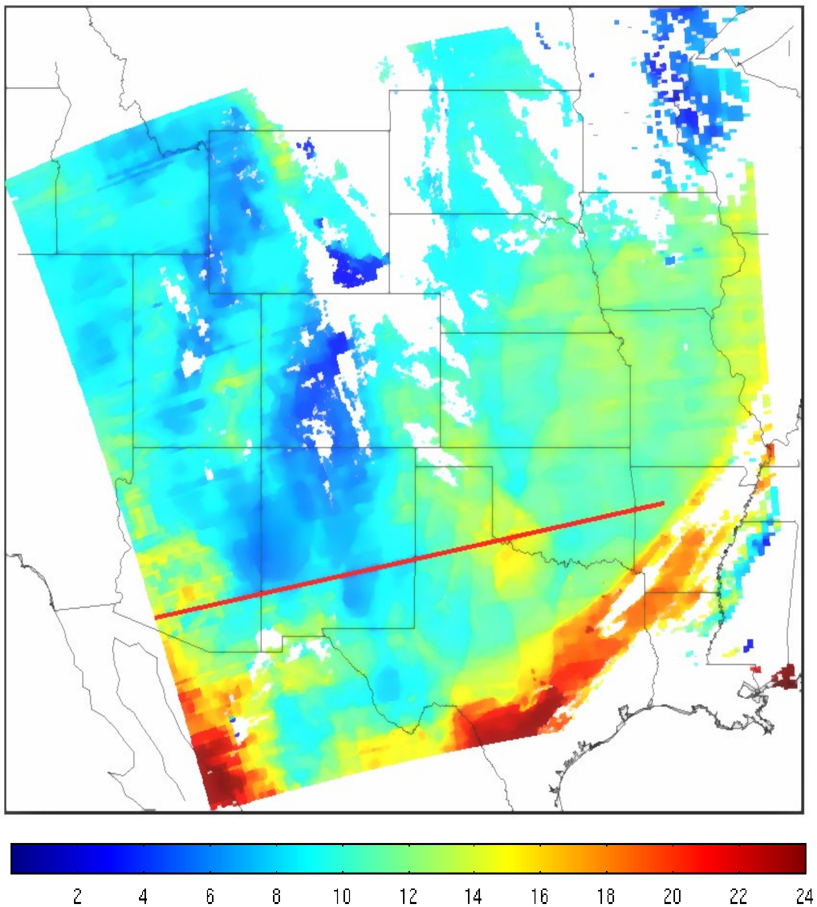

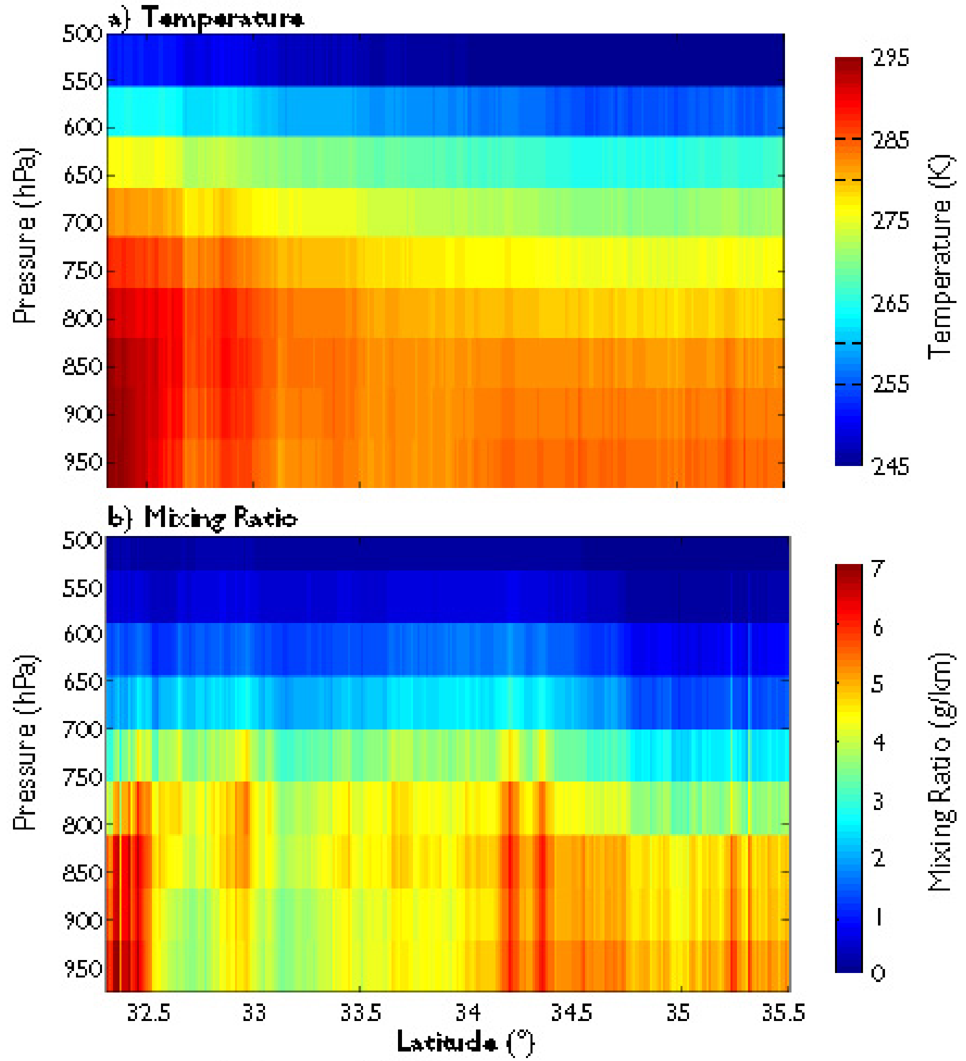

Clear sky layers of temperature and moisture on 2 June 2001

RTE in Cloudy Conditions

$$I_\lambda = \eta I^{cd}_\lambda + (1 - \eta) I^c_\lambda$$ where cd = cloud, c = clear, η = cloud fraction

$$I^c_\lambda = B_\lambda(T_s)\, \tau_\lambda(p_s) + \int_{p_s}^{o} B_\lambda(T(p))\, d\tau_\lambda \,.$$

$$I^{cd}_\lambda = (1-\varepsilon_\lambda)\, B_\lambda(T_s)\, \tau_\lambda(p_s) + (1-\varepsilon_\lambda) \int_{p_s}^{p_c} B_\lambda(T(p))\, d\tau_\lambda$$

$$+ \varepsilon_\lambda B_\lambda(T(p_c))\, \tau_\lambda(p_c) + \int_{p_c}^{o} B_\lambda(T(p))\, d\tau_\lambda$$

ε_λ is emittance of cloud. First two terms are from below cloud, third term is cloud contribution, and fourth term is from above cloud. After rearranging

$$I_\lambda - I_\lambda{}^c = \eta\varepsilon_\lambda \int_{p_s}^{p_c} \tau(p) \frac{dB_\lambda}{dp}\, dp \,.$$

Techniques for dealing with clouds fall into three categories: (a) searching for cloudless fields of view, (b) specifying cloud top pressure and sounding down to cloud level as in the cloudless case, and (c) employing adjacent fields of view to determine clear sky signal from partly cloudy observations.

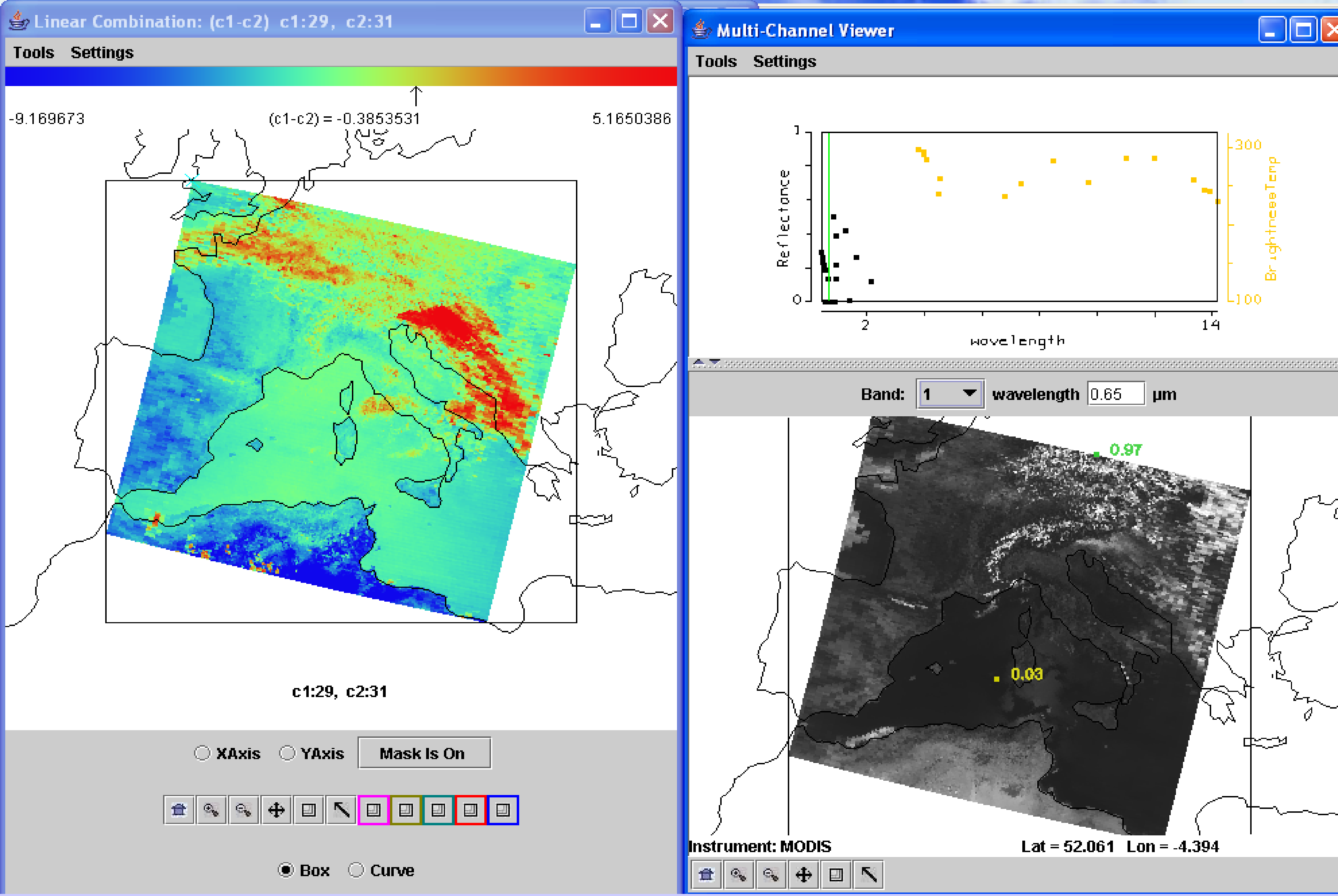

Ice clouds are revealed with BT8.6-BT11>0 & water clouds and fog show in r0.65

Cloud Properties

RTE for cloudy conditions indicates dependence of cloud forcing (observed minus clear sky radiance) on cloud amount ($\eta\varepsilon_\lambda$) and cloud top pressure (p_c)

$$(I_\lambda - I_\lambda^{clr}) = \eta\varepsilon_\lambda \int_{p_s}^{p_c} \tau_\lambda \, dB_\lambda \, .$$

Higher colder cloud or greater cloud amount produces greater cloud forcing; dense low cloud can be confused for high thin cloud. Two unknowns require two equations.

p_c can be inferred from radiance measurements in two spectral bands where cloud emissivity is the same. $\eta\varepsilon_\lambda$ is derived from the infrared window, once p_c is known. This is the essence of the CO2 slicing technique.

Cloud Clearing

For a single layer of clouds, radiances in one spectral band vary linearly with those of another as cloud amount varies from one field of view (fov) to another

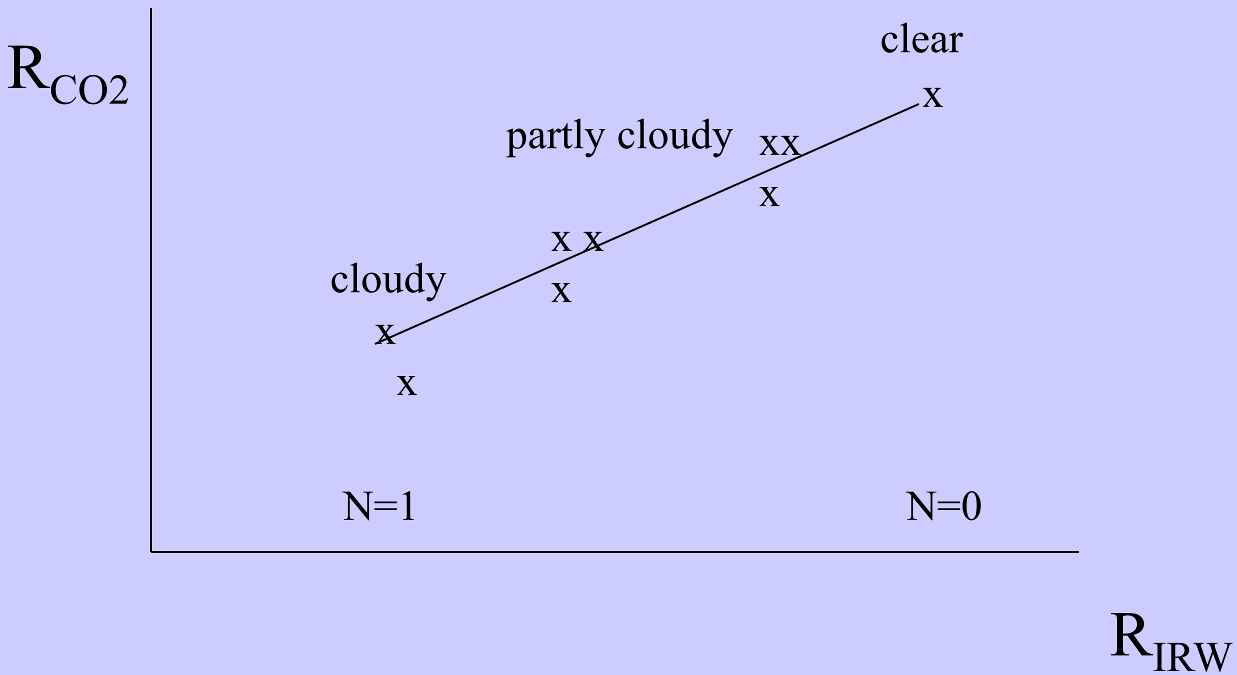

Clear radiances can be inferred by extrapolating to cloud free conditions.

Moisture

Moisture attenuation in atmospheric windows varies linearly with optical depth.

$$\tau_\lambda = e^{-k_\lambda u} = 1 - k_\lambda u$$

For same atmosphere, deviation of brightness temperature from surface temperature is a linear function of absorbing power. Thus moisture corrected SST can inferred by using split window measurements and extrapolating to zero k_λ

Moisture content of atmosphere inferred from slope of linear relation.

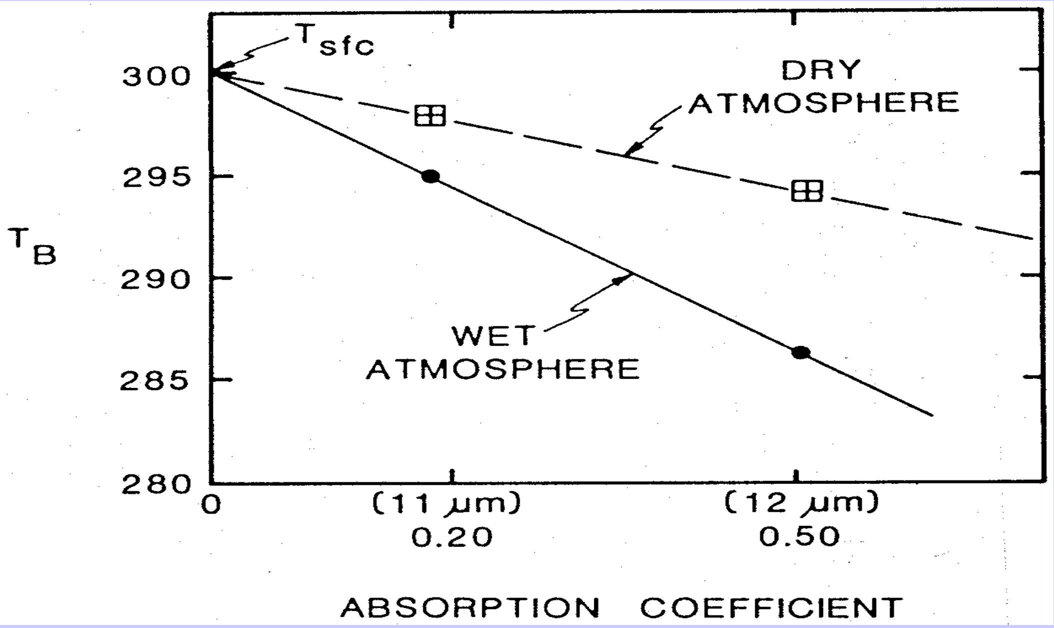

Spectral Separation with a Prism: longer wavelengths deflected less

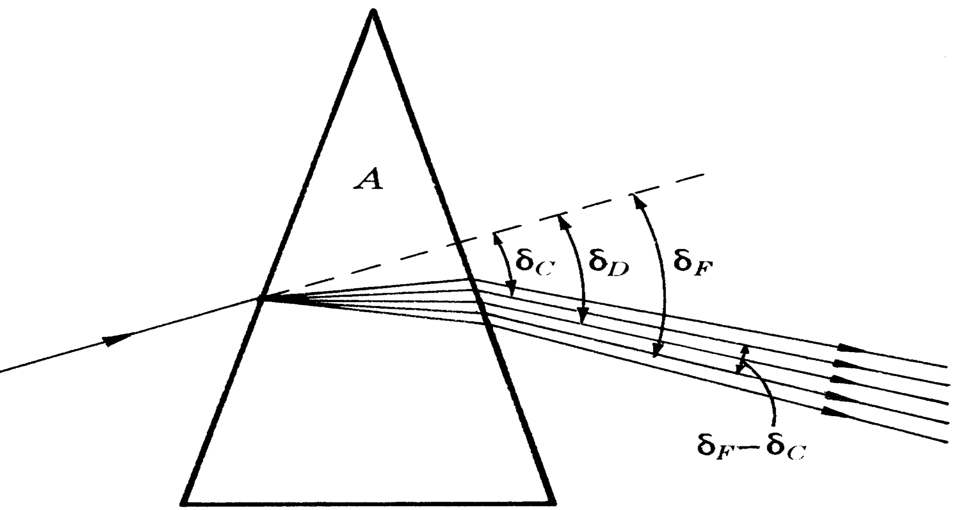

Spectral Separation with a Grating: path difference from slits produces positive and negative wavelet interference on screen

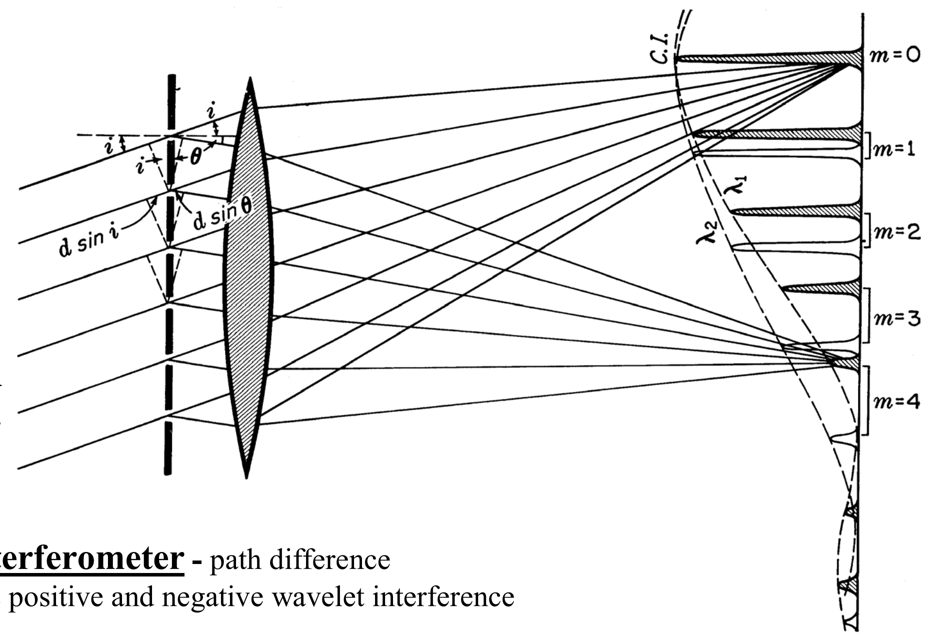

Spectral Separation with an Interferometer - path difference (or delay) from two mirrors produces positive and negative wavelet interference

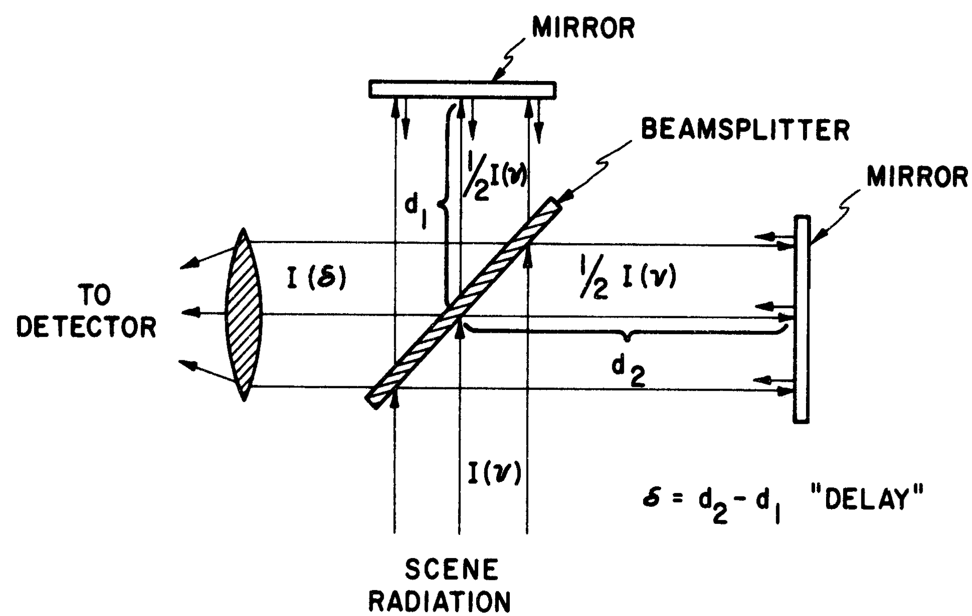

MODIS Instrument Overview

- 36 spectral bands (490 detectors) cover wavelength range from 0.4 to 14.5 μm
- Spatial resolution at nadir: 250m (2 bands), 500m (5 bands) and 1000m
- 4 FPAs: VIS, NIR, SMIR, LWIR
- On-Board Calibrators: SD/SDSM, SRCA, and BB (plus space view)
- 12 bit (0-4095) dynamic range
- 2-sided Paddle Wheel Scan Mirror scans 2330 km swath in 1.47 sec
- Day data rate = 10.6 Mbps; night data rate = 3.3 Mbps (100% duty cycle, 50% day and 50% night)

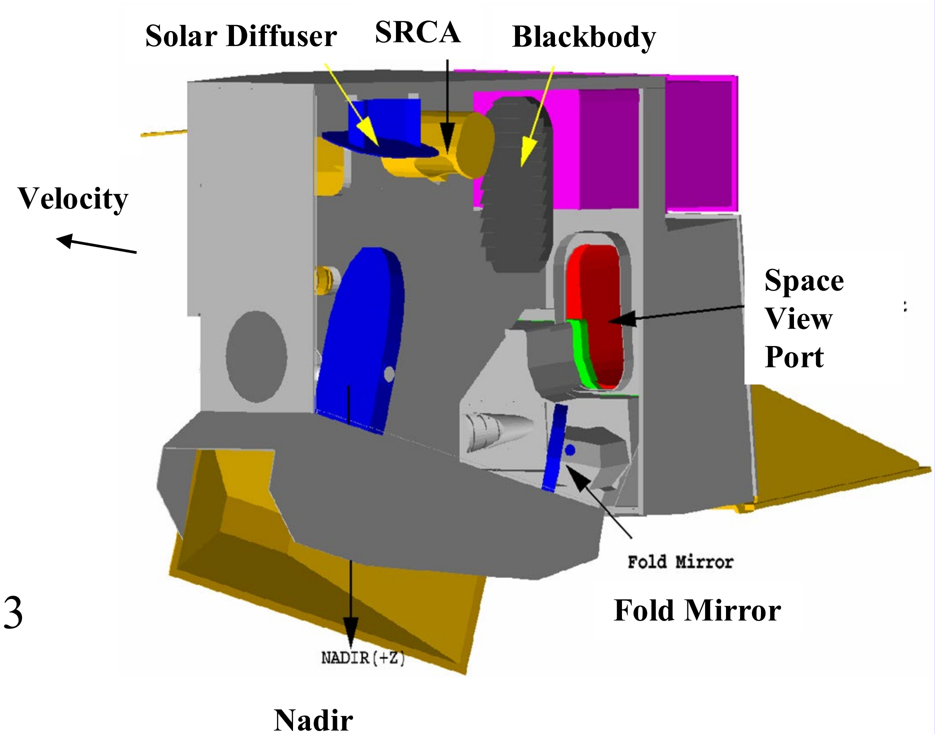

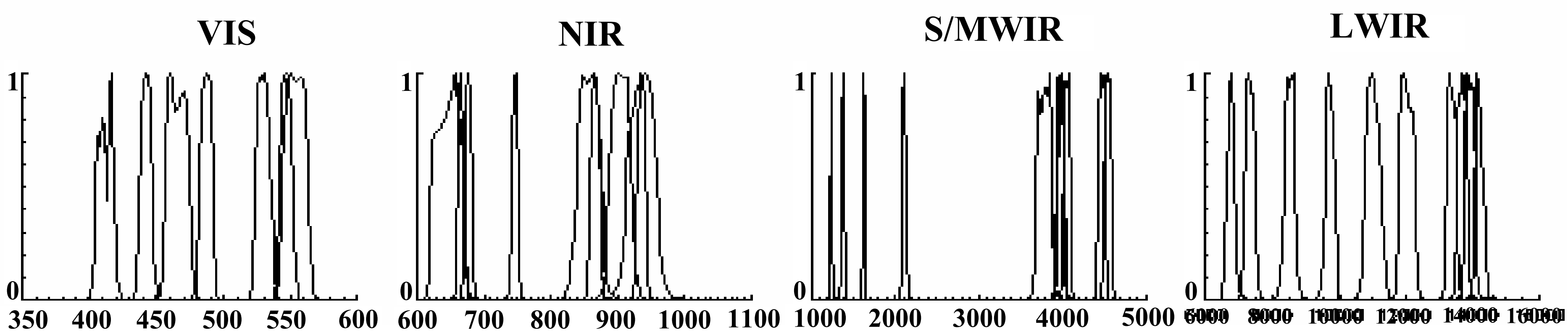

MODIS Performance

Performance Issue	Terra	Aqua
Band 26 Striping and elevated background signal	Correction in L1B now in place for Collect 4.	No Improvement Correction will be necessary
S/MWIR Electronic Crosstalk	An ongoing issue No on-orbit correction	Improved (reduced but not eliminated)
PC LWIR Band Optical Leak	Corrected in L1B; 1-2% uncertainty	Fixed during prelaunch
Detector Striping	Exists in several thermal IR bands. EDF algorithm now available	Improved, but still present. EDF algorithm now available.

MODIS Performance
cont.

Performance Issue	Terra	Aqua
5um thermal leak into SWIR	Small influence; Effectively Corrected in L1B	Improved; Correction in L1B TBD
SWIR Band Subsample Departure	On going issue No on-orbit correction	Much Improved
Noisy Detectors	Several in LWIR CO2 bands, one in B24, 25, 27, 28,30	Much Improved (B36 chan 5)
Saturation in Band 2	Saturation on thick water cloud, sunglint regions	Slightly Worse (lower saturation level)

MODIS Performance
cont.

Performance Issue	Terra	Aqua
Scan Mirror reflectance vs. angle of incidence	Much Improved after Deep Space Maneuver	Much Improved Good prelaunch characterization
Dead detectors in SWIR bands	None	B6 severely impacted; B5 has one dead detector

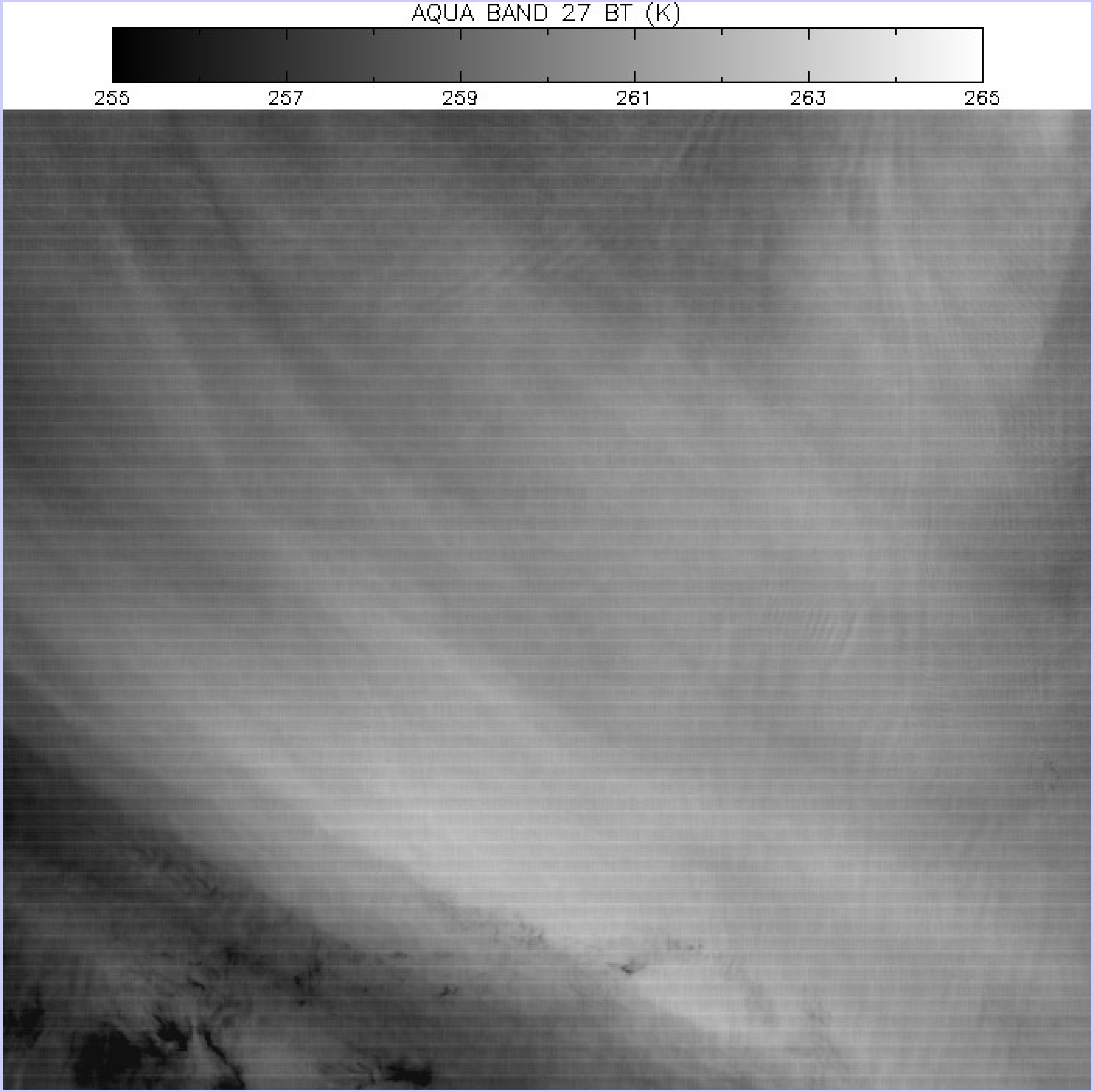
AQUA BAND 27 BT (K)
255
257
259
261
263
265

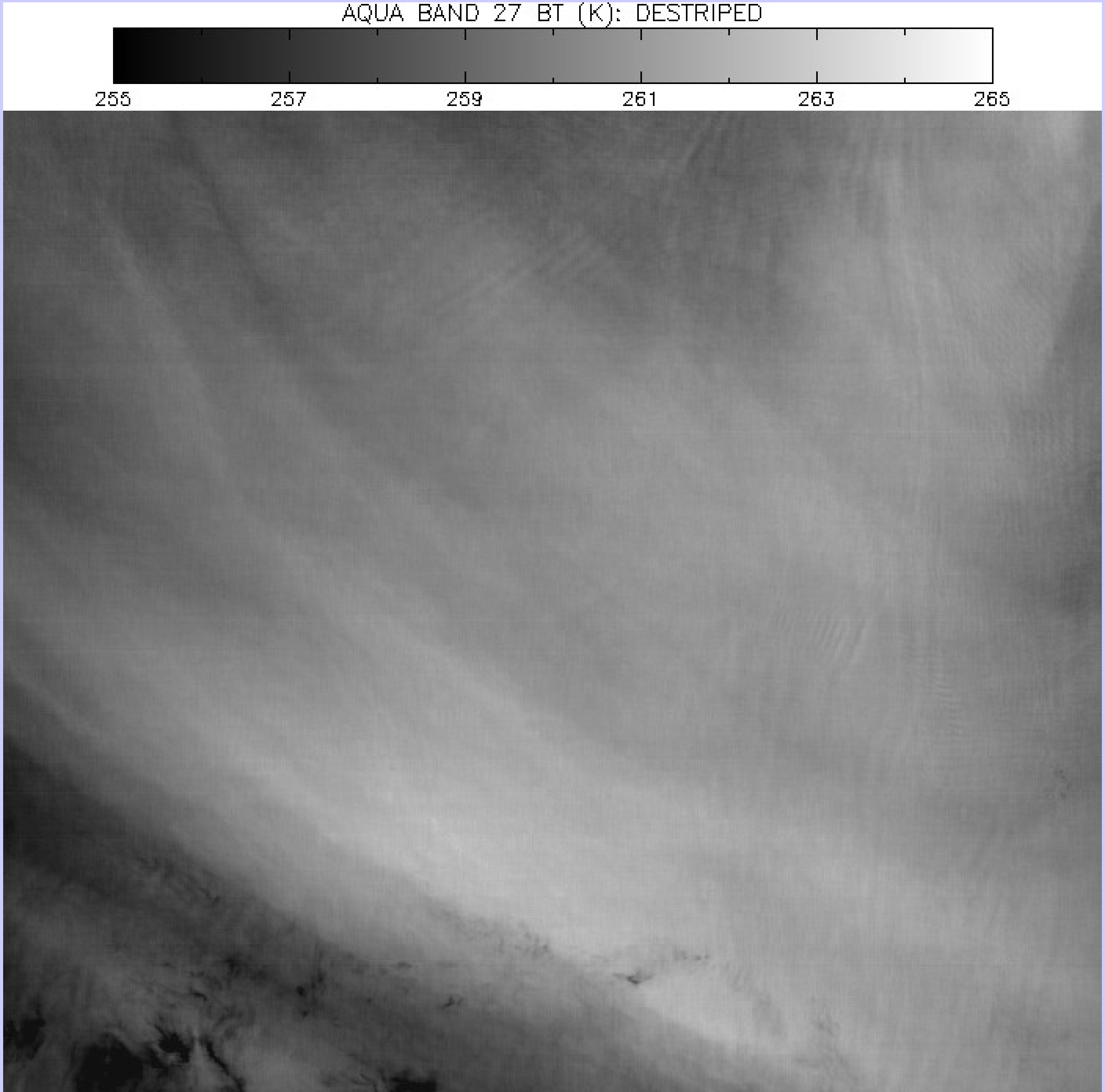
AQUA BAND 27 BT (K): DESTRIPED
255
257
259
261
263
265

temperature weighting functions sorted by pressure of their peak (blue = 0)

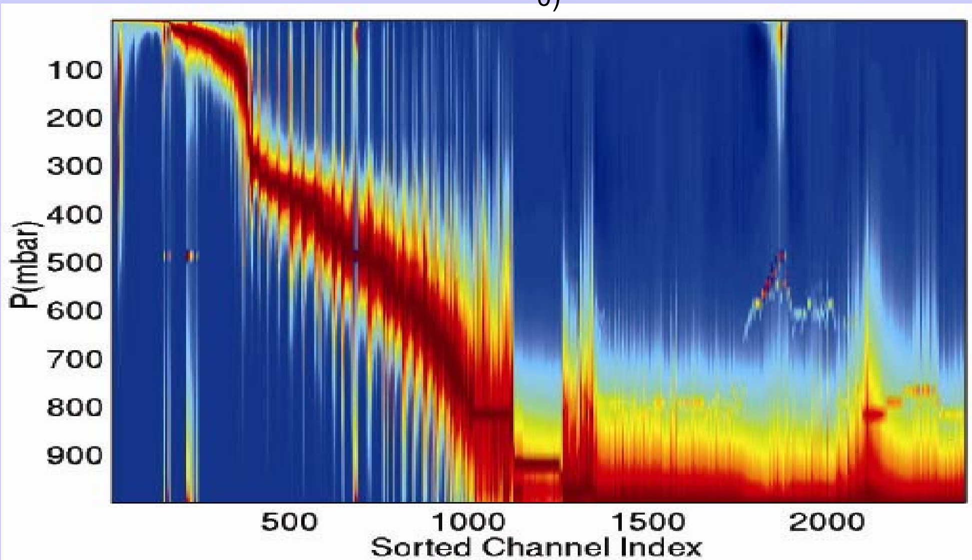

AIRS On Aqua

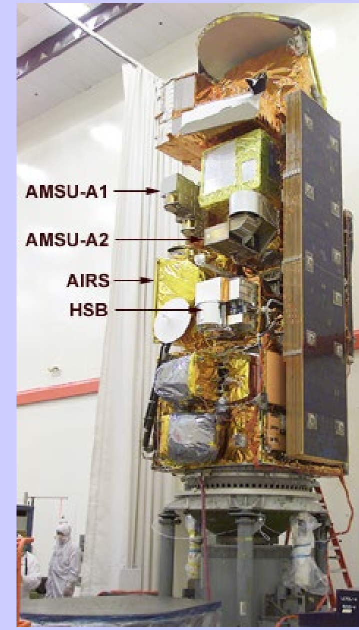

Instrument

- Hyperspectral radiometer with **resolution of 0.5 – 2 cm^{-1}**
- Extremely well calibrated pre-launch
- **Spectral range: 650 – 2700 cm^{-1}**
- Associated microwave instruments (AMSU, HSB)

Design

- Grating Spectrometer passively cooled to 160K, stabilized to 30 mK
- **PV and PC HdCdTe focal plane cooled to 60K** with redundant active pulse tube cryogenic coolers
- **Focal plane has ~5000 detectors,** 2378 channels. PV detectors (all below 13 microns) are doubly redundant. Two channels per resolution element (n/Dn = 1200)
- 310 K Blackbody and space view provides radiometric calibration
- Paralyene coating on calibration mirror and upwelling radiation provides spectral calibration
- **NEDT (per resolution element) ranges from 0.05K to 0.5K**

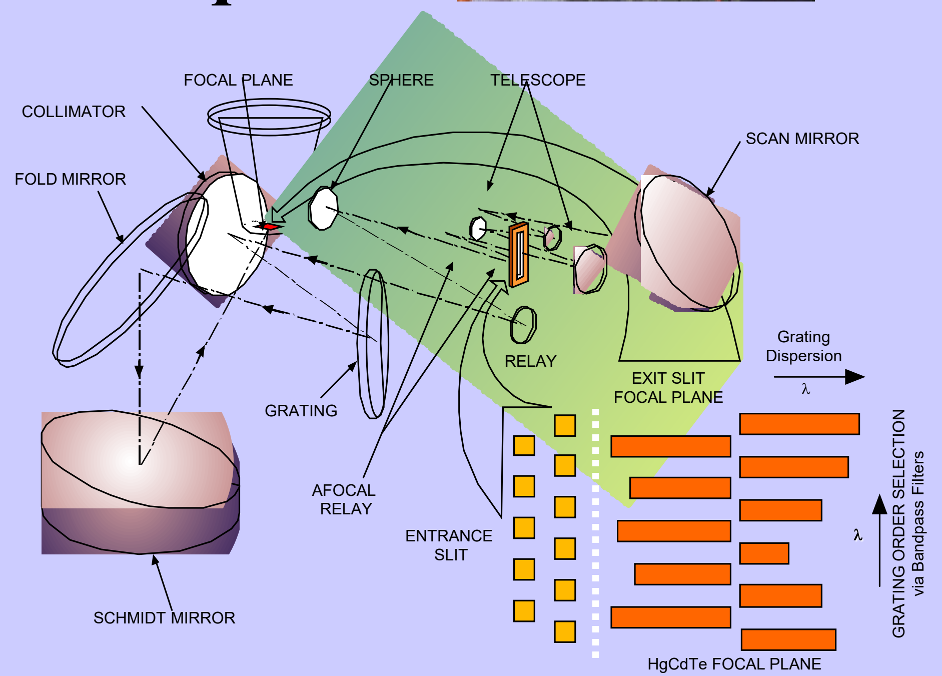

Spectral filters at each entrance slit and over each FPA array isolate color band (grating order) of interest

AIRS data from 28 Aug 2005

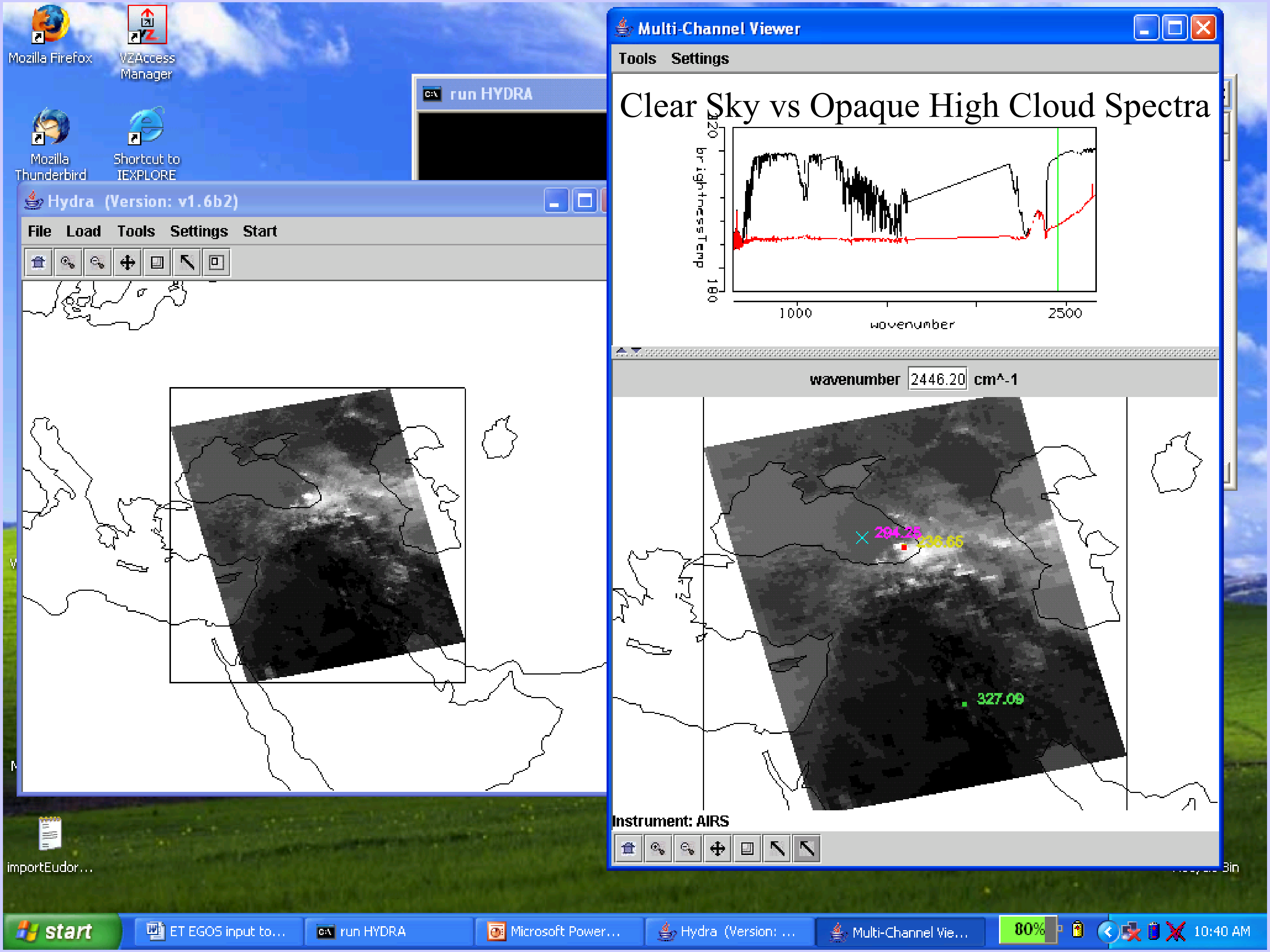

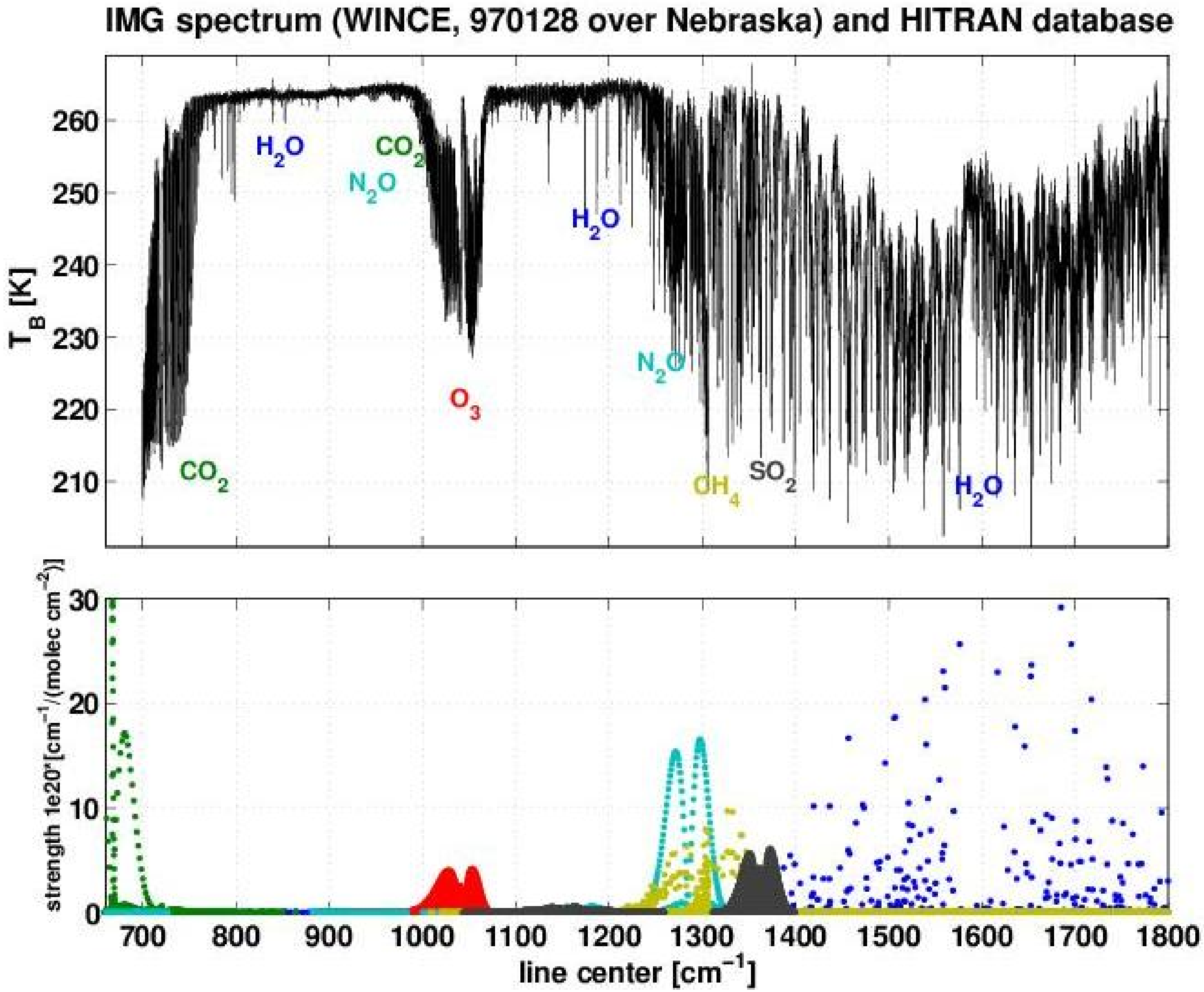

IMG spectrum (WINCE, 970128 over Nebraska) and HITRAN database
T_B [K]
260
250
240
230
220
210
H2O
CO2
N2O
H2O
N2O
O3
CO2
CH4
SO2
H2O
strength 1e20*[cm^-1/(molec cm^-2)]
30
20
10
0
700
800
900
1000
1100
1200
1300
1400
1500
1600
1700
1800
line center [cm^-1]

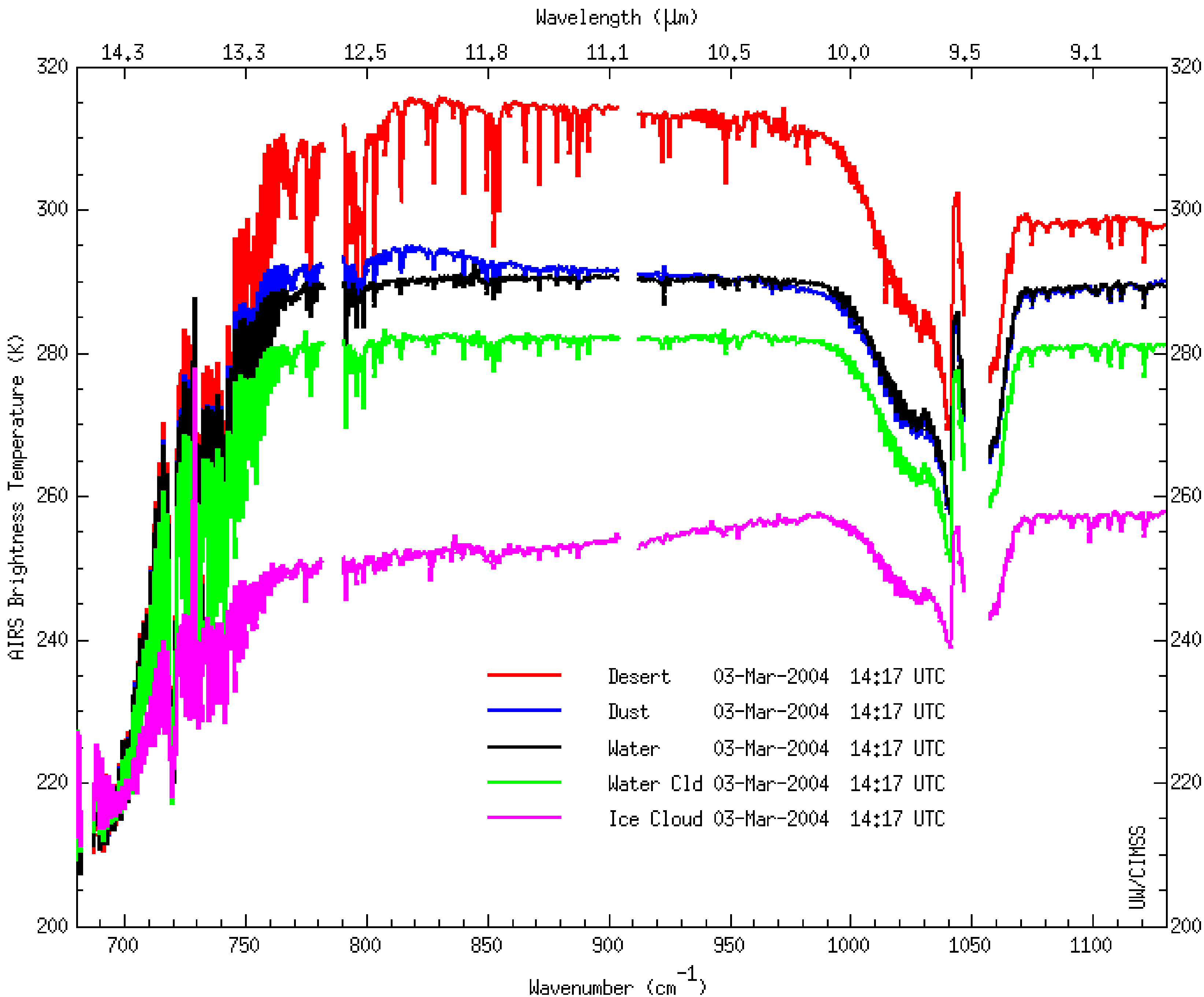

Wavelength (μm)
14.3
13.3
12.5
11.8
11.1
10.5
10.0
9.5
9.1
AIRS Brightness Temperature (K)
320
300
280
260
240
220
200
700
750
800
850
900
950
1000
1050
1100
Wavenumber (cm^{-1})
Desert 03-Mar-2004 14:17 UTC
Dust 03-Mar-2004 14:17 UTC
Water 03-Mar-2004 14:17 UTC
Water Cld 03-Mar-2004 14:17 UTC
Ice Cloud 03-Mar-2004 14:17 UTC
UW/CIMSS

Silicate (ash cloud) signal at Anatahan, Mariana Is

Image is ECMWF bias difference of 1227 cm^{-1} - 984 cm^{-1} (double difference)

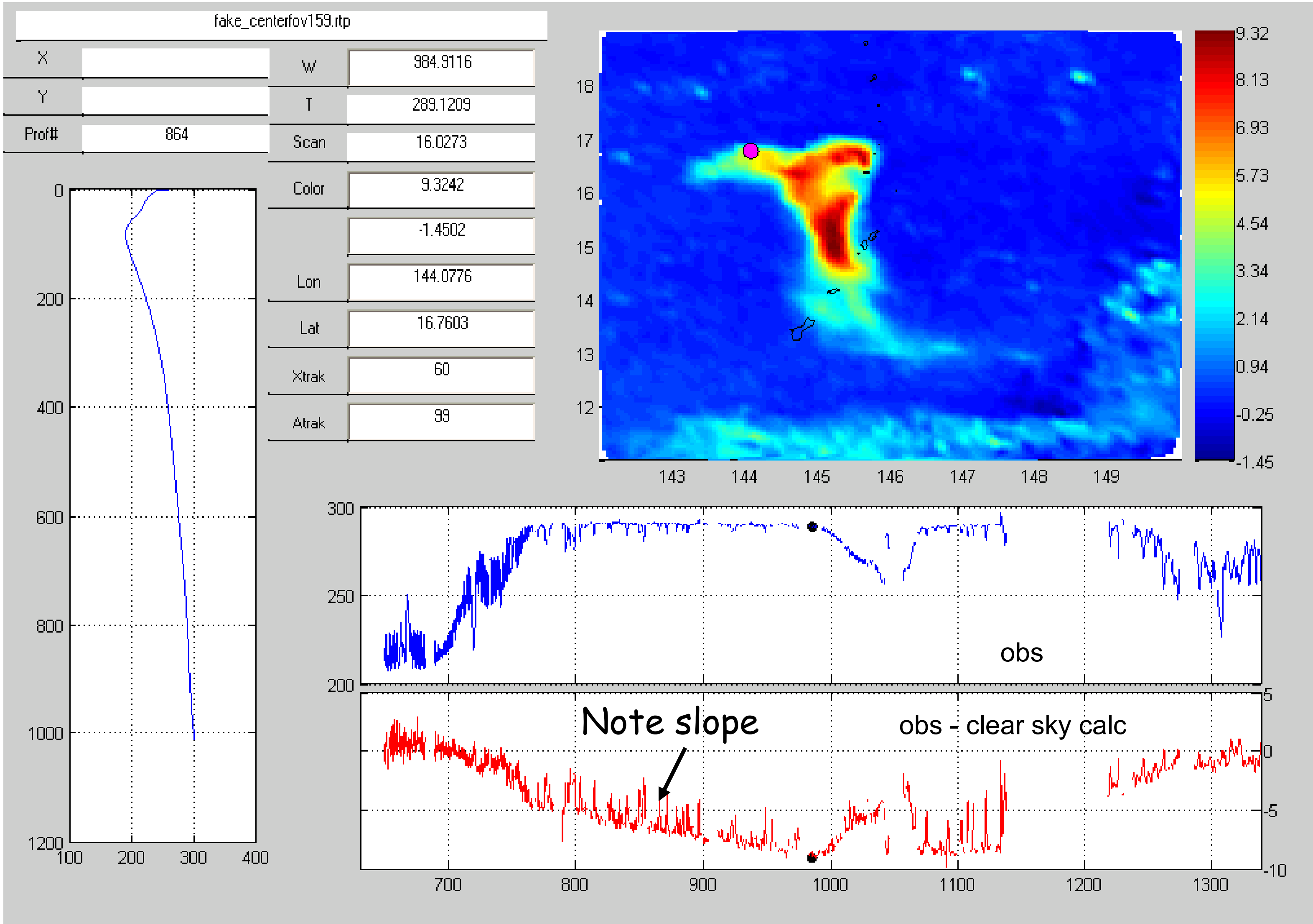

Cirrus signal at Anatahan

Image is ECMWF T_b bias difference of 1227 cm^{-1} - 781 cm^{-1} (double difference)

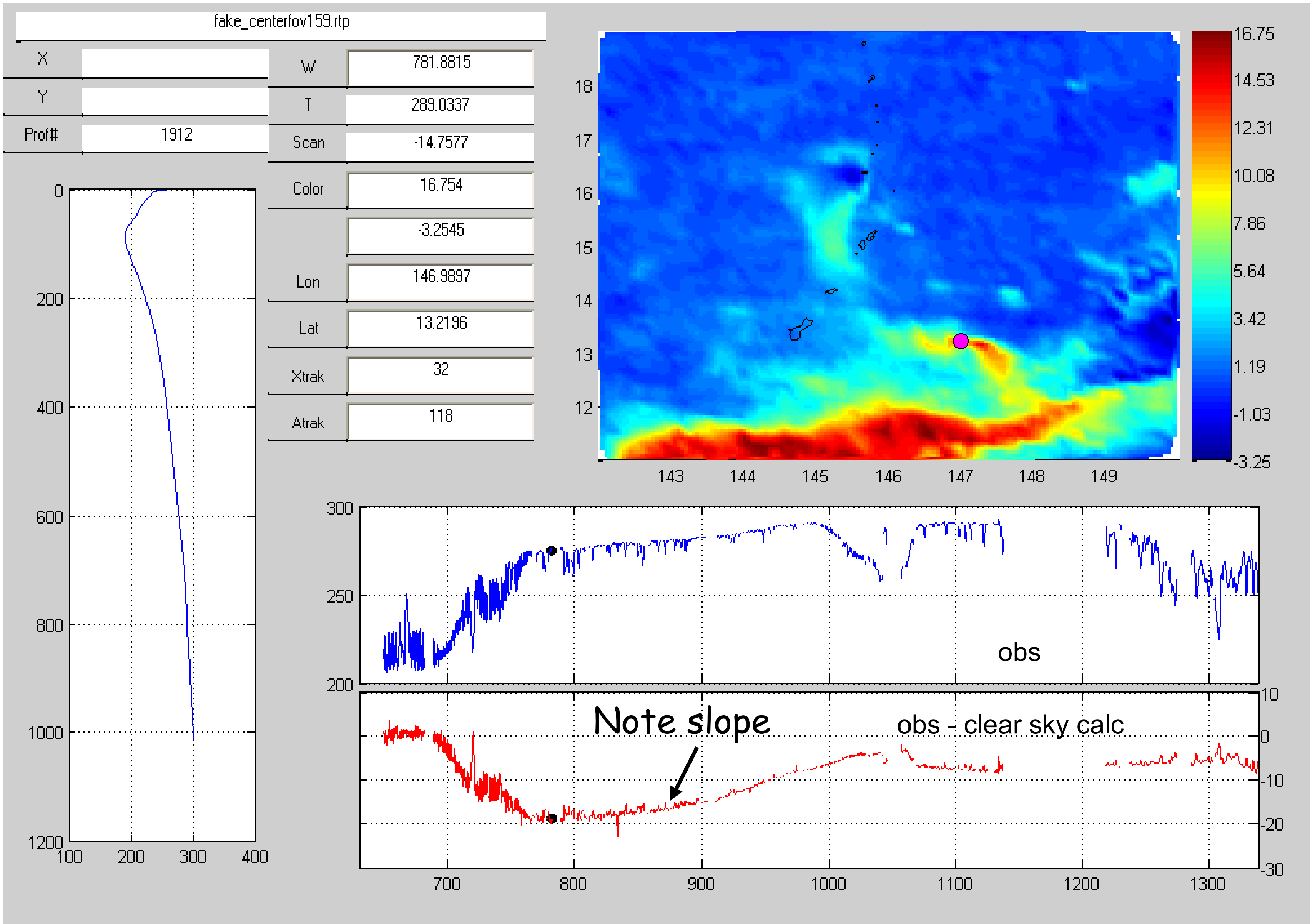

AIRS Spectra from around the Globe

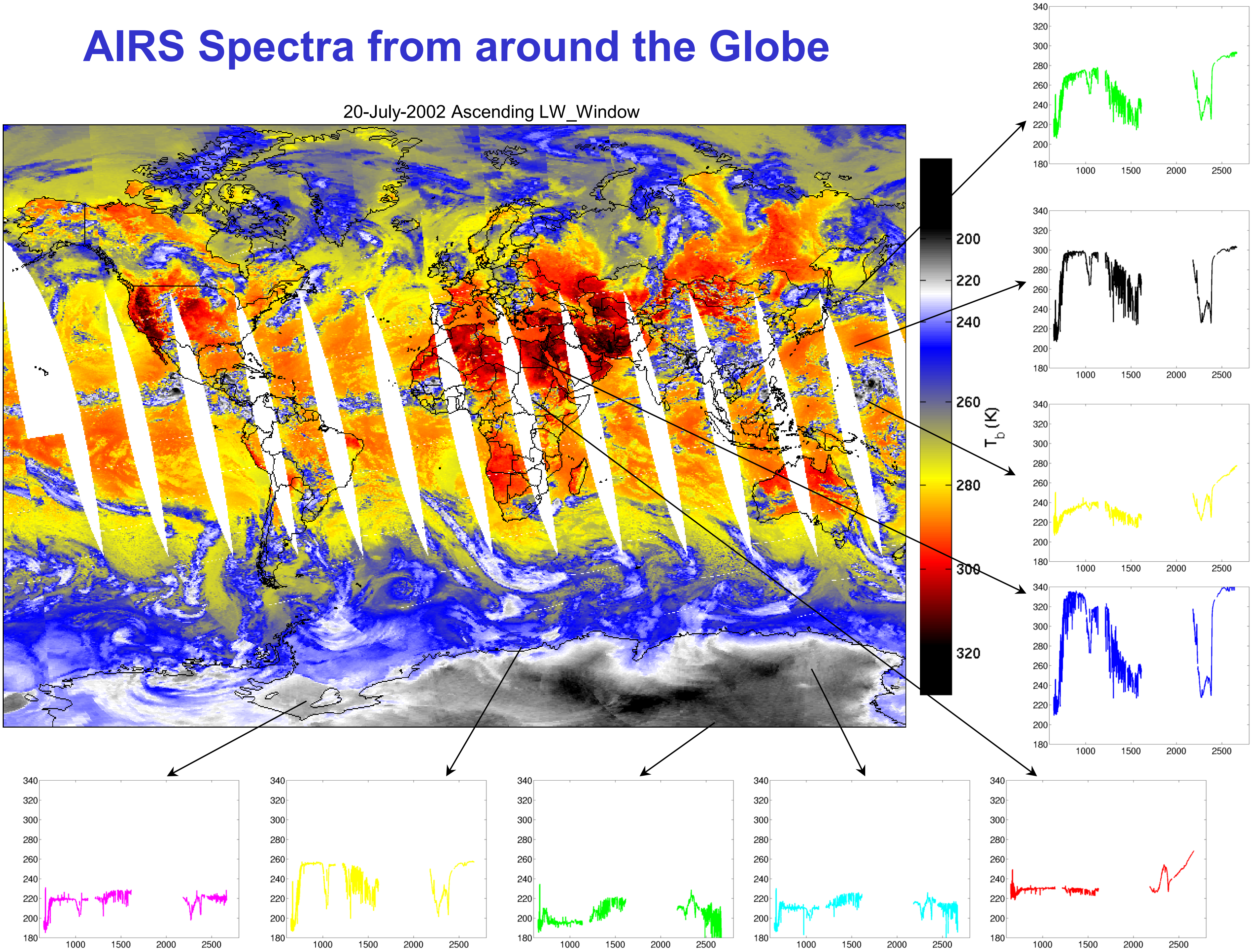

Inferring surface properties with AIRS high spectral resolution data

Barren region detection if T1086 < T981

Barren vs Water/Vegetated

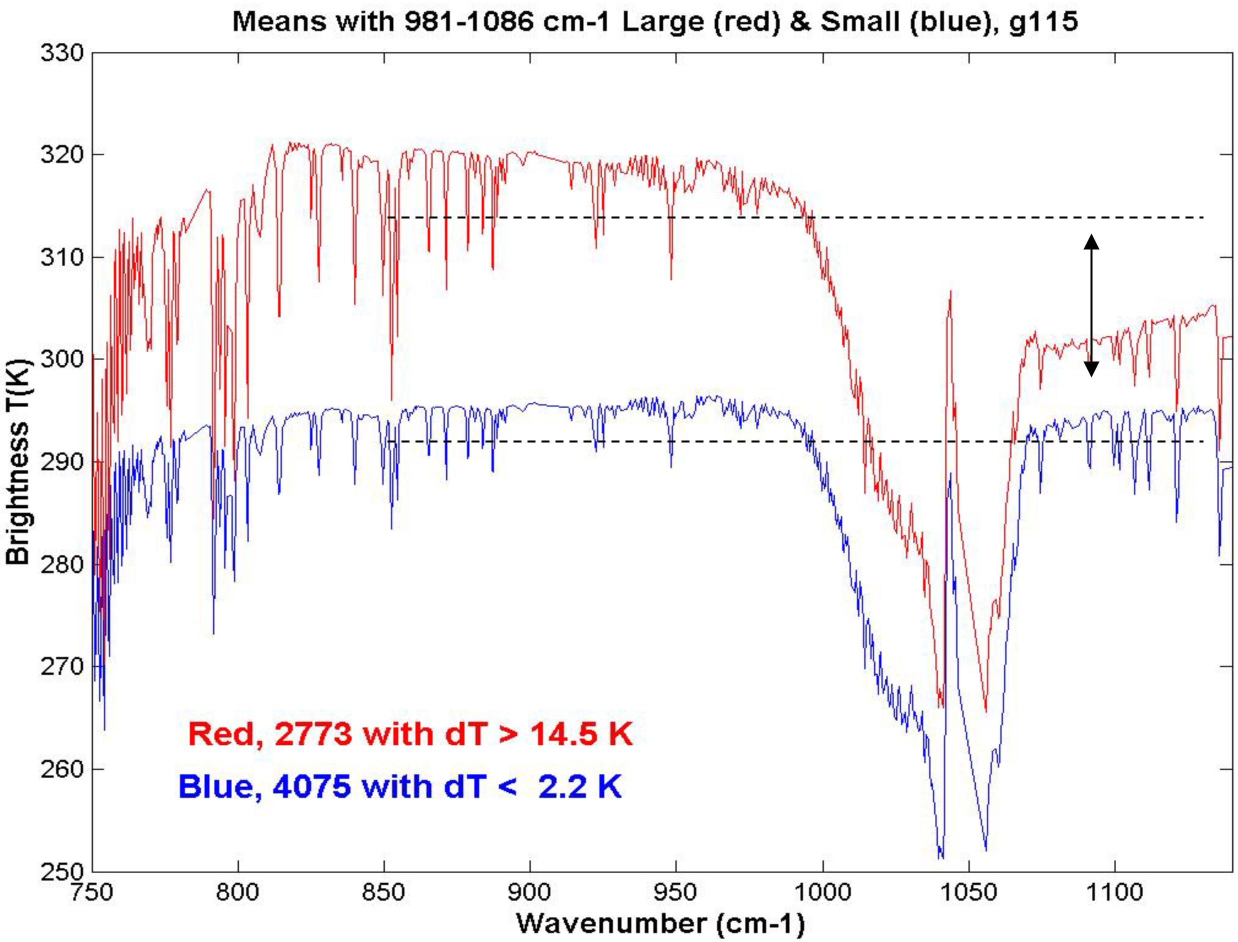

AIRS data from 14 June 2002

T(981 cm^{-1})-T(1086 cm^{-1})

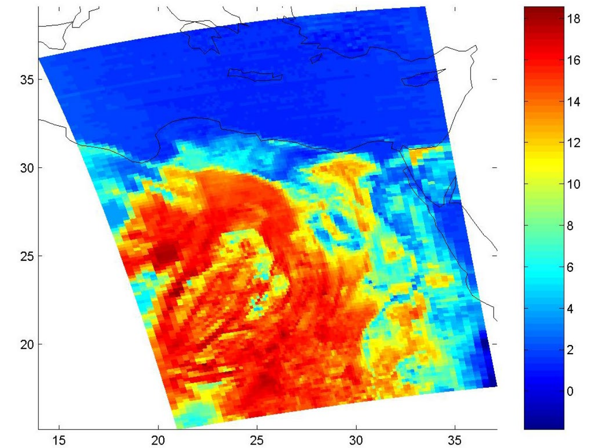

T(1086 cm^{-1})

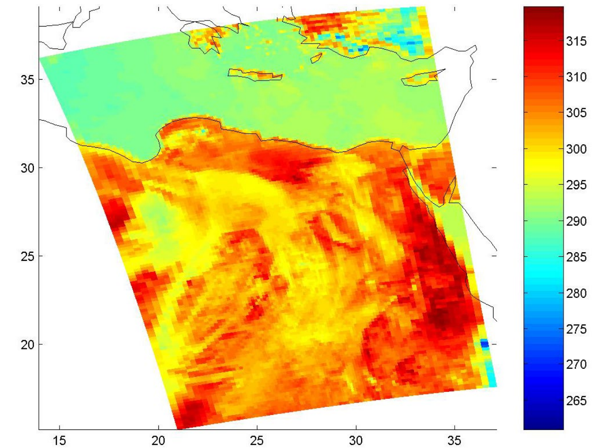

Sensitivity of High Spectral Resolution to Boundary Layer Inversions and Surface/atmospheric Temperature differences

(from IMG Data, October, December 1996)

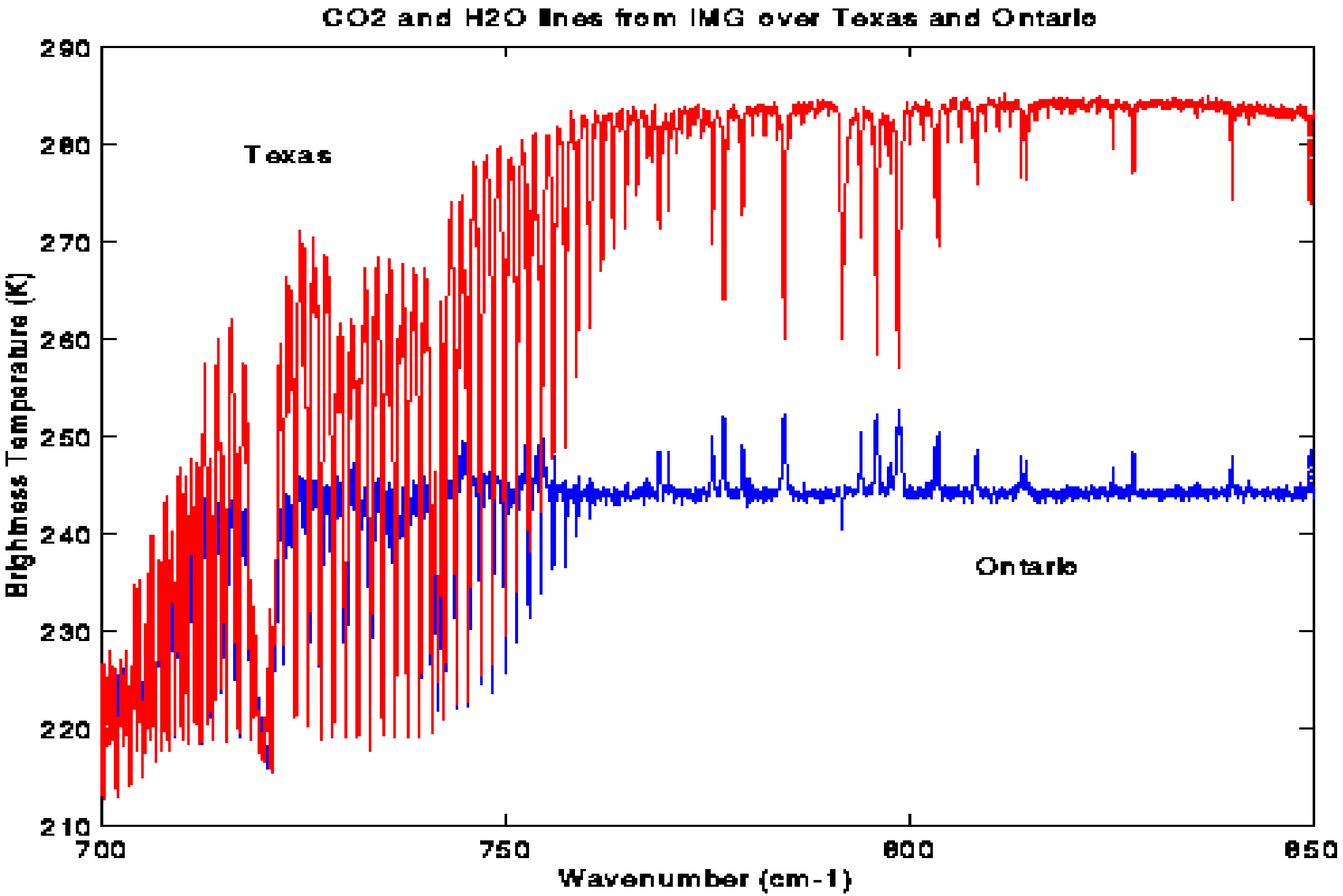

Twisted Ribbon formed by CO_2 spectrum:

Tropopause inversion causes On-line & off-line patterns to cross

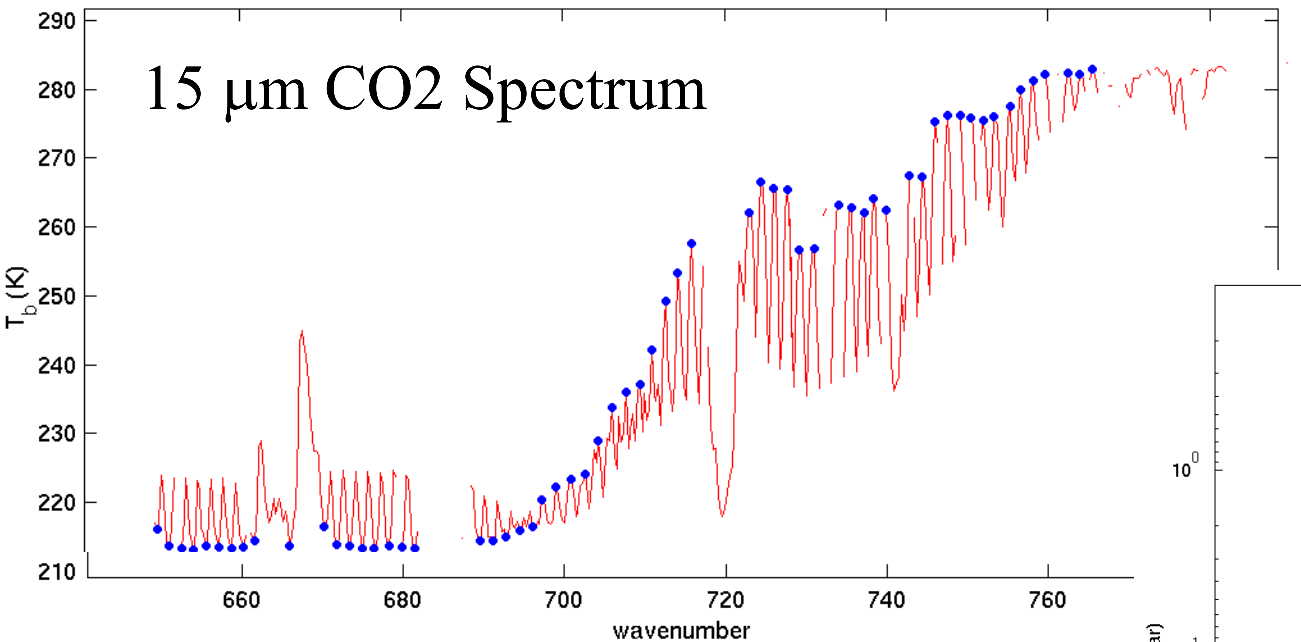

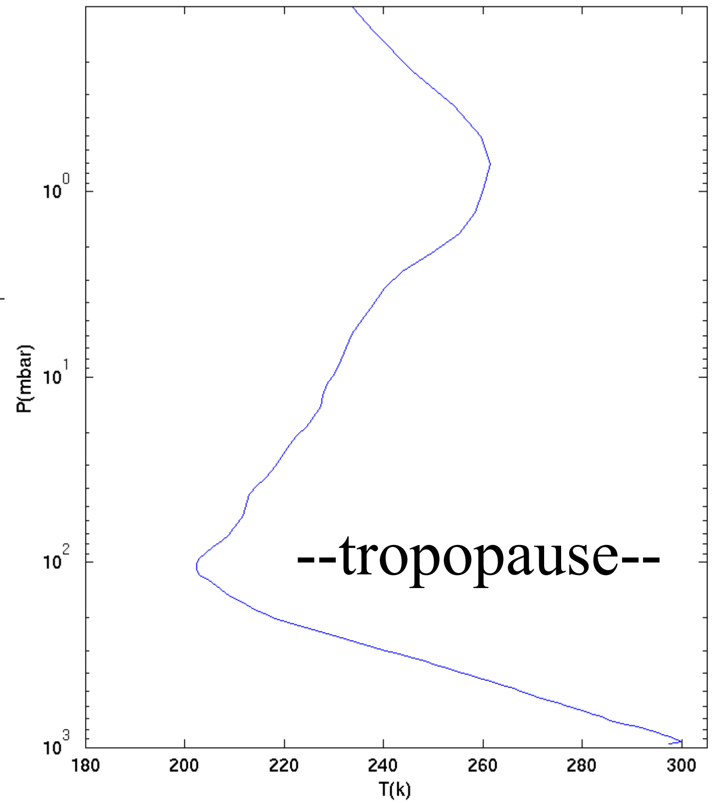

Blue between-line T_b

<u>warmer</u> for tropospheric channels,

<u>colder</u> for stratospheric channels

Signature not available at low resolution

Offline-Online in LW IRW showing low level moisture

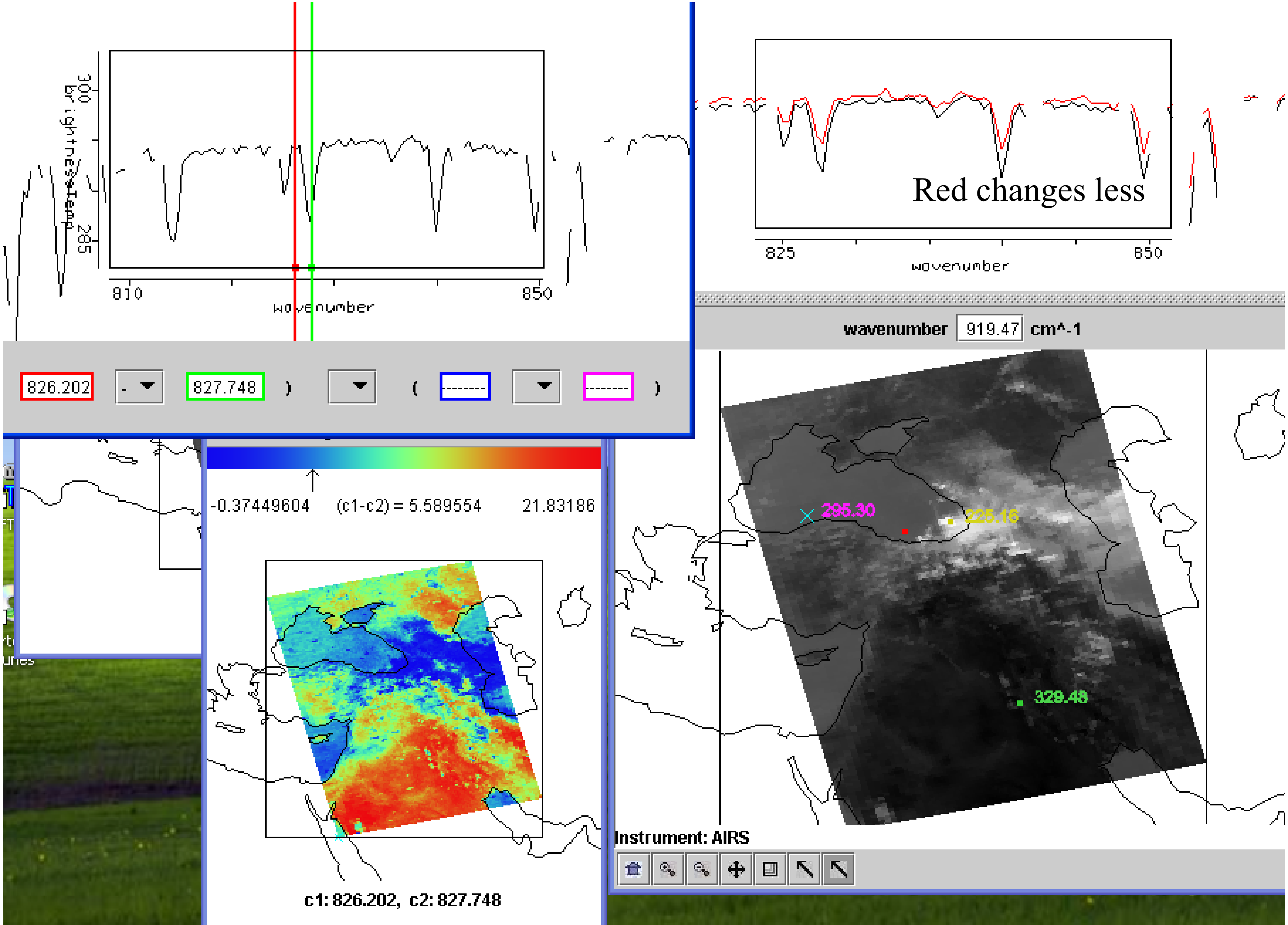

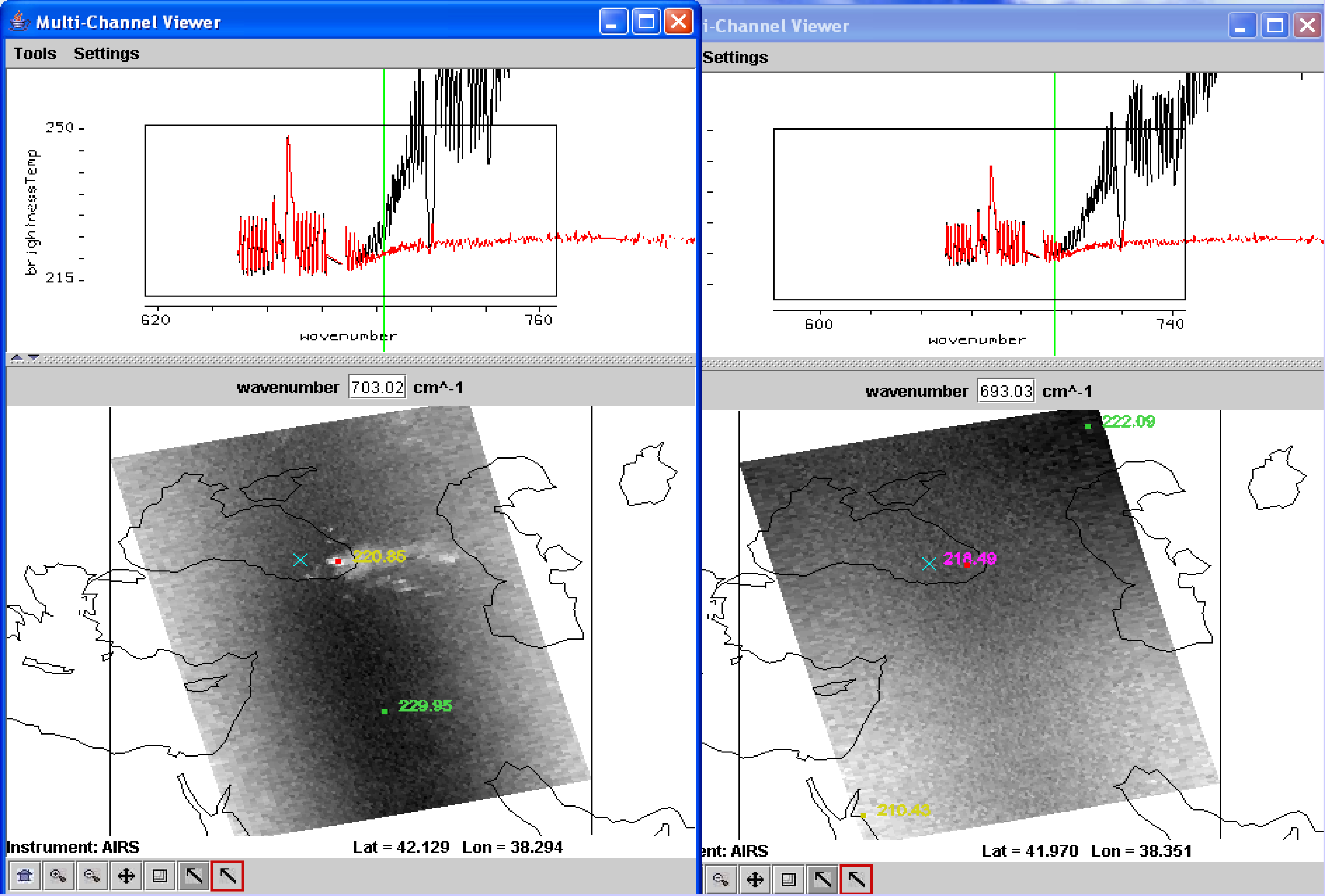

Cld and clr spectra in CO2 absorption separate when weighting functions sink to cloud level

IASI data display on HYDRA

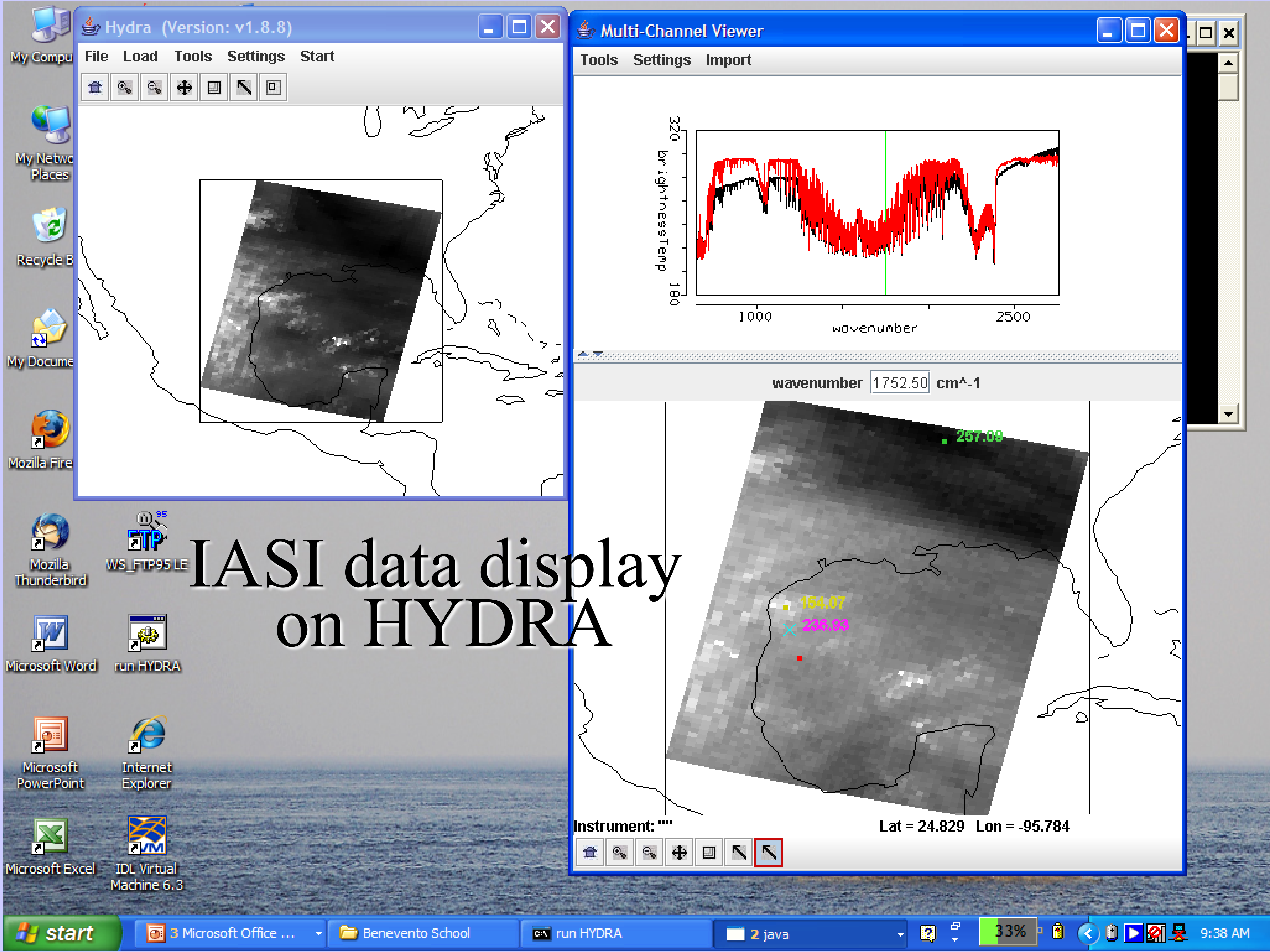

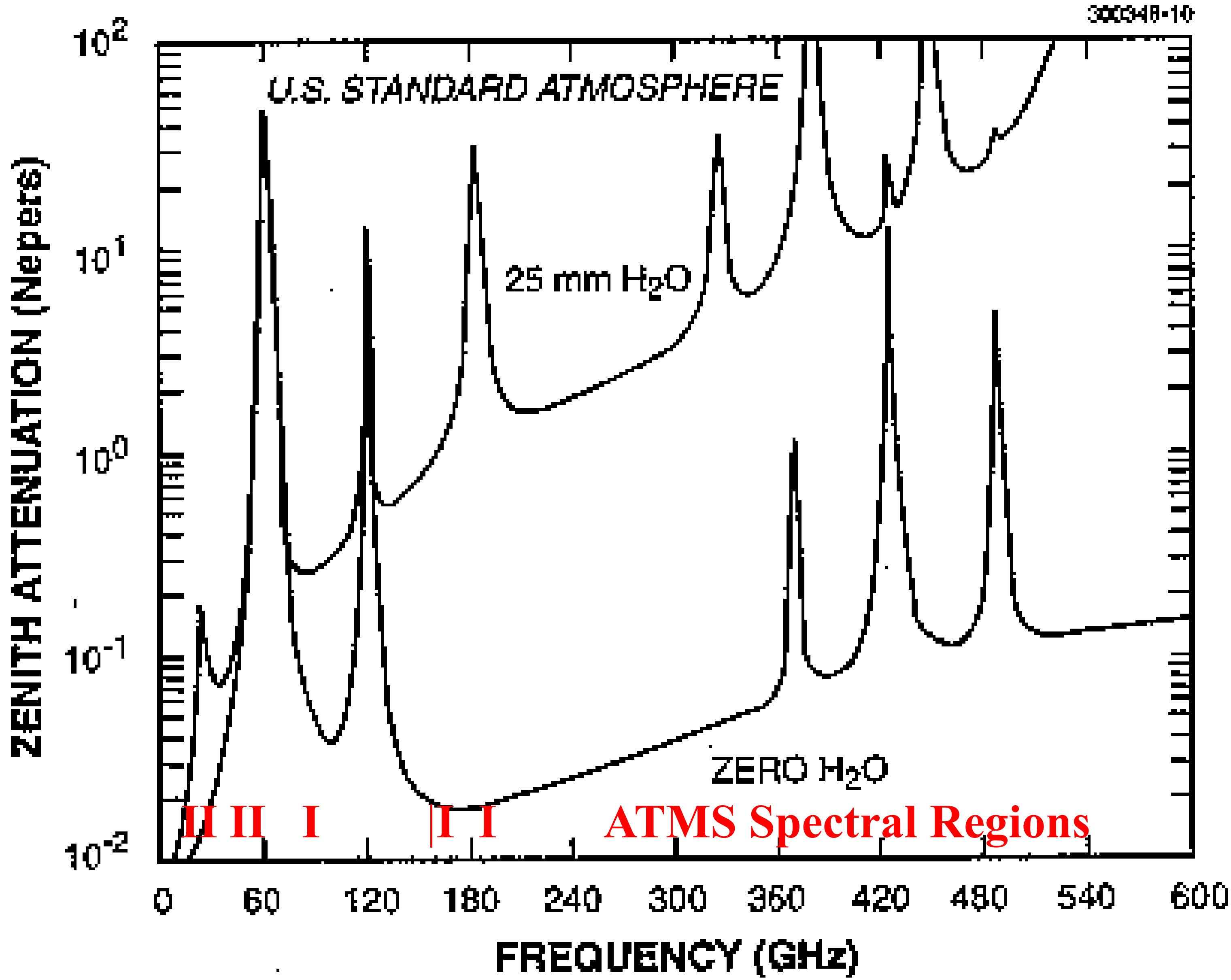
300348-10
U.S. STANDARD ATMOSPHERE
25 mm H2O
ZERO H2O
II II I
|I I
ATMS Spectral Regions
ZENITH ATTENUATION (Nepers)
FREQUENCY (GHz)
10^2
10^1
10^0
10^-1
10^-2
0
60
120
180
240
300
360
420
480
540
600

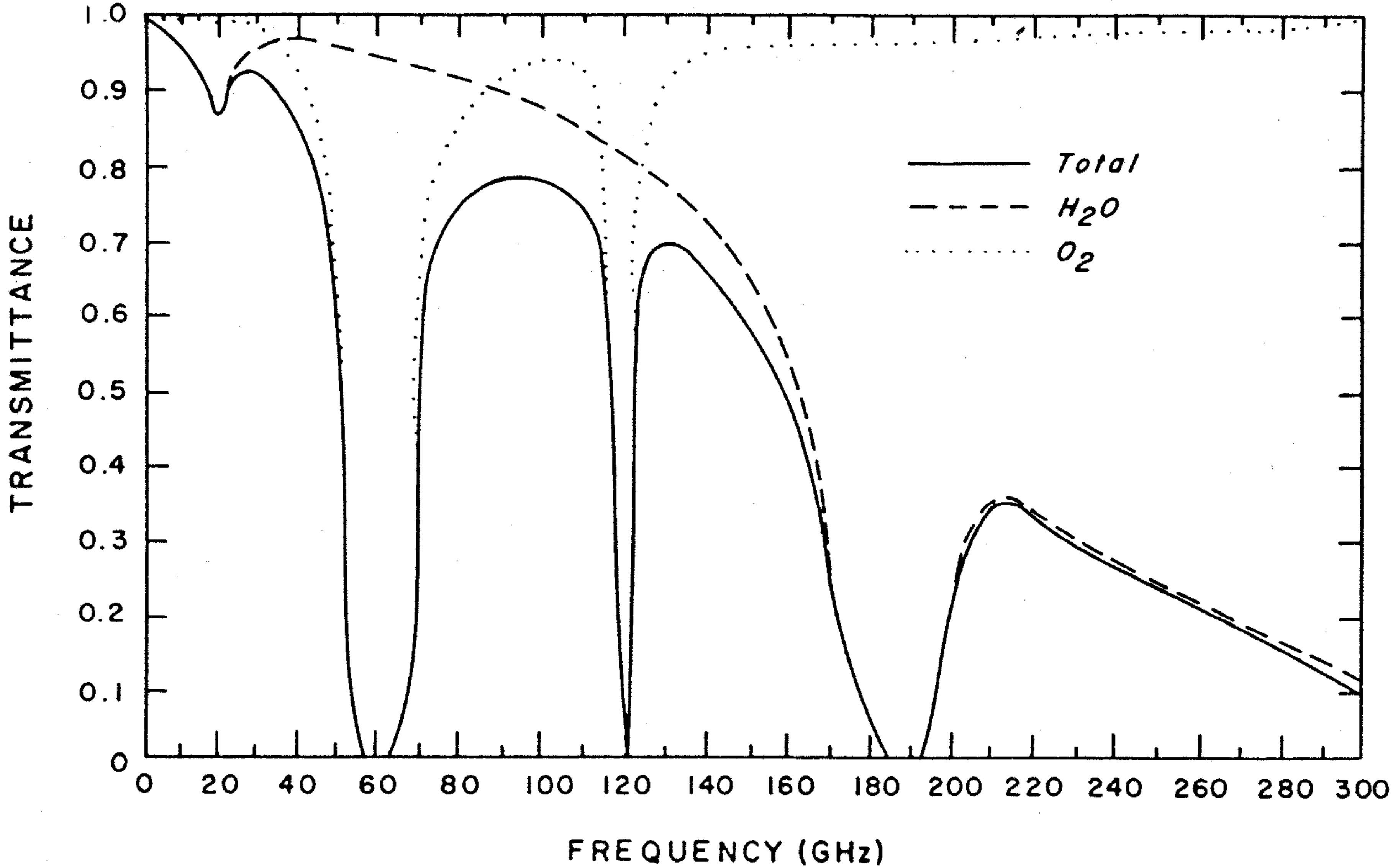

TRANSMITTANCE
1.0
0.9
0.8
0.7
0.6
0.5
0.4
0.3
0.2
0.1
0
0
20
40
60
80
100
120
140
160
180
200
220
240
260
280
300
FREQUENCY (GHz)
Total
H_2O
O_2

Radiation is governed by Planck's Law

$$B(\lambda,T) = c_1 / \{ \lambda^5 [e^{c_2/\lambda T} - 1] \}$$

In microwave region $c_2/\lambda T << 1$ so that

$$e^{c_2/\lambda T} = 1 + c_2/\lambda T + \text{second order}$$

And classical Rayleigh Jeans radiation equation emerges

$$B_\lambda(T) \approx [c_1 / c_2] [T / \lambda^4]$$

Radiance is linear function of brightness temperature.

Microwave Form of RTE

$$I^{sfc}_{\lambda} = \varepsilon_\lambda B_\lambda(T_s)\, \tau_\lambda(p_s) + (1-\varepsilon_\lambda)\, \tau_\lambda(p_s) \int_{o}^{p_s} B_\lambda(T(p)) \frac{\partial \tau'_\lambda(p)}{\partial \ln p}\, d \ln p$$

$$I_\lambda = \varepsilon_\lambda B_\lambda(T_s)\, \tau_\lambda(p_s) + (1-\varepsilon_\lambda)\, \tau_\lambda(p_s) \int_{o}^{p_s} B_\lambda(T(p)) \frac{\partial \tau'_\lambda(p)}{\partial \ln p}\, d \ln p$$

$$+ \int_{p_s}^{o} B_\lambda(T(p)) \frac{\partial \tau_\lambda(p)}{\partial \ln p}\, d \ln p$$

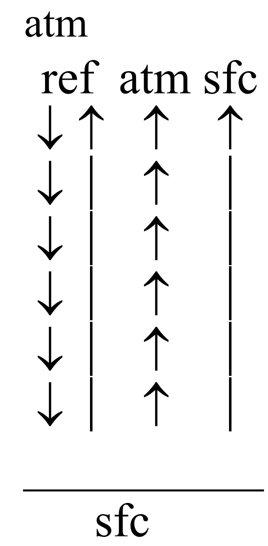

In the microwave region $c_2 / \lambda T << 1$, so the Planck radiance is linearly proportional to the temperature

$$B_\lambda(T) \approx [c_1 / c_2]\, [T / \lambda^4]$$

So

$$T_{b\lambda} = \varepsilon_\lambda T_s(p_s)\, \tau_\lambda(p_s) + \int_{p_s}^{o} T(p)\, F_\lambda(p) \frac{\partial \tau_\lambda(p)}{\partial \ln p}\, d \ln p$$

where

$$F_\lambda(p) = \{ 1 + (1 - \varepsilon_\lambda) \left[\frac{\tau_\lambda(p_s)}{\tau_\lambda(p)}\right]^2 \} .$$

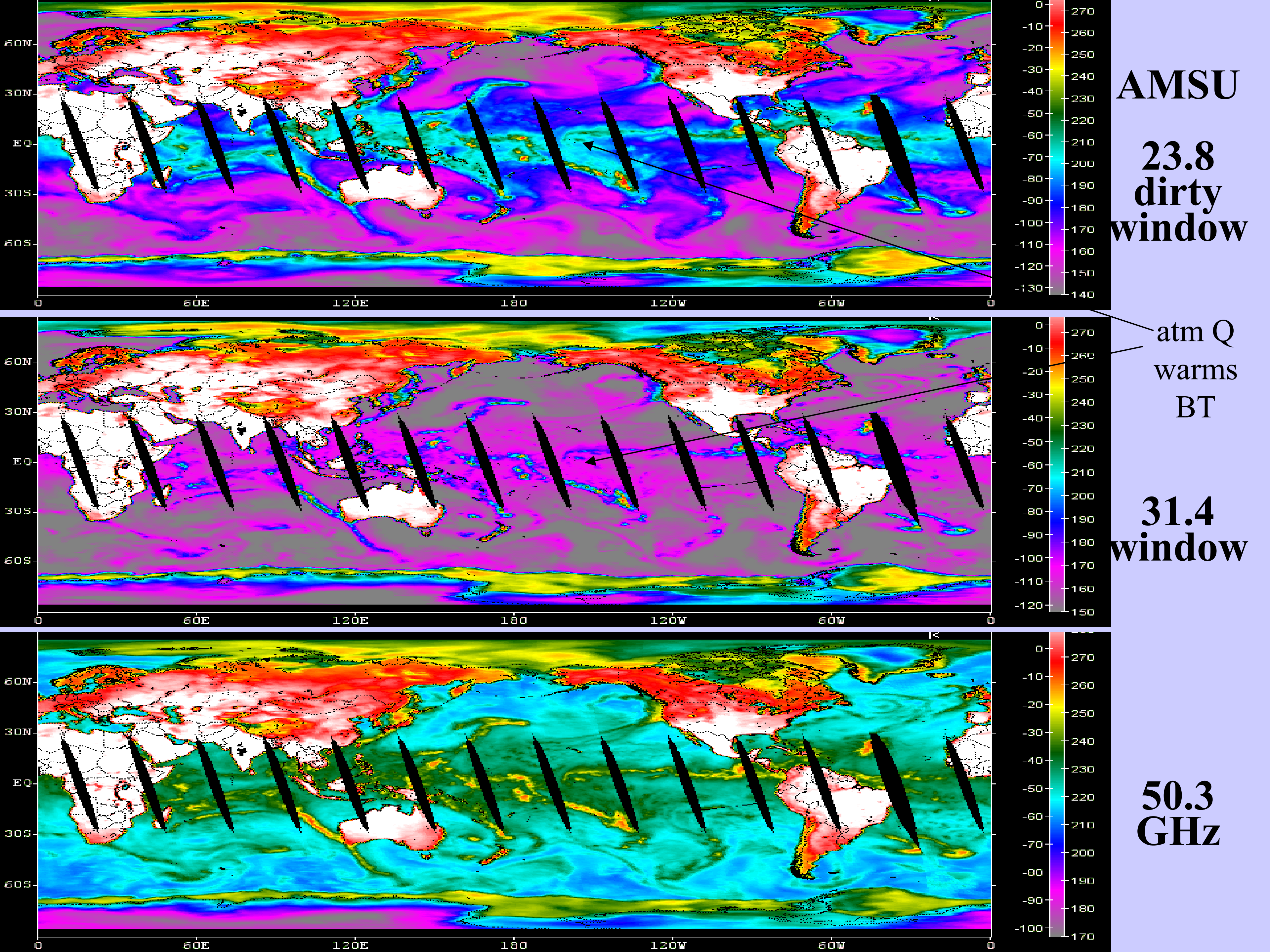

AMSU
23.8
dirty
window
atm Q
warms
BT
31.4
window
50.3
GHz
60N
30N
EQ
30S
60S
0
60E
120E
180
120W
60W

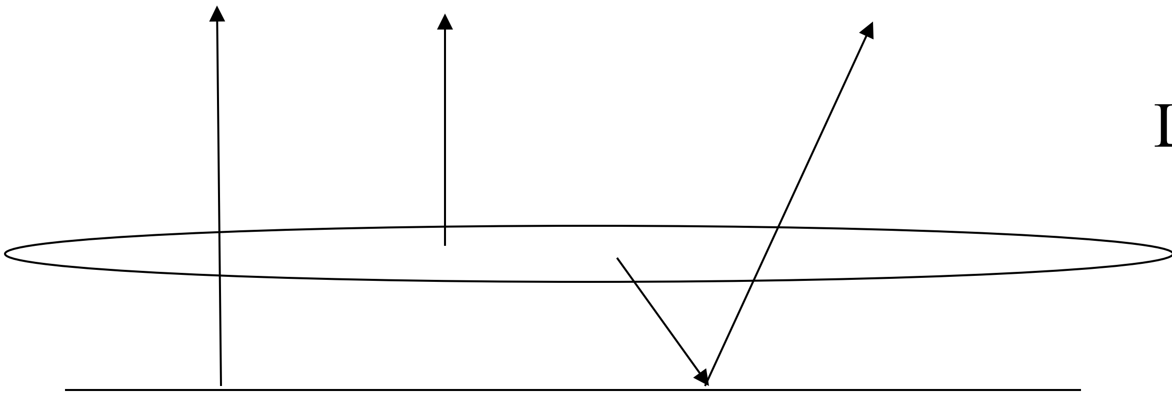

Low mist over ocean

$$T_b = \varepsilon_s T_s (1-\sigma_m) + \sigma_m T_m + \sigma_m (1-\varepsilon_s) (1-\sigma_m) T_s$$

So

$$\Delta T_b = - \varepsilon_s \sigma_m T_s + \sigma_m T_m + \sigma_m (1-\varepsilon_s) (1-\sigma_m) T_s$$

For $\varepsilon_s \sim 0.5$ and $T_s \sim T_m$ this is always positive for $0 < \sigma_m < 1$

Accuracy of Satellite Derived Met Parameters

T(p) within 1.5 C of raobs for 1 km layers

SST within 0.5 C of buoys

Q(p) within 15-20% of raobs for 2 km layers

TPW with 3 mm of ground based MW

TO3 within 30 Dobsons of ozone profilers

LI adjusted 3 C lower (for better agreement with raobs)

gradients in space and time more reliable than absolute

AMVs within 7 m/s (upper trop) and 5 m/s (lower trop)

CTPs within 50 hPa of lidar determination

Geopotential heights within 20 to 30 m

for 500 to 300 hPa

For TC, Psfc within 6 hPa and Vmax within 10 kts

(from MW ΔT250)

Trajectory forecast 72 hour error reduction about 10%

GEO vs LEO

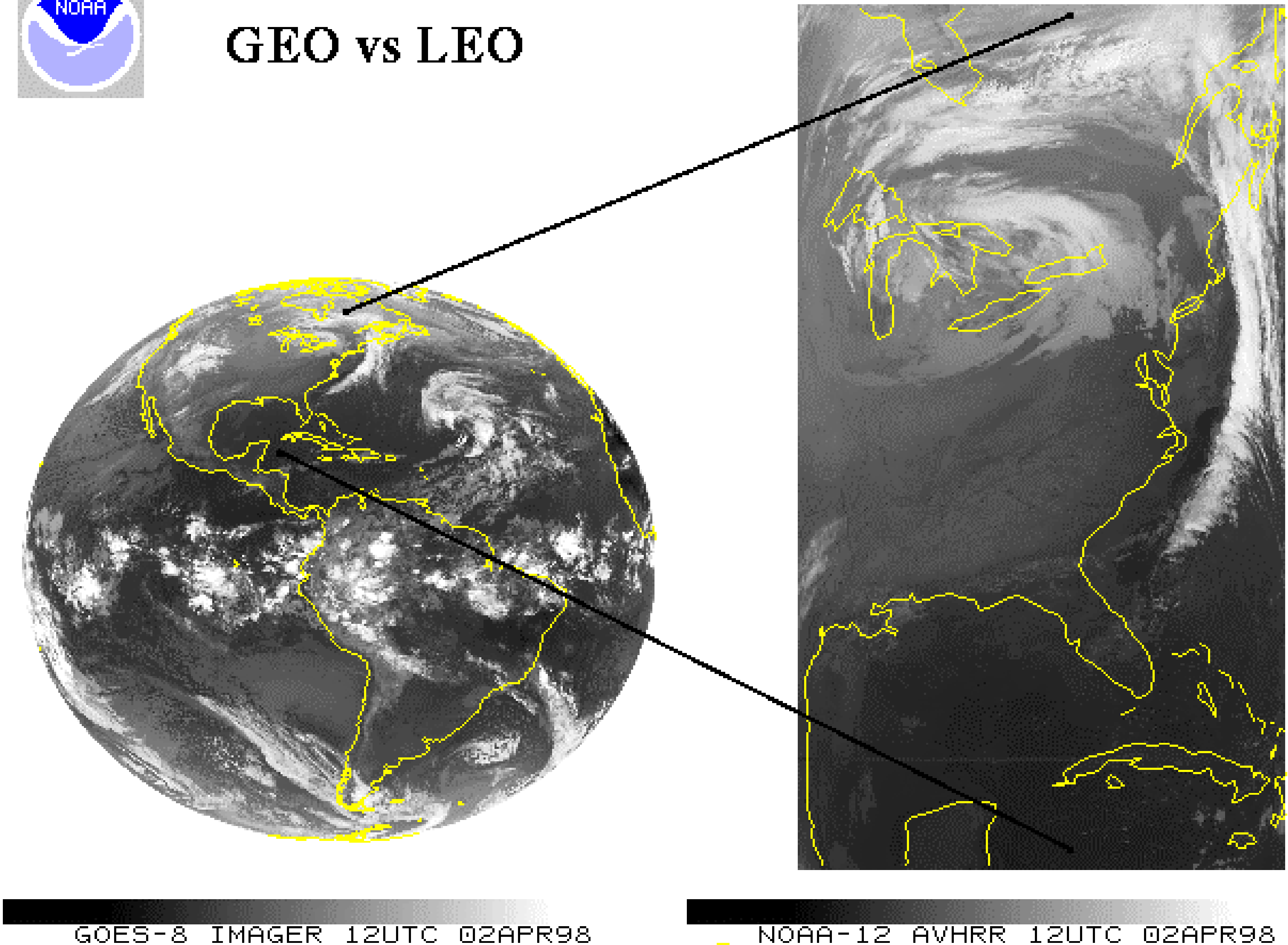

All Sats on NASA J-track

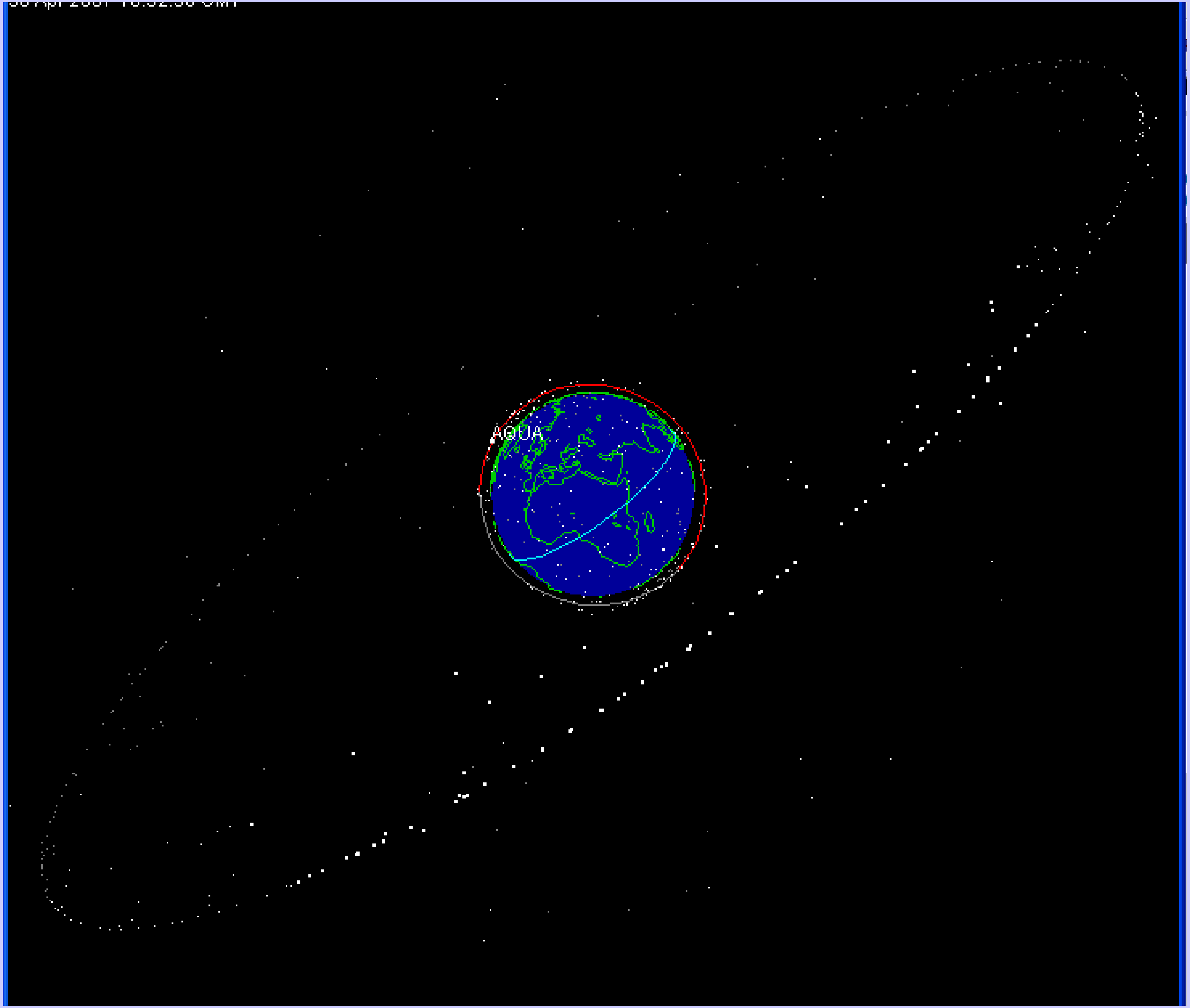

Comparison of geostationary (geo) and low earth orbiting (leo) satellite capabilities

Geo	Leo
observes process itself (motion and targets of opportunity)	observes effects of process
repeat coverage in minutes ($\Delta t \leq 30$ minutes)	repeat coverage twice daily ($\Delta t = 12$ hours)
full earth disk only	global coverage
best viewing of tropics	best viewing of poles
same viewing angle	varying viewing angle
differing solar illumination	same solar illumination
visible, IR imager (1, 4 km resolution)	visible, IR imager (1, 1 km resolution)
one visible band	multispectral in visible (veggie index)
IR only sounder (8 km resolution)	IR and microwave sounder (17, 50 km resolution)
filter radiometer	filter radiometer, interferometer, and grating spectrometer
diffraction more than leo	diffraction less than geo

HYperspectral viewer for Development of Research Applications - HYDRA

MSG,
GOES

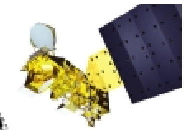

MODIS,
AIRS

Freely available software
For researchers and educators
Computer platform independent
Extendable to more sensors and applications
Based in VisAD
(Visualization for Algorithm Development)
Uses Jython (Java implementation of Python)
runs on most machines
512MB main memory & 32MB graphics card suggested
on-going development effort

Developed at CIMSS by
Tom Rink
Tom Whittaker
Kevin Baggett

With guidance from
Paolo Antonelli
Liam Gumley
Paul Menzel

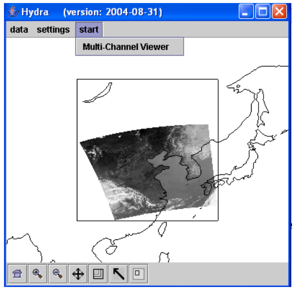

CIMSS

http://www.ssec.wisc.edu/hydra/

For hydra
http://www.ssec.wisc.edu/hydra/

For MODIS data and quick browse images
http://rapidfire.sci.gsfc.nasa/realtime

For MODIS data orders
http://ladsweb.nascom.nasa.gov/

For AIRS data orders
http://daac.gsfc.nasa.gov/

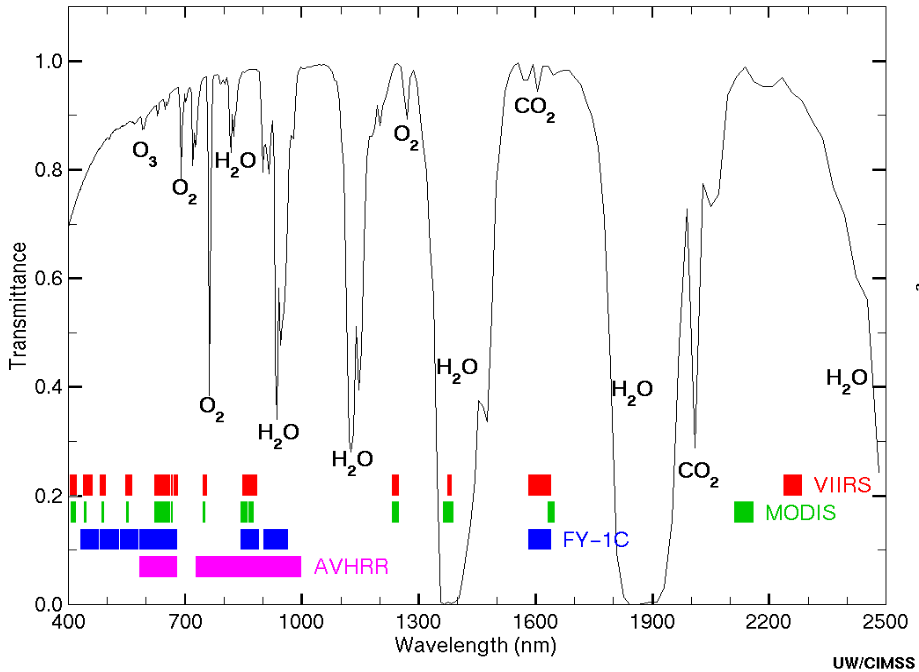

Transmittance
Wavelength (nm)
1.0
0.8
0.6
0.4
0.2
0.0
400
700
1000
1300
1600
1900
2200
2500
O_3
O_2
H_2O
O_2
H_2O
H_2O
O_2
H_2O
CO_2
H_2O
CO_2
H_2O
VIIRS
MODIS
FY-1C
AVHRR
UW/CIMSS

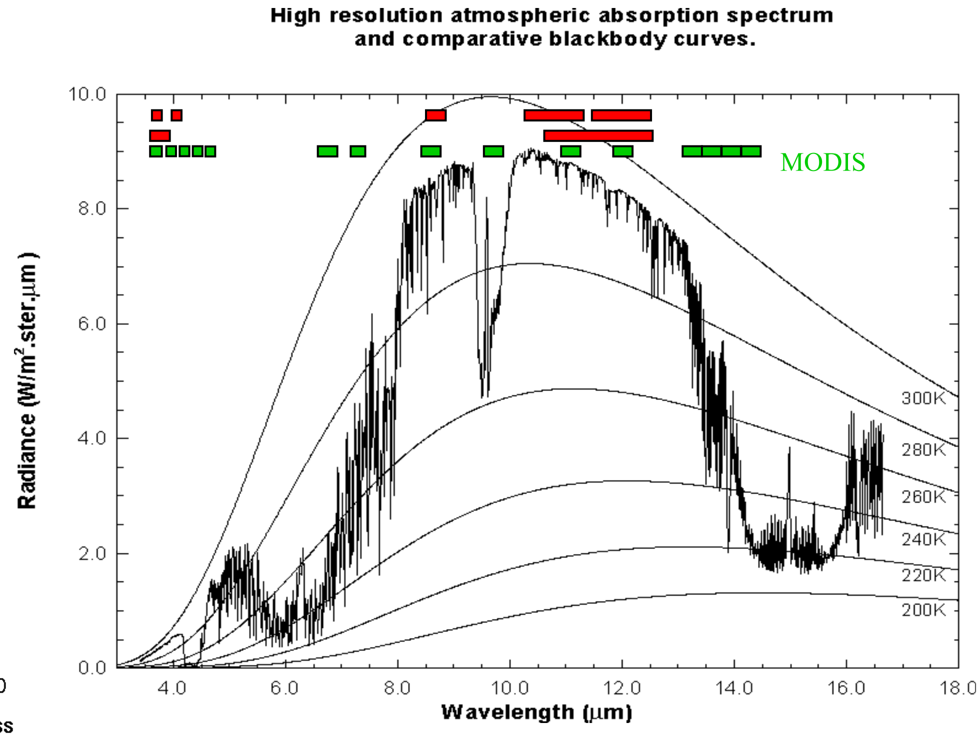

High resolution atmospheric absorption spectrum
and comparative blackbody curves.
Radiance (W/m^2.ster.μm)
Wavelength (μm)
10.0
8.0
6.0
4.0
2.0
0.0
4.0
6.0
8.0
10.0
12.0
14.0
16.0
18.0
MODIS
300K
280K
260K
240K
220K
200K

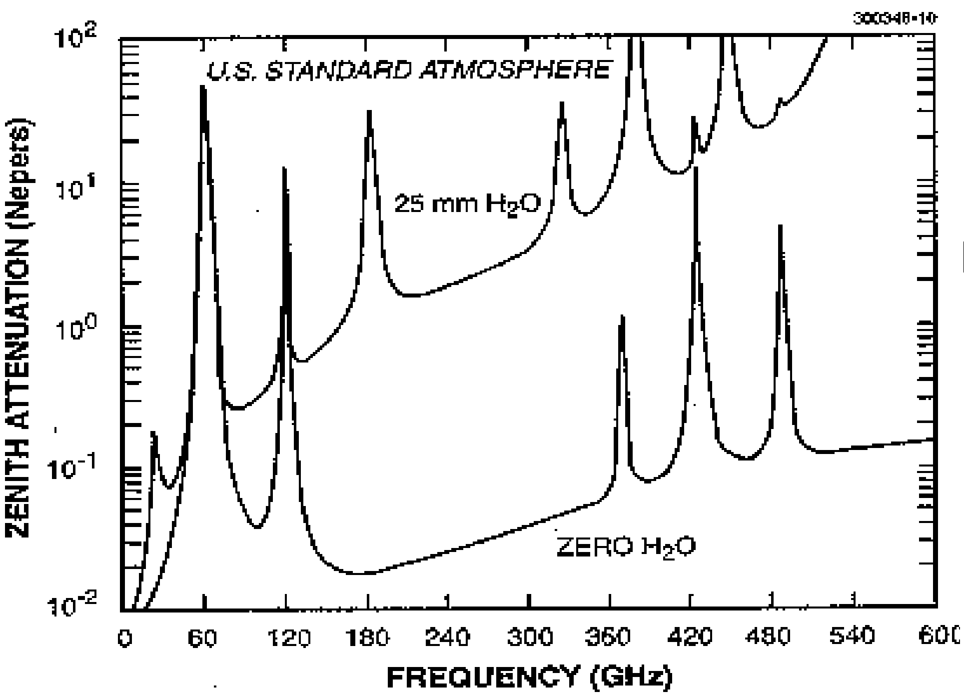

U.S. STANDARD ATMOSPHERE
ZENITH ATTENUATION (Nepers)
FREQUENCY (GHz)
10^2
10^1
10^0
10^{-1}
10^{-2}
0
60
120
180
240
300
360
420
480
540
600
25 mm H_2O
ZERO H_2O

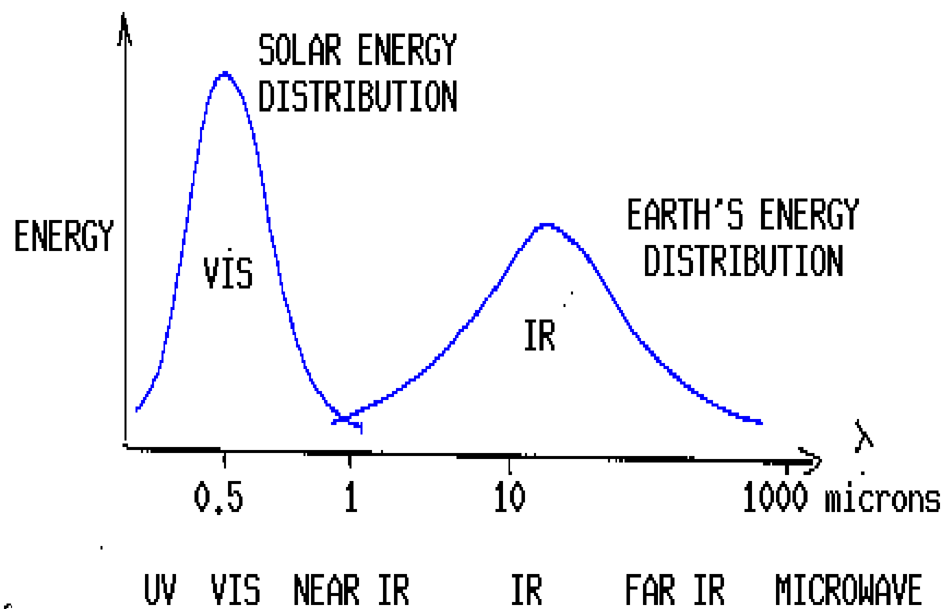

SOLAR ENERGY
DISTRIBUTION
ENERGY
VIS
EARTH'S ENERGY
DISTRIBUTION
IR
λ
0.5
1
10
1000 microns
UV
VIS
NEAR IR
IR
FAR IR
MICROWAVE